THE IMPACT OF POST-TRANSLATIONAL MODIFICATIONS ON AGGREGATION OF CU, ZN SUPEROXIDE DISMUTASE IN AMYOTROPHIC LATERAL SCLEROSIS

Rachel L. Redler

A dissertation submitted to the faculty at the University of North Carolina at Chapel Hill in partial fulfillment of the requirements for the degree of Doctor of Philosophy in the Department of Biochemistry and Biophysics in the School of Medicine.

Chapel Hill
2014

Approved by:

Sharon Campbell

Michael Caplow

Mohanish Deshmukh

Nikolay V. Dokholyan

Hengming Ke

ABSTRACT

Rachel L. Redler: The impact of post-translational modifications on aggregation of Cu, Zn superoxide dismutase in amyotrophic lateral sclerosis
(Under the direction of Nikolay V. Dokholyan)

Aberrant conformers of disease-linked proteins have been proposed as cytotoxic agents in several late-onset neurodegenerative disorders, including Alzheimer's disease and amyotrophic lateral sclerosis (ALS). Mutations in the gene encoding Cu, Zn superoxide dismutase (SOD1) are present in a subset of familial ALS (FALS) cases; most of these mutations destabilize the protein, although typically by a small margin relative to SOD1's exceptionally high stability. Therefore, SOD1 with FALS-linked substitutions often misfolds and aggregates, adopting aberrant conformations that interact with numerous cellular components and disrupt their functioning, despite having a more stable folded state than would be expected for an aggregation-prone protein. This fact, together with the specific death of motor neurons late in life despite ubiquitous expression of mutant SOD1 since birth, implicates factors in the cellular environment as substantial contributors to the cytotoxicity of mutant SOD1 in FALS. One non-genetic factor likely to influence misfolding and aggregation of SOD1 in human tissue is its susceptibility to abundant post-translational modifications, including phosphorylation and numerous oxidative modifications. We find that reversible oxidative modification of Cys-111 by the glutathione tripeptide destabilizes the native SOD1 homodimer, increasing the equilibrium dissociation constant of the WT dimer from low nanomolar to the low micromolar range, and

further destabilizes SOD1 containing a FALS-linked substitution within the dimer interface (A4V). Assessment of the effect of glutathionylation on dimer dissociation kinetics using surface plasmon resonance revealed that this modification causes minimal change in dimer dissociation rate; therefore, the increased K_d observed for glutathionylated WT and A4V SOD1 must result from slowed association of modified monomers. In addition to inducing dissociation of the native dimer, Cys-111 glutathionylation promotes the assembly of soluble non-native oligomers that contain an epitope specific to disease-relevant misfolded SOD1. Our findings suggest that soluble non-native SOD1 oligomers share structural similarity to pathogenic misfolded species found in ALS patients, and therefore represent potential cytotoxic agents and therapeutic targets in ALS. Furthermore, the induction of SOD1 misfolding and aggregation by glutathionylation represents a possible mechanism by which oxidative stress brought on by aging triggers the transition of SOD1 from its natively folded state to cytotoxic conformations.

ACKNOWLEDGEMENTS

This work was supported by the National Institutes of Health Predoctoral Fellowship F31NS073435 from the National Institute of Neurological Disorders and Stroke to R.L.R., as well as the National Institutes of Health grant R01GM080742 and the ARRA supplement 3R01GM080742-03S1 to N.V.D and National Institutes of Health Predoctoral Fellowship F31AG039266 from the National Institute on Aging to E.A.P. This research is based in part upon work conducted using the UNC Michael Hooker Proteomics Center, which is supported in part by the NIH-NCI Grant No. CA016086 to the Lineberger Comprehensive Cancer Center.

I thank Kyle C. Wilcox, Lanette Fee, Elizabeth A. Proctor, Michael Caplow, and Nikolay V. Dokholyan for their contributions to the design, execution, and analysis of work described in Chapter 2. I thank Lanette Fee, James Fay, Michael Caplow, and Nikolay V. Dokholyan for their contributions to the design, execution, and analysis of the work described in Chapter 3. I thank Hengming Ke, Elizabeth Proctor, Lanette Fee, James Fay, Kyle Wilcox, Huanchen Wang, Wenjun Cui, Michael Caplow, and Nikolay V. Dokholyan for their contributions to the design, execution, and analysis of the work described in Chapter 4. DMD simulations and analysis, the results of which are shown in Figures 2.5, 2.6, and 4.4, were performed by Elizabeth A. Proctor. We thank Joan S. Valentine for providing the EG118 yeast strain and yEP351:hwtSOD1 vector. I also thank Drs. Feng Ding, Xian Chen, Ashutosh Tripathy, David Smalley, and Brian Kuhlman for helpful discussions.

PREFACE

Chapter 1 is reprinted from "Redler, R. L. and Dokholyan, N.V. (2012) The complex molecular biology of amyotrophic lateral sclerosis (ALS). *Prog Mol Biol Transl Sci* 107:215-262", Copyright 2012, with permission from Elsevier.

Chapter 2 is reproduced with permission from "Redler, R. L., Wilcox, K. C., Proctor, E. A., Fee, L., Caplow, M., and Dokholyan, N. V. (2011) Glutathionylation at Cys 111 triggers dissociation of wild type and FALS mutant SOD1 dimers. *Biochemistry* 50:7057-7066". Copyright 2011 American Chemical Society.

TABLE OF CONTENTS

LIST OF TABLES

LIST OF FIGURES

LIST OF ABBREVIATIONS

ALS	Amyotrophic lateral sclerosis
CNS	Central nervous system
DMD	Discrete molecular dynamics
EDTA	Ethylenediaminetetraacetic acid
EMG	Electromyography
FALS	Familial amyotrophic lateral sclerosis
FTLD	Frontotemporal lobar dementia
GSSG	Oxidized glutathione
GS-SOD1	Glutathionylated SOD1
LMN	Lower motor neuron
μ-ESI-FT-ICR-MS	Microcapillary electrospray ionization Fourier transform ion cyclotron resonance mass spectrometry
MALS	Multi-angle light scattering
MS/MS	Tandem mass spectrometry
p-SOD1	Phosphorylated SOD1
RNS	Reactive nitrogen species
ROS	Reactive oxygen species
SALS	Sporadic amyotrophic lateral sclerosis

SEC	Size exclusion chromatography
SOD1	Cu, Zn superoxide dismutase
SPR	Surface plasmon resonance
TDP-43	43 kDa trans-activating response region DNA-binding protein
UMN	Upper motor neuron

CHAPTER ONE: INTRODUCTION

ALS is a deadly neurodegenerative disorder

Amyotrophic lateral sclerosis (ALS) was first described by the noted French neurologist Jean-Martin Charcot in 1869, who connected the progressive paralytic syndrome with lesions in both white and grey matter of the central nervous system (CNS) (1). Over 140 years later, ALS is the most common adult-onset motor neuron disorder, affecting approximately 1-2 per 100,000 people worldwide. Considering the short course of disease progression (death/tracheotomy typically within 2-5 years of diagnosis), 1 of every 800 individuals is expected to face ALS in his/her lifetime (2-4).

As described by Charcot, ALS involves degeneration of the upper motor neurons (UMN) of the motor cortex and of the lower motor neurons (LMN), which extend through the brainstem and spinal cord to innervate skeletal muscle. Though the upper and lower motor systems are known to be interconnected, controlling voluntary muscle movement in concert, the primary site of dysfunction in ALS has long been a source of debate (5-7). Questions of UMN/LMN primacy aside, ALS is clearly specific for motor neurons and largely spares cognitive ability, sensation and autonomic nervous functions. Muscles controlling eye movement and the pelvic floor are the only skeletal musculature left unaffected. However, in a minority of cases (5-10%), patients also develop frontotemporal lobar dementia (FTLD). It has been suggested that a greater percentage

of patients experience some cognitive change (such as loss in executive function) without crossing the threshold required for a diagnosis of dementia (8).

Clinical presentation varies but most commonly consists of weakness, fasciculations (twitching muscles), and/or hyperreflexivity of facial muscles (bulbar onset) or limbs (spinal onset). Interestingly, initial symptoms usually appear at a focal site and later spread along contiguous anatomic paths (9). Diagnosis is achieved by a combination of clinical examination and electromyography (EMG), in which positive sharp waves and fibrillation potentials provide evidence for active denervation. The El Escorial criteria were developed in 1990 and are still utilized to diagnose and classify ALS cases as "possible," "probable," or "definite" (10) (Figure 1.1). Guidelines on implementation of the El Escorial criteria have been revised to place greater emphasis on electrophysiological abnormalities, which can be detected earlier and thus facilitate timely diagnosis (11).

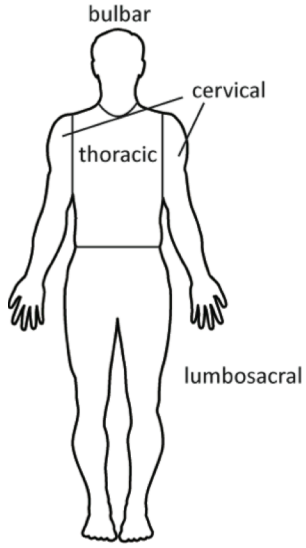

	Clinical presentation
Definite ALS	UMN and LMN signs in three regions (pictured left)
Probable ALS	UMN and LMN signs in two regions ***AND*** some UMN signs must be rostral to (above) LMN signs
Possible ALS	UMN and LMN signs in one region ***OR*** UMN signs alone in two or more regions ***OR*** UMN signs alone in two regions
Suspected ALS	LMN signs alone in two or more regions
All	Signs of degeneration spread within or between regions ***AND*** Lack of electrophysiological or neuroimaging evidence for other disorders which would explain observed degeneration

UMN signs: spasticity, hyperreflexivity *LMN signs: weakness, atrophy, fasciculation*

Figure 1.1. El Escorial criteria for diagnosis of ALS. UMN = upper motor neuron; LMN = lower motor neuron.

Etiology of ALS

The majority of ALS cases (≈ 82%) are sporadic (SALS) (9), having no apparent heritability. Up to 5% of SALS cases are caused by mutations in the 43 kDa trans-activating response region DNA-binding protein (TDP-43). TDP-43 mutations have also been linked to ≈ 3% of inherited, or "familial" ALS (FALS) (12). The most commonly-occurring mutations in FALS patients are found in the gene for Cu, Zn superoxide dismutase (SOD1) and account for approximately 20% of all FALS (13, 14). Most of these mutations are missense mutations that cause autosomal dominant ALS, except the D90A polymorphism, which can also behave as a recessive mutation (15). FALS-causative mutations have also been found in genetic loci corresponding to alsin, a guanine exchange factor for Rac1 that plays a role in cytoskeletal dynamics (16, 17); senataxin, a DNA/RNA helicase that may be involved in RNA processing (18, 19); vesicle-associated membrane protein-associated protein B (VAPB), which facilitates intracellular vesicular trafficking (20); and angiogenin (21-23) (Table 1.1). Some polymorphisms found in ALS patients do not segregate completely with disease and may represent genetic risk factors rather than causative mutations.

	Locus	Chromosome	Gene	Characteristics
CLASSICAL ALS:	ALS1	12q22.1	superoxide dismutase 1 (SOD1)	AD, adult onset
	ALS2	2q33	alsin	AR, juvenile onset
	ALS3	18q21	unknown	AD, adult onset
	ALS4	9q34	senataxin (SETX)	AD, juvenile onset
	ALS5	15q15.1-21.1	unknown	AR, juvenile onset
	ALS6	16q12.1-12.2	fused in sarcoma (FUS)	AD, adult onset
	ALS7	20p13	unknown	AD, adult onset
	ALS8	20q13.33	vesicle-associated membrane protein-associated protein B (VAPB)	AD, adult onset
	ALS9	14q11	angiogenin (ANG)	AD, adult onset
	ALS10	1p36	Tar DNA-binding protein (TARDBP)	AD, adult onset
	ALSX	X	unknown	XD, adult onset
ATYPICAL ALS:	ALS/ FTLD	9q21-22 9p13.3-21.3	unknown	AD, adult onset
	ALS-PDC	17q21.1	membrane-associated protein tau (MAPT)	AD, adult onset

AD = autosomal dominant; AR = autosomal recessive; XD = X-linked dominant; FTLD = frontotemporal lobar dementia; PDC = Parkinsonism-dementia complex
Updated references for each locus at the ALS Online Genetics Database (http://alsod.iop.kcl.ac.uk)

Table 1.1. Genetic loci associated with ALS

Mutations in the neurofilament-heavy subunit (24, 25), vascular endothelial growth factor (VEGF) (26) and ciliary neurotrophic factor (CNTF) (27, 28) fall under this category. All genetic loci that have been reported as putative modifiers of ALS susceptibility are listed in the ALS Online Genetics Database (http://alsod.iop.kcl.ac.uk).

There is evidence to suggest that specific environmental factors play a prominent role in the etiology of some ALS cases. Geographically-limited populations with dramatically increased ALS incidence, such as inhabitants of the Kii peninsula in Japan (29), the Chamorro people of Guam, Gulf War veterans (30, 31), and Italian soccer players (32), certainly lead one to suspect the environment as a potential modifier of disease susceptibility. There also have been reports of ALS in individuals with intense exposure to particular stressors, such as harsh chemicals and heavy metals (33, 34), viral infection (35), electrical shock (36) and traumatic nerve injury (37). Most of these reports, however, involve a very small number of cases and do not permit rigorous evaluation of these stressors as potential risk factors for ALS.

SOD1-related pathology as a general model for ALS

The discovery of SOD1's role in FALS (14) offered the first insight into the molecular mechanisms of ALS and the study of SOD1-mediated pathology has contributed much to our current understanding of the disease. The majority of *in vivo* work has utilized transgenic mice expressing FALS mutants of human SOD, which develop a progressive motor neuron syndrome reminiscent of the human ALS phenotype (reviewed in (38)). The sporadic disease differs little clinically from SOD1-related FALS, leading to the widespread supposition that all cases of ALS share some common mechanism(s) of pathology (2, 39, 40).

Misfolding and aggregation is the most likely source of SOD1 toxicity

SOD1 is a ubiquitous cytosolic enzyme whose primary function is the dismutation of the superoxide radical ($O_2^{-}\bullet$) to a less oxidizing species (H_2O_2) via a bound Cu^{2+} ligand. Although this enzyme plays an important role as a cellular antioxidant, the ability of SOD1 mutants to selectively kill motor neurons is not linked to a loss of dismutase function. Not only do many FALS mutants retain enzymatic activity at or near wild type levels (41-43), SOD null mice do not exhibit neurodegeneration (44). Furthermore, the toxicity of SOD1 mutants cannot be rescued by co-expression of wild type SOD1 (45). This evidence has lead to widespread acceptance of the hypothesis that SOD1 mutants acquire a novel toxic property independent of their enzymatic function.

Despite over 15 years of research, the mode(s) by which SOD1 mutants selectively kill motor neurons has not been clearly delineated. However, a large body of evidence implicates a common propensity to misfold and aggregate as the primary toxic gain of function. Destabilization of the native fold is an attractive hypothesis for SOD1 mutant pathogenicity, offering a plausible explanation for the common disease outcome of over 140 mutants spanning the sequence and structure. Early *in silico* studies by our laboratory predicted that a majority of SOD1 mutations would destabilize the native fold or quaternary structure (46), a trend that since has been verified experimentally (47-50). Especially severe destabilization caused by certain mutations could account for their inherently higher aggressiveness (short disease duration) (51, 52). Indeed, several recent analyses of *in vitro* SOD1 mutant behavior and FALS patient survival showed that protein instability and increased aggregation rate correlated with decreased survival time (53, 54). Furthermore, the presence of SOD1-immunoreactive proteinaceous aggregates in SALS patient motor neurons (55-58) suggests that aberrant oligomerization of SOD1 could be a

common feature of ALS, regardless of genotype. It thus appears that ALS is a protein conformational disorder, akin to other neurodegenerative diseases such as Alzheimer's, Parkinson's and Huntington's (2).

Though a primary role for SOD1 aggregation in FALS seems likely, deconstruction of the molecular determinants and mechanisms of this process is incomplete. SOD1 is an extremely stable enzyme in its fully mature, homodimeric form, remaining active in the presence of 6 M guanidinium or 8 M urea (59, 60). SOD1 owes its extraordinary stability largely to the coordination of Zn^{2+}, which constrains the relatively unstructured electrostatic and zinc-binding loops, "tethering" them together and protecting the protein core, an eight-stranded Greek key β-barrel (47, 61, 62) (Figure 1.2). The catalytic copper ligand and an intrasubunit disulfide bridge between Cys-57 and Cys-146 appear to contribute relatively little to monomer thermodynamic stability, but the latter modification constrains loop mobility and facilitates dimer formation (59, 61, 63). Metal-bound, disulfide-oxidized SOD1 forms an exceptionally stable homodimer, with low nanomolar binding affinity (64, 65). These maturation events are mutually interdependent—metal binding promotes disulfide bond formation, disulfide bond formation and metal binding promote dimerization, and dimeric SOD1 is more resistant to disulfide reduction/metal loss (61, 64, 66).

In vitro studies show that dimer dissociation is a necessary initiating step in SOD1 aggregation (65, 67). The resultant monomeric SOD1 is more susceptible to the loss of the stabilizing zinc ligand and disulfide bridge (68, 69), leading to freer loop movement (70) and exposure of β-barrel edge strands (61, 71). Dynamical studies of wild type and FALS mutant SOD1 revealed a transient "excited state" whose population is enhanced by mutations and zinc loss, but unaffected by disulfide status (72). Increased surface hydrophobicity of metal-free,

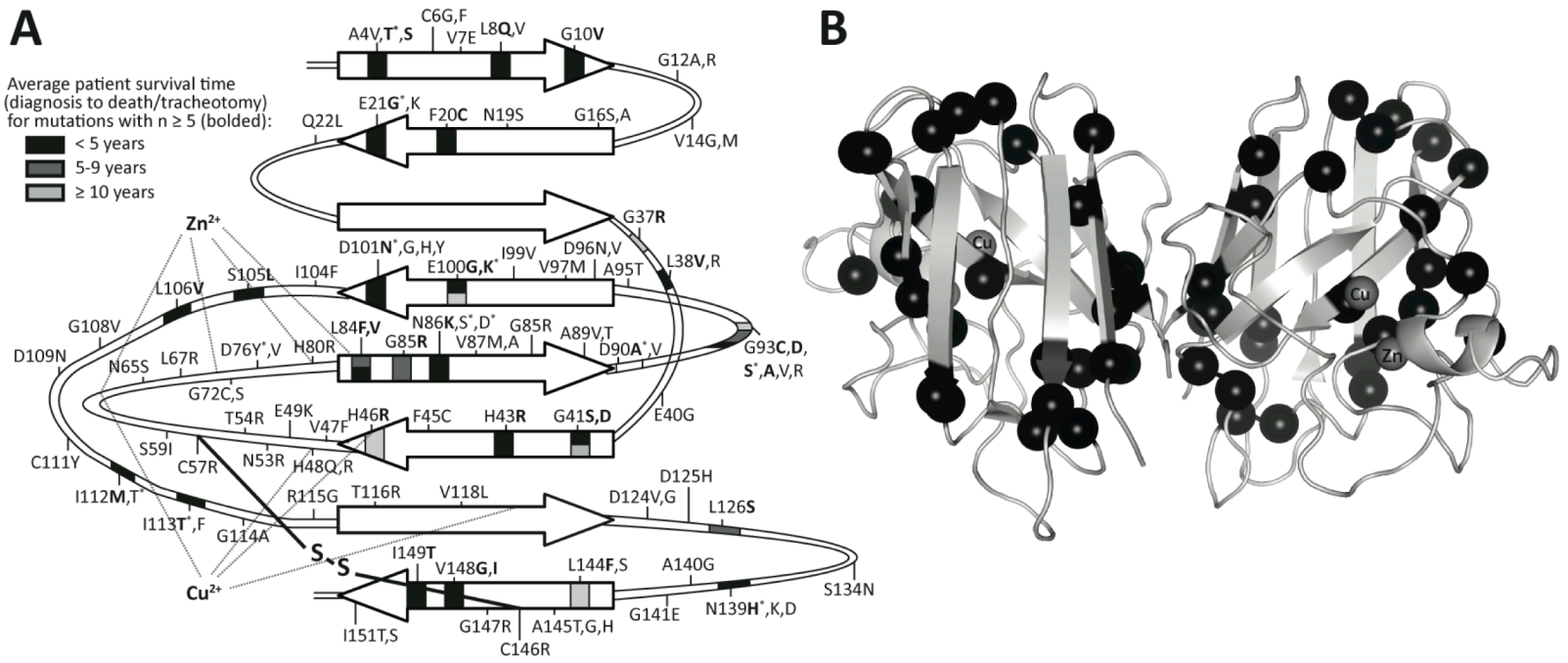

Figure 1.2. Location of FALS-causative mutations on the SOD1 structure. (A) Map of SOD1 secondary structure showing locations of FALS missense mutations, residues that coordinate Cu^{2+} (His-46, His-48, His-120, His-63) and Zn^{2+} (His-63, His-71, His-80, and Asp-83) ligands and the intramolecular disulfide bridge. Arrows indicate β-strands. Epidemiological data was taken from (39, 54, 108-111); mutations with survival data for at least five patients are bolded and the residue position is colored to indicate the corresponding average survival time. For positions with more than one n ≥ 5 mutation, the upper color corresponds to the first mutation listed. (B) Crystal structure (PDB code 1spd) of fully mature (metal-bound, disulfide-intact) homodimeric SOD1 with positions of aggressive (survival time < 5 years) mutations indicated by black spheres.

disulfide reduced mutant SOD1 was shown directly by Tiwari *et al.* using 1-anilinonaphthalene-8-sulfonic acid (ANS), a fluorescent dye that binds to hydrophobic surfaces (73). Munch *et al.* obtained similar results using a different hydrophobic dye, Sypro Orange, and found that increased exposure of hydrophobic regions promotes aggregation (74). A general model of SOD1 aggregation in ALS has emerged in which dimer dissociation and subsequent metal loss (and/or disulfide reduction) induce structural distortions that favor assembly into non-native oligomers (oligomers other than the native homodimer) (Figure 1.3). FALS mutations promote aggregation by increasing the tendency of SOD1 to lose its stabilizing post-translational modifications and/or by decreasing the intrinsic stability of the apo-monomer (46, 48-50, 61, 75-77). Substantial gaps remain in our understanding of the relation between SOD1 aggregation and ALS pathology. These include aggregate structure, mechanism of formation and toxicity.

SOD1 aggregate structure

No high-resolution structural information is available for misfolded monomeric SOD1 or non-native oligomers. The transient nature of many structurally-perturbed SOD1 species makes

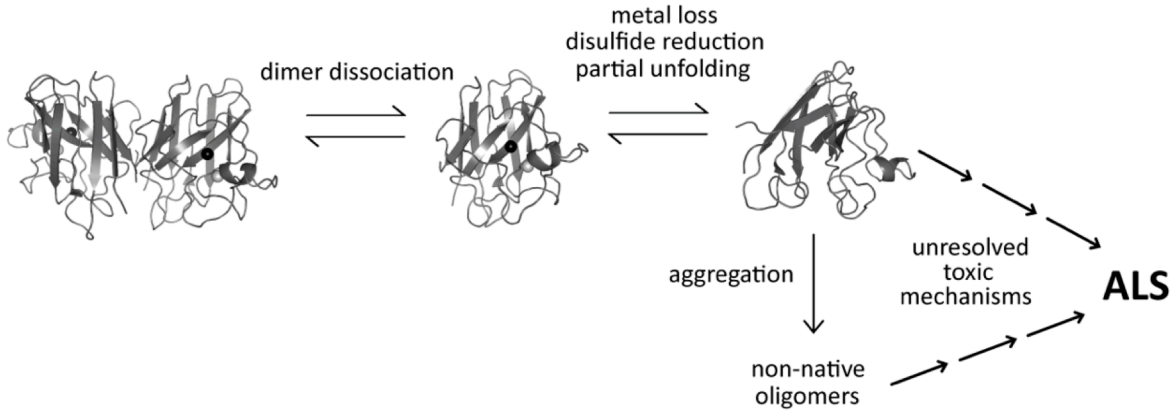

Figure 1.3. General mechanism of SOD1 aggregation.

their isolation for study impractical. However, misfolded dimeric or monomeric SOD1 can be detected using an antibody specific for residues 145-151, which are normally buried within the native dimer interface (78). SOD1 monomers with a more substantially disrupted fold can be tracked using an antibody recognizing the natively-buried residues of β-strand 4 (residues 42-48) (79). Chromatographic methods have also been utilized to isolate misfolded SOD1 using their affinity to hydrophobic resins (80). Continued study using these and similar methods will be useful in tracking the spatial and temporal distribution of misfolded SOD1 in cell culture, transgenic mouse models, and ALS patients, providing insight into the molecular determinants and cellular consequences of SOD1 destabilization.

Electron microscopic, immunohistological, and biochemical studies have shed some light on the structural properties of SOD1 aggregates. Both insoluble, detergent-resistant aggregates and soluble oligomers have been noted in cell culture, transgenic mice and *in vitro* (56, 57, 81-83). These species contain metal-free SOD1 that is full-length and usually lacks the native disulfide bridge (84). Aggregates formed *in vitro* under near-physiological conditions are often fibrillar and bind thioflavin T (ThT^+, suggestive of amyloid character) (75, 85-87), while *in vivo* aggregates sometime appear amorphous or pore-shaped and do not always bind amyloid-sensitive dyes (79, 82, 88-90). Soluble misfolded SOD1 populates a wide range of oligomeric states and also accumulates as non-native monomers, dimers or trimers (55, 80, 85). The instability of some soluble oligomers may preclude the use of static structural techniques, such as x-ray crystallography, to determine structural details, but solution-state methods such as nuclear magnetic resonance (NMR) or limited proteolysis, especially coupled with computational structural modeling, may yield insights into their conformations.

Mechanism of SOD1 aggregation

The likelihood that misfolded SOD1 samples a multitude of conformational and energetic states also complicates detailed mechanistic study of oligomer formation. However, it is clear that post-translational modifications of the SOD1 polypeptide modulate oligomer formation to some extent. As discussed above, the native intramolecular disulfide bridge and metal binding both impart exceptional stability to SOD1 and, unsurprisingly, loss of these factors drives misfolding and aggregation. However, reduction of the native Cys57-Cys146 disulfide has been putatively linked to the initiation, but not elongation, of amyloid-like fibril formation *in vitro* (75, 86). Fully mature, but metal-free, SOD1 incubated at physiological pH and temperature can be induced to aggregate by disrupting noncovalent interactions with a chaotrope, but treatment with a reducing agent instead results in a 20-fold shorter lag period (86). Disulfide bond reduction, while apparently dispensible for fibril formation *in vitro*, may specifically accelerate nucleation. Indeed, the presence of a small amount of disulfide-reduced wild type or mutant SOD1 appeared to "recruit" disulfide-intact wild type SOD1 into fibrils without need for additional reducing agent (86). The mechanism by which disulfide-reduced SOD1 facilitates fibril nucleation has not yet been demonstrated, although the requirement of cysteines 57 and 146 suggest that intermolecular cross-linking between these two residues may play a role (86). It is also unclear whether *in vivo* SOD1 aggregation, which is not always amyloid-like, proceeds by elongation of nuclei.

The two free cysteines in SOD1, at positions 6 and 111, also appear to be involved in SOD1 oligomer assembly. *In vitro* aggregation of metal-free wild type SOD1 coincides with a loss of free cysteines and oligomer formation is ablated by mutations at either or both sites (85, 91), leading to the hypothesis that intermolecular disulfide cross-linking mediates

oligomerization. However, more recent studies in mutant SOD1 transgenic mice show that aberrant disulfide linkages are present only in large-scale aggregates appearing late in the disease (92, 93). A secondary role for intermolecular disulfide cross-linking in aggregation is unsurprising given the reducing environment of the cytosol and may be due to kinetic "trapping" of SOD1 in a misfolded state after an initial destabilizing trigger, such as Zn^{2+} loss or altered conformational dynamics resulting from mutation (76, 77). Cell culture experiments reveal a key role for Cys-111 in the promotion of SOD1 oligomerization, as mutation of this residue, but not Cys-6, attenuated oligomer formation and protected cells from mutant SOD1-mediated toxicity (94).

An emerging question in the study of mutant-mediated SOD1 aggregation is the extent of involvement of wild type protein. Since most FALS patients with SOD1 mutations are heterozygous, recent studies have utilized transgenic mice expressing both human wild type and FALS mutant protein to more accurately recapitulate SOD1 behavior *in vivo*. Co-expression of $SOD1^{WT}$ exacerbates the disease phenotypes of $SOD1^{G93A}$ (95, 96), $SOD1^{G85R}$ (97), $SOD1^{L126Z}$ and $SOD1^{A4V}$ mice (81), hastening the appearance of cellular pathologies and shortening survival times. The effect of the wild type protein on $SOD1^{A4V}$ mice is particularly dramatic; even though FALS patients with this mutation exhibit particularly rapid disease progression, mice expressing only $SOD1^{A4V}$ do not develop motor neuron disease within their lifetimes (42). The toxic effect of co-expressing wild type protein may be a simple issue of protein copy number. An earlier study of G85R mice (45) did not find any effect of human wild type co-expression on survival, but both $SOD1^{G85R}$ and $SOD1^{WT}$ were expressed at lower levels than in the more recent model (97). The observation that mutant SOD1 toxicity depends heavily on protein abundance, while not surprising, is troubling since nearly all mutant SOD1 transgenic mice dramatically

overexpress the protein (38). However, mice overexpressing $SOD1^{WT}$ alone, while exhibiting minor deficits in motor function, do not experience paralysis or die prematurely (96). Thus, FALS mutants clearly possess intrinsic pathogenicity independent of gene dosage. Mutant-wild type heterodimers and disulfide-linked aggregates containing both wild-type and mutant SOD1 have been observed (81, 97), suggesting that wild type SOD1 is "recruited" into non-native oligomers by pathogenic mutants, possibly under conditions of oxidative stress. These studies present an incomplete picture of the role of $SOD1^{WT}$ in aggregation but highlight the need for further scrutiny of the physiological relevance of commonly-used transgenic mouse models.

Toxicity of SOD1 aggregates

While misfolding and aggregation has been convincingly linked to ALS pathogenesis, the species responsible for motor neuron death has not been identified. Insoluble inclusion bodies appear in brain stem and spinal cord coincident with symptom onset and accumulate progressively in the terminal stages (98-102), leading to an initial belief that large-scale aggregates are themselves toxic. However, the ability to detect soluble misfolded SOD1 led to the discovery that these non-native forms are present from birth (80, 103) and selectively enriched in motor neurons (78, 80) of FALS transgenic mice. It thus appears that small misfolded SOD1 may be the actual toxic culprit(s), present throughout life but causing symptoms only when cells can no longer keep their deleterious effects in check. In such a scenario, assembly of soluble misfolded SOD1 into relatively inert inclusions is expected to be neuroprotective, a phenomenon that has been demonstrated for aggregation of Aβ and huntingtin in Alzheimer's and Huntington's diseases, respectively (104-106). However, the relative

toxicities of small soluble oligomers and large-scale aggregates of SOD1 remain to be directly proven. Similarly, no consensus has yet been reached on the mode(s) by which non-native SOD1 kills cells. The evidence at present, though sometimes contradictory, identifies a diverse set of targeted organelles, signaling pathways, and other cellular processes (107). On a subcellular level, ALS pathology is staggeringly complex and includes abnormalities in nearly all cellular compartments (Figure 1.4). Many of these are undoubtedly secondary effects or compensatory mechanisms for an initial dysfunctional "trigger," the identification of which has remained elusive despite nearly 20 years of research on the molecular bases of ALS.

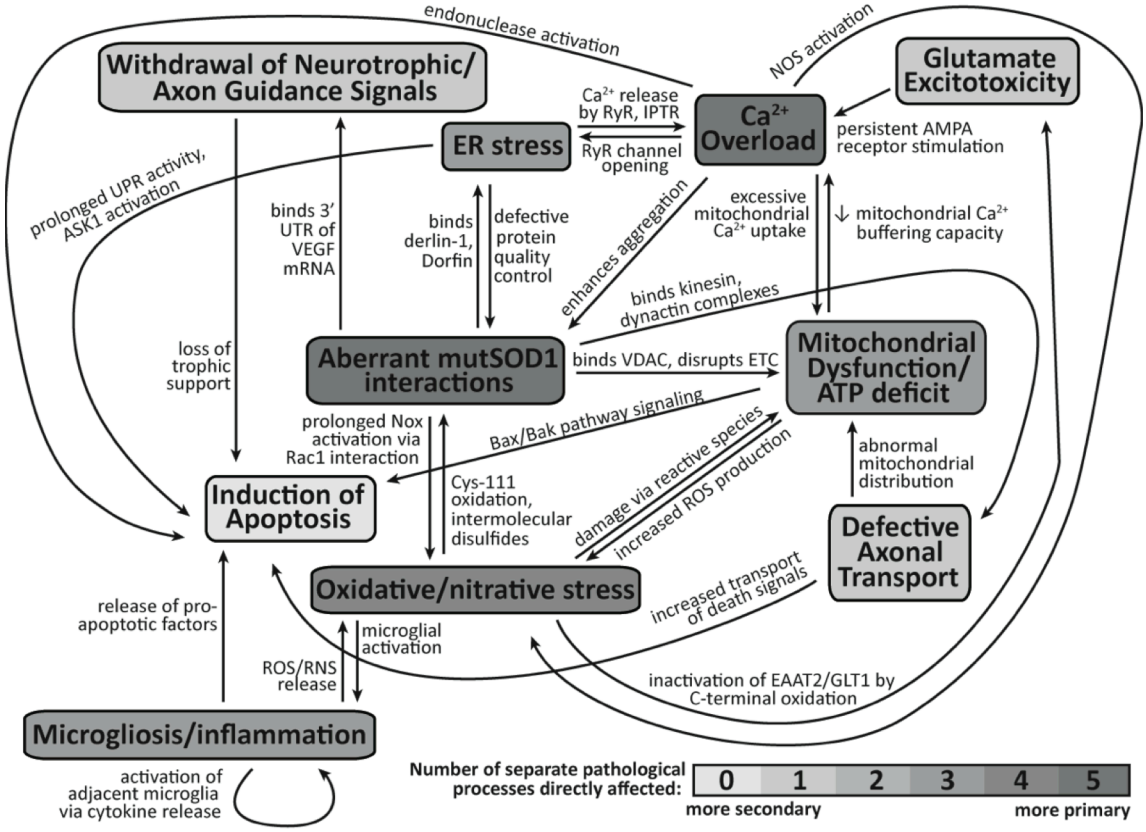

Figure 1.4. Diverse pathological processes in SOD1-related FALS are highly interrelated and many stem directly from SOD1 misfolding/aggregation and cytosolic calcium overload. mutSOD1 = mutant SOD1; UTR = untranslated region; VDAC = voltage-dependent anion channel; ETC = electron transport chain; UPR = unfolded protein response; ROS/RNS = reactive oxygen/nitrogen species.

REFERENCES

1. Goetz, C. G. (2000) Amyotrophic lateral sclerosis: early contributions of Jean-Martin Charcot. Muscle Nerve. 23, 336.

2. Bruijn, L. I., Miller, T. M. and Cleveland, D. W. (2004) Unraveling the mechanisms involved in motor neuron degeneration in ALS. Annu.Rev.Neurosci. 27, 723.

3. Cleveland, D. W. and Rothstein, J. D. (2001) From Charcot to Lou Gehrig: deciphering selective motor neuron death in ALS. Nat.Rev Neurosci. 2, 806.

4. Rothstein, J. D. (2009) Current hypotheses for the underlying biology of amyotrophic lateral sclerosis. Ann.Neurol. 65 Suppl 1, S3.

5. Chou, S. M. and Norris, F. H. (1993) Amyotrophic lateral sclerosis: lower motor neuron disease spreading to upper motor neurons. Muscle Nerve. 16, 864.

6. Eisen, A. and Weber, M. (2001) The motor cortex and amyotrophic lateral sclerosis. Muscle Nerve. 24, 564.

7. Mochizuki, Y., Mizutani, T. and Takasu, T. (1995) Amyotrophic lateral sclerosis with marked neurological asymmetry: clinicopathological study. Acta Neuropathol. 90, 44.

8. Lomen-Hoerth, C., Anderson, T. and Miller, B. (2002) The overlap of amyotrophic lateral sclerosis and frontotemporal dementia. Neurology. 59, 1077.

9. Ravits, J. M. and La Spada, A. R. (2009) ALS motor phenotype heterogeneity, focality, and spread: deconstructing motor neuron degeneration. Neurology. 73, 805.

10. Brooks, B. R. (1994) El Escorial World Federation of Neurology criteria for the diagnosis of amyotrophic lateral sclerosis. Subcommittee on Motor Neuron Diseases/Amyotrophic Lateral Sclerosis of the World Federation of Neurology Research Group on Neuromuscular Diseases and the El Escorial "Clinical limits of amyotrophic lateral sclerosis" workshop contributors. J Neurol Sci. 124 Suppl, 96-107.

11. de Carvalho, M., Dengler, R., Eisen, A., England, J. D., Kaji, R., Kimura, J., Mills, K., Mitsumoto, H., Nodera, H., Shefner, J. and Swash, M. (2008) Electrodiagnostic criteria for diagnosis of ALS. Clin Neurophysiol. 119, 497-503.

12. Beleza-Meireles, A. and Al-Chalabi, A. (2009) Genetic studies of amyotrophic lateral sclerosis: controversies and perspectives. Amyotroph.Lateral.Scler. 10, 1.

13. Deng, H. X., Hentati, A., Tainer, J. A., Iqbal, Z., Cayabyab, A., Hung, W. Y., Getzoff, E. D., Hu, P., Herzfeldt, B. and Roos, R. P. (1993) Amyotrophic lateral sclerosis and structural defects in Cu,Zn superoxide dismutase. Science. 261, 1047.

14. Rosen, D. R., Siddique, T., Patterson, D., Figlewicz, D. A., Sapp, P., Hentati, A., Donaldson, D., Goto, J., O'Regan, J. P. and Deng, H. X. (1993) Mutations in Cu/Zn superoxide dismutase gene are associated with familial amyotrophic lateral sclerosis. Nature. 362, 59.

15. Al-Chalabi, A., Andersen, P. M., Chioza, B., Shaw, C., Sham, P. C., Robberecht, W., Matthijs, G., Camu, W., Marklund, S. L., Forsgren, L., Rouleau, G., Laing, N. G., Hurse, P. V., Siddique, T., Leigh, P. N. and Powell, J. F. (1998) Recessive amyotrophic lateral sclerosis families with the D90A SOD1 mutation share a common founder: evidence for a linked protective factor. Hum.Mol.Genet. 7, 2045.

16. Hadano, S., Hand, C. K., Osuga, H., Yanagisawa, Y., Otomo, A., Devon, R. S., Miyamoto, N., Showguchi-Miyata, J., Okada, Y., Singaraja, R., Figlewicz, D. A., Kwiatkowski, T., Hosler, B. A., Sagie, T., Skaug, J., Nasir, J., Brown, R. H., Jr., Scherer, S. W., Rouleau, G. A., Hayden, M. R. and Ikeda, J. E. (2001) A gene encoding a putative GTPase regulator is mutated in familial amyotrophic lateral sclerosis. Nat.Genet. 29, 166.

17. Yang, Y., Hentati, A., Deng, H. X., Dabbagh, O., Sasaki, T., Hirano, M., Hung, W. Y., Ouahchi, K., Yan, J., Azim, A. C., Cole, N., Gascon, G., Yagmour, A., Ben-Hamida, M., Pericak-Vance, M., Hentati, F. and Siddique, T. (2001) The gene encoding alsin, a protein with three guanine-nucleotide exchange factor domains, is mutated in a form of recessive amyotrophic lateral sclerosis. Nat.Genet. 29, 160.

18. Chance, P. F., Rabin, B. A., Ryan, S. G., Ding, Y., Scavina, M., Crain, B., Griffin, J. W. and Cornblath, D. R. (1998) Linkage of the gene for an autosomal dominant form of juvenile amyotrophic lateral sclerosis to chromosome 9q34. Am.J.Hum.Genet. 62, 633.

19. Chen, Y. Z., Bennett, C. L., Huynh, H. M., Blair, I. P., Puls, I., Irobi, J., Dierick, I., Abel, A., Kennerson, M. L., Rabin, B. A., Nicholson, G. A., Auer-Grumbach, M., Wagner, K., De, J. P., Griffin, J. W., Fischbeck, K. H., Timmerman, V., Cornblath, D. R. and Chance, P. F. (2004) DNA/RNA helicase gene mutations in a form of juvenile amyotrophic lateral sclerosis (ALS4). Am.J.Hum.Genet. 74, 1128.

20. Nishimura, A. L., Mitne-Neto, M., Silva, H. C., Richieri-Costa, A., Middleton, S., Cascio, D., Kok, F., Oliveira, J. R., Gillingwater, T., Webb, J., Skehel, P. and Zatz, M. (2004) A mutation in the vesicle-trafficking protein VAPB causes late-onset spinal muscular atrophy and amyotrophic lateral sclerosis. Am.J.Hum.Genet. 75, 822.

21. Greenway, M. J., Alexander, M. D., Ennis, S., Traynor, B. J., Corr, B., Frost, E., Green, A. and Hardiman, O. (2004) A novel candidate region for ALS on chromosome 14q11.2. Neurology. 63, 1936.

22. Greenway, M. J., Andersen, P. M., Russ, C., Ennis, S., Cashman, S., Donaghy, C., Patterson, V., Swingler, R., Kieran, D., Prehn, J., Morrison, K. E., Green, A., Acharya, K. R., Brown, R. H., Jr. and Hardiman, O. (2006) ANG mutations segregate with familial and 'sporadic' amyotrophic lateral sclerosis. Nat.Genet. 38, 411.

23. Wu, D., Yu, W., Kishikawa, H., Folkerth, R. D., Iafrate, A. J., Shen, Y., Xin, W., Sims, K. and Hu, G. F. (2007) Angiogenin loss-of-function mutations in amyotrophic lateral sclerosis. Ann.Neurol. 62, 609.

24. Al-Chalabi, A., Andersen, P. M., Nilsson, P., Chioza, B., Andersson, J. L., Russ, C., Shaw, C. E., Powell, J. F. and Leigh, P. N. (1999) Deletions of the heavy neurofilament subunit tail in amyotrophic lateral sclerosis. Hum.Mol.Genet. **8**, 157.

25. Figlewicz, D. A., Krizus, A., Martinoli, M. G., Meininger, V., Dib, M., Rouleau, G. A. and Julien, J. P. (1994) Variants of the heavy neurofilament subunit are associated with the development of amyotrophic lateral sclerosis. Hum.Mol.Genet. **3**, 1757.

26. Lambrechts, D., Storkebaum, E., Morimoto, M., Del-Favero, J., Desmet, F., Marklund, S. L., Wyns, S., Thijs, V., Andersson, J., van, M. I., Al-Chalabi, A., Bornes, S., Musson, R., Hansen, V., Beckman, L., Adolfsson, R., Pall, H. S., Prats, H., Vermeire, S., Rutgeerts, P., Katayama, S., Awata, T., Leigh, N., Lang-Lazdunski, L., Dewerchin, M., Shaw, C., Moons, L., Vlietinck, R., Morrison, K. E., Robberecht, W., Van, B. C., Collen, D., Andersen, P. M. and Carmeliet, P. (2003) VEGF is a modifier of amyotrophic lateral sclerosis in mice and humans and protects motoneurons against ischemic death. Nat.Genet. **34**, 383.

27. Al-Chalabi, A., Scheffler, M. D., Smith, B. N., Parton, M. J., Cudkowicz, M. E., Andersen, P. M., Hayden, D. L., Hansen, V. K., Turner, M. R., Shaw, C. E., Leigh, P. N. and Brown, R. H., Jr. (2003) Ciliary neurotrophic factor genotype does not influence clinical phenotype in amyotrophic lateral sclerosis. Ann.Neurol. **54**, 130.

28. Giess, R., Goetz, R., Schrank, B., Ochs, G., Sendtner, M. and Toyka, K. (1998) Potential implications of a ciliary neurotrophic factor gene mutation in a German population of patients with motor neuron disease. Muscle Nerve. **21**, 236.

29. Kokubo, Y., Kuzuhara, S. and Narita, Y. (2000) Geographical distribution of amyotrophic lateral sclerosis with neurofibrillary tangles in the Kii Peninsula of Japan. J Neurol. 247, 850-852.

30. Haley, R. W. (2003) Excess incidence of ALS in young Gulf War veterans. Neurology. 61, 750.

31. Horner, R. D., Kamins, K. G., Feussner, J. R., Grambow, S. C., Hoff-Lindquist, J., Harati, Y., Mitsumoto, H., Pascuzzi, R., Spencer, P. S., Tim, R., Howard, D., Smith, T. C., Ryan, M. A., Coffman, C. J. and Kasarskis, E. J. (2003) Occurrence of amyotrophic lateral sclerosis among Gulf War veterans. Neurology. 61, 742.

32. Chio, A., Benzi, G., Dossena, M., Mutani, R. and Mora, G. (2005) Severely increased risk of amyotrophic lateral sclerosis among Italian professional football players. Brain. 128, 472.

33. Sutedja, N. A., Fischer, K., Veldink, J. H., Van Der Heijden, G. J., Kromhout, H., Heederik, D., Huisman, M. H., Wokke, J. J. and Van den Berg, L. H. (2009) What we truly know about occupation as a risk factor for ALS: A critical and systematic review. Amyotroph.Lateral.Scler., 10, 295.

34. Sutedja, N. A., Veldink, J. H., Fischer, K., Kromhout, H., Heederik, D., Huisman, M. H., Wokke, J. H. and Van den Berg, L. H. (2009) Exposure to chemicals and metals and risk of amyotrophic lateral sclerosis: A systematic review. Amyotroph.Lateral.Scler., 10, 302.

35. Mattson, M. P. (2004) Infectious agents and age-related neurodegenerative disorders. Ageing Res.Rev. 3, 105.

36. Jafari, H., Couratier, P. and Camu, W. (2001) Motor neuron disease after electric injury. J.Neurol.Neurosurg.Psychiatry. 71, 265.

37. Kurtzke, J. F. (1991) Risk factors in amyotrophic lateral sclerosis. Adv.Neurol. 56, 245.

38. Turner, B. J. and Talbot, K. (2008) Transgenics, toxicity and therapeutics in rodent models of mutant SOD1-mediated familial ALS. Prog.Neurobiol. 85, 94.

39. Andersen, P. M., Nilsson, P., Keranen, M. L., Forsgren, L., Hagglund, J., Karlsborg, M., Ronnevi, L. O., Gredal, O. and Marklund, S. L. (1997) Phenotypic heterogeneity in motor neuron disease patients with CuZn-superoxide dismutase mutations in Scandinavia. Brain. 120 (Pt 10), 1723.

40. Hand, C. K., Khoris, J., Salachas, F., Gros-Louis, F., Lopes, A. A., Mayeux-Portas, V., Brewer, C. G., Brown, R. H., Jr., Meininger, V., Camu, W. and Rouleau, G. A. (2002) A novel locus for familial amyotrophic lateral sclerosis, on chromosome 18q. Am.J.Hum.Genet. 70, 251.

41. Bruijn, L. I., Becher, M. W., Lee, M. K., Anderson, K. L., Jenkins, N. A., Copeland, N. G., Sisodia, S. S., Rothstein, J. D., Borchelt, D. R., Price, D. L. and Cleveland, D. W. (1997) ALS-linked SOD1 mutant G85R mediates damage to astrocytes and promotes rapidly progressive disease with SOD1-containing inclusions. Neuron. 18, 327.

42. Gurney, M. E., Pu, H., Chiu, A. Y., Dal Canto, M. C., Polchow, C. Y., Alexander, D. D., Caliendo, J., Hentati, A., Kwon, Y. W. and Deng, H. X. (1994) Motor neuron degeneration in mice that express a human Cu,Zn superoxide dismutase mutation. Science. 264, 1772.

43. Wong, P. C., Pardo, C. A., Borchelt, D. R., Lee, M. K., Copeland, N. G., Jenkins, N. A., Sisodia, S. S., Cleveland, D. W. and Price, D. L. (1995) An adverse property of a familial ALS-linked SOD1 mutation causes motor neuron disease characterized by vacuolar degeneration of mitochondria. Neuron. 14, 1105.

44. Reaume, A. G., Elliott, J. L., Hoffman, E. K., Kowall, N. W., Ferrante, R. J., Siwek, D. F., Wilcox, H. M., Flood, D. G., Beal, M. F., Brown, R. H., Jr., Scott, R. W. and Snider, W. D. (1996) Motor neurons in Cu/Zn superoxide dismutase-deficient mice develop normally but exhibit enhanced cell death after axonal injury. Nat.Genet. 13, 43.

45. Bruijn, L. I., Houseweart, M. K., Kato, S., Anderson, K. L., Anderson, S. D., Ohama, E., Reaume, A. G., Scott, R. W. and Cleveland, D. W. (1998) Aggregation and motor neuron toxicity of an ALS-linked SOD1 mutant independent from wild-type SOD1. Science. 281, 1851.

46. Khare, S. D., Caplow, M. and Dokholyan, N. V. (2006) FALS mutations in Cu, Zn superoxide dismutase destabilize the dimer and increase dimer dissociation propensity: a large-scale thermodynamic analysis. Amyloid. 13, 226.

47. Furukawa, Y. and O'Halloran, T. V. (2005) Amyotrophic lateral sclerosis mutations have the greatest destabilizing effect on the apo- and reduced form of SOD1, leading to unfolding and oxidative aggregation. J.Biol.Chem. 280, 17266.

48. Hough, M. A., Grossmann, J. G., Antonyuk, S. V., Strange, R. W., Doucette, P. A., Rodriguez, J. A., Whitson, L. J., Hart, P. J., Hayward, L. J., Valentine, J. S. and Hasnain, S. S. (2004) Dimer destabilization in superoxide dismutase may result in disease-causing properties: structures of motor neuron disease mutants. Proc Natl Acad Sci U S A. 101, 5976.

49. Rodriguez, J. A., Shaw, B. F., Durazo, A., Sohn, S. H., Doucette, P. A., Nersissian, A. M., Faull, K. F., Eggers, D. K., Tiwari, A., Hayward, L. J. and Valentine, J. S. (2005) Destabilization of apoprotein is insufficient to explain Cu,Zn-superoxide dismutase-linked ALS pathogenesis. Proc.Natl.Acad.Sci.U.S.A. 102, 10516.

50. Shaw, B. F. and Valentine, J. S. (2007) How do ALS-associated mutations in superoxide dismutase 1 promote aggregation of the protein? Trends Biochem Sci. 32, 78.

51. Radunovic, A. and Leigh, P. N. (1996) Cu/Zn superoxide dismutase gene mutations in amyotrophic lateral sclerosis: correlation between genotype and clinical features. J.Neurol.Neurosurg.Psychiatry. 61, 565.

52. Cudkowicz, M. E., McKenna-Yasek, D., Sapp, P. E., Chin, W., Geller, B., Hayden, D. L., Schoenfeld, D. A., Hosler, B. A., Horvitz, H. R. and Brown, R. H. (1997) Epidemiology of mutations in superoxide dismutase in amyotrophic lateral sclerosis. Ann.Neurol. 41, 210.

53. Bystrom, R., Andersen, P. M., Grobner, G. and Oliveberg, M. (2010) SOD1 mutations targeting surface hydrogen bonds promote amyotrophic lateral sclerosis without reducing apo-state stability. J.Biol.Chem. 285, 19544.

54. Wang, Q., Johnson, J. L., Agar, N. Y. and Agar, J. N. (2008) Protein aggregation and protein instability govern familial amyotrophic lateral sclerosis patient survival. PLoS Biol. 6, e170.

55. Gruzman, A., Wood, W. L., Alpert, E., Prasad, M. D., Miller, R. G., Rothstein, J. D., Bowser, R., Hamilton, R., Wood, T. D., Cleveland, D. W., Lingappa, V. R. and Liu, J. (2007) Common molecular signature in SOD1 for both sporadic and familial amyotrophic lateral sclerosis. Proc.Natl.Acad.Sci.U.S.A. 104, 12524.

56. Shibata, N., Asayama, K., Hirano, A. and Kobayashi, M. (1996) Immunohistochemical study on superoxide dismutases in spinal cords from autopsied patients with amyotrophic lateral sclerosis. Dev Neurosci. 18, 492.

57. Shibata, N., Hirano, A., Kobayashi, M., Sasaki, S., Kato, T., Matsumoto, S., Shiozawa, Z., Komori, T., Ikemoto, A. and Umahara, T. (1994) Cu/Zn superoxide dismutase-like immunoreactivity in Lewy body-like inclusions of sporadic amyotrophic lateral sclerosis. Neurosci.Lett. 179, 149.

58. Matsumoto, S., Kusaka, H., Ito, H., Shibata, N., Asayama, T. and Imai, T. (1996) Sporadic amyotrophic lateral sclerosis with dementia and Cu/Zn superoxide dismutase-positive Lewy body-like inclusions. Clin.Neuropathol. 15, 41.

59. Bartnikas, T. B. and Gitlin, J. D. (2003) Mechanisms of biosynthesis of mammalian copper/zinc superoxide dismutase. J.Biol.Chem. 278, 33602.

60. Forman, H. J. and Fridovich, I. (1973) On the stability of bovine superoxide dismutase. The effects of metals. J.Biol.Chem. 248, 2645.

61. Ding, F. and Dokholyan, N. V. (2008) Dynamical roles of metal ions and the disulfide bond in Cu, Zn superoxide dismutase folding and aggregation. Proc.Natl.Acad.Sci.U.S.A. 105, 19696.

62. Tiwari, A. and Hayward, L. J. (2005) Mutant SOD1 instability: implications for toxicity in amyotrophic lateral sclerosis. Neurodegener.Dis. 2, 115.

63. Banci, L., Bertini, I., Cantini, F., D'Onofrio, M. and Viezzoli, M. S. (2002) Structure and dynamics of copper-free SOD: The protein before binding copper. Protein Sci. 11, 2479.

64. Doucette, P. A., Whitson, L. J., Cao, X., Schirf, V., Demeler, B., Valentine, J. S., Hansen, J. C. and Hart, P. J. (2004) Dissociation of human copper-zinc superoxide dismutase dimers using chaotrope and reductant. Insights into the molecular basis for dimer stability. J Biol Chem. 279, 54558.

65. Khare, S. D., Caplow, M. and Dokholyan, N. V. (2004) The rate and equilibrium constants for a multistep reaction sequence for the aggregation of superoxide dismutase in amyotrophic lateral sclerosis. Proc Natl Acad Sci U S A. 101, 15094.

66. Arnesano, F., Banci, L., Bertini, I., Martinelli, M., Furukawa, Y. and O'Halloran, T. V. (2004) The unusually stable quaternary structure of human Cu,Zn-superoxide dismutase 1 is controlled by both metal occupancy and disulfide status. J.Biol.Chem. 279, 47998.

67. Rakhit, R., Crow, J. P., Lepock, J. R., Kondejewski, L. H., Cashman, N. R. and Chakrabartty, A. (2004) Monomeric Cu,Zn-superoxide dismutase is a common misfolding intermediate in the oxidation models of sporadic and familial amyotrophic lateral sclerosis. J Biol Chem. 279, 15499.

68. Lindberg, M. J., Normark, J., Holmgren, A. and Oliveberg, M. (2004) Folding of human superoxide dismutase: disulfide reduction prevents dimerization and produces marginally stable monomers. Proc.Natl.Acad.Sci.U.S.A. 101, 15893.

69. Ray, S. S., Nowak, R. J., Strokovich, K., Brown, R. H., Jr., Walz, T. and Lansbury, P. T., Jr. (2004) An intersubunit disulfide bond prevents in vitro aggregation of a superoxide dismutase-1 mutant linked to familial amytrophic lateral sclerosis. Biochemistry. 43, 4899.

70. Molnar, K. S., Karabacak, N. M., Johnson, J. L., Wang, Q., Tiwari, A., Hayward, L. J., Coales, S. J., Hamuro, Y. and Agar, J. N. (2009) A common property of amyotrophic

lateral sclerosis-associated variants: destabilization of the copper/zinc superoxide dismutase electrostatic loop. J.Biol.Chem. 284, 30965.

71. Durazo, A., Shaw, B. F., Chattopadhyay, M., Faull, K. F., Nersissian, A. M., Valentine, J. S. and Whitelegge, J. P. (2009) Metal-free superoxide dismutase-1 and three different amyotrophic lateral sclerosis variants share a similar partially unfolded beta-barrel at physiological temperature. J.Biol.Chem. 284, 34382.

72. Teilum, K., Smith, M. H., Schulz, E., Christensen, L. C., Solomentsev, G., Oliveberg, M. and Akke, M. (2009) Transient structural distortion of metal-free Cu/Zn superoxide dismutase triggers aberrant oligomerization. Proc Natl Acad Sci U S A. 106, 18273.

73. Tiwari, A., Liba, A., Sohn, S. H., Seetharaman, S. V., Bilsel, O., Matthews, C. R., Hart, P. J., Valentine, J. S. and Hayward, L. J. (2009) Metal deficiency increases aberrant hydrophobicity of mutant superoxide dismutases that cause amyotrophic lateral sclerosis. J.Biol.Chem. 284, 27746.

74. Munch, C. and Bertolotti, A. (2010) Exposure of hydrophobic surfaces initiates aggregation of diverse ALS-causing superoxide dismutase-1 mutants. J.Mol.Biol. 399, 512.

75. Furukawa, Y., Kaneko, K., Yamanaka, K., O'Halloran, T. V. and Nukina, N. (2008) Complete loss of post-translational modifications triggers fibrillar aggregation of SOD1 in the familial form of amyotrophic lateral sclerosis. J.Biol.Chem. 283, 24167.

76. Khare, S. D., Ding, F. and Dokholyan, N. V. (2003) Folding of Cu, Zn superoxide dismutase and familial amyotrophic lateral sclerosis. J.Mol.Biol. 334, 515.

77. Khare, S. D. and Dokholyan, N. V. (2006) Common dynamical signatures of familial amyotrophic lateral sclerosis-associated structurally diverse Cu, Zn superoxide dismutase mutants. Proc.Natl.Acad.Sci.U.S.A. 103, 3147.

78. Rakhit, R., Robertson, J., Vande, V. C., Horne, P., Ruth, D. M., Griffin, J., Cleveland, D. W., Cashman, N. R. and Chakrabartty, A. (2007) An immunological epitope selective for pathological monomer-misfolded SOD1 in ALS. Nat.Med. 13, 754.

79. Kerman, A., Liu, H. N., Croul, S., Bilbao, J., Rogaeva, E., Zinman, L., Robertson, J. and Chakrabartty, A. (2010) Amyotrophic lateral sclerosis is a non-amyloid disease in which extensive misfolding of SOD1 is unique to the familial form. Acta Neuropathol. 119, 335.

80. Zetterstrom, P., Stewart, H. G., Bergemalm, D., Jonsson, P. A., Graffmo, K. S., Andersen, P. M., Brannstrom, T., Oliveberg, M. and Marklund, S. L. (2007) Soluble misfolded subfractions of mutant superoxide dismutase-1s are enriched in spinal cords throughout life in murine ALS models. Proc.Natl.Acad.Sci.U.S.A. 104, 14157.

81. Deng, H. X., Shi, Y., Furukawa, Y., Zhai, H., Fu, R., Liu, E., Gorrie, G. H., Khan, M. S., Hung, W. Y., Bigio, E. H., Lukas, T., Dal Canto, M. C., O'Halloran, T. V. and Siddique, T. (2006) Conversion to the amyotrophic lateral sclerosis phenotype is associated with intermolecular linked insoluble aggregates of SOD1 in mitochondria. Proc.Natl.Acad.Sci.U.S.A. 103, 7142.

82. Johnston, J. A., Dalton, M. J., Gurney, M. E. and Kopito, R. R. (2000) Formation of high molecular weight complexes of mutant Cu, Zn-superoxide dismutase in a mouse model for familial amyotrophic lateral sclerosis. Proc Natl Acad Sci U S A. 97, 12571.

83. Shibata, N., Hirano, A., Kobayashi, M., Siddique, T., Deng, H. X., Hung, W. Y., Kato, T. and Asayama, K. (1996) Intense superoxide dismutase-1 immunoreactivity in intracytoplasmic hyaline inclusions of familial amyotrophic lateral sclerosis with posterior column involvement. J Neuropathol Exp.Neurol. 55, 481.

84. Shaw, B. F., Lelie, H. L., Durazo, A., Nersissian, A. M., Xu, G., Chan, P. K., Gralla, E. B., Tiwari, A., Hayward, L. J., Borchelt, D. R., Valentine, J. S. and Whitelegge, J. P. (2008) Detergent-insoluble aggregates associated with amyotrophic lateral sclerosis in transgenic mice contain primarily full-length, unmodified superoxide dismutase-1. J.Biol.Chem. 283, 8340.

85. Banci, L., Bertini, I., Durazo, A., Girotto, S., Gralla, E. B., Martinelli, M., Valentine, J. S., Vieru, M. and Whitelegge, J. P. (2007) Metal-free superoxide dismutase forms soluble oligomers under physiological conditions: a possible general mechanism for familial ALS. Proc Natl Acad Sci U S A. 104, 11263.

86. Chattopadhyay, M., Durazo, A., Sohn, S. H., Strong, C. D., Gralla, E. B., Whitelegge, J. P. and Valentine, J. S. (2008) Initiation and elongation in fibrillation of ALS-linked superoxide dismutase. Proc.Natl.Acad.Sci.U.S.A. 105, 18663.

87. DiDonato, M., Craig, L., Huff, M. E., Thayer, M. M., Cardoso, R. M., Kassmann, C. J., Lo, T. P., Bruns, C. K., Powers, E. T., Kelly, J. W., Getzoff, E. D. and Tainer, J. A. (2003) ALS mutants of human superoxide dismutase form fibrous aggregates via framework destabilization. J Mol Biol. 332, 601.

88. Jonsson, P. A., Graffmo, K. S., Andersen, P. M., Brannstrom, T., Lindberg, M., Oliveberg, M. and Marklund, S. L. (2006) Disulphide-reduced superoxide dismutase-1 in CNS of transgenic amyotrophic lateral sclerosis models. Brain. 129, 451.

89. Matsumoto, G., Kim, S. and Morimoto, R. I. (2006) Huntingtin and mutant SOD1 form aggregate structures with distinct molecular properties in human cells. J.Biol.Chem. 281, 4477.

90. Matsumoto, G., Stojanovic, A., Holmberg, C. I., Kim, S. and Morimoto, R. I. (2005) Structural properties and neuronal toxicity of amyotrophic lateral sclerosis-associated Cu/Zn superoxide dismutase 1 aggregates. J Cell Biol. 171, 75.

91. Niwa, J., Yamada, S., Ishigaki, S., Sone, J., Takahashi, M., Katsuno, M., Tanaka, F., Doyu, M. and Sobue, G. (2007) Disulfide bond mediates aggregation, toxicity, and ubiquitylation of familial amyotrophic lateral sclerosis-linked mutant SOD1. J.Biol.Chem. 282, 28087.

92. Karch, C. M., Prudencio, M., Winkler, D. D., Hart, P. J. and Borchelt, D. R. (2009) Role of mutant SOD1 disulfide oxidation and aggregation in the pathogenesis of familial ALS. Proc.Natl.Acad.Sci.U.S.A. 106, 7774.

93. Karch, C. M. and Borchelt, D. R. (2008) A limited role for disulfide cross-linking in the aggregation of mutant SOD1 linked to familial amyotrophic lateral sclerosis. J.Biol.Chem. 283, 13528.

94. Cozzolino, M., Amori, I., Pesaresi, M. G., Ferri, A., Nencini, M. and Carri, M. T. (2008) Cysteine 111 affects aggregation and cytotoxicity of mutant Cu,Zn-superoxide dismutase associated with familial amyotrophic lateral sclerosis. J.Biol.Chem. 283, 866.

95. Fukada, K., Nagano, S., Satoh, M., Tohyama, C., Nakanishi, T., Shimizu, A., Yanagihara, T. and Sakoda, S. (2001) Stabilization of mutant Cu/Zn superoxide dismutase (SOD1) protein by coexpressed wild SOD1 protein accelerates the disease progression in familial amyotrophic lateral sclerosis mice. Eur.J.Neurosci. 14, 2032.

96. Jaarsma, D., Haasdijk, E. D., Grashorn, J. A., Hawkins, R., van, D. W., Verspaget, H. W., London, J. and Holstege, J. C. (2000) Human Cu/Zn superoxide dismutase (SOD1) overexpression in mice causes mitochondrial vacuolization, axonal degeneration, and premature motoneuron death and accelerates motoneuron disease in mice expressing a familial amyotrophic lateral sclerosis mutant SOD1. Neurobiol.Dis. 7, 623.

97. Wang, L., Deng, H. X., Grisotti, G., Zhai, H., Siddique, T. and Roos, R. P. (2009) Wild-type SOD1 overexpression accelerates disease onset of a G85R SOD1 mouse. Hum.Mol.Genet. 18, 1642.

98. Sasaki, S., Warita, H., Murakami, T., Shibata, N., Komori, T., Abe, K., Kobayashi, M. and Iwata, M. (2005) Ultrastructural study of aggregates in the spinal cord of transgenic mice with a G93A mutant SOD1 gene. Acta Neuropathol. 109, 247.

99. Turner, B. J., Lopes, E. C. and Cheema, S. S. (2003) Neuromuscular accumulation of mutant superoxide dismutase 1 aggregates in a transgenic mouse model of familial amyotrophic lateral sclerosis. Neurosci.Lett. 350, 132.

100. Wang, J., Xu, G. and Borchelt, D. R. (2002) High molecular weight complexes of mutant superoxide dismutase 1: age-dependent and tissue-specific accumulation. Neurobiol.Dis. 9, 139.

101. Wang, J., Xu, G., Gonzales, V., Coonfield, M., Fromholt, D., Copeland, N. G., Jenkins, N. A. and Borchelt, D. R. (2002) Fibrillar inclusions and motor neuron degeneration in transgenic mice expressing superoxide dismutase 1 with a disrupted copper-binding site. Neurobiol.Dis. 10, 128.

102. Wang, J., Xu, G., Li, H., Gonzales, V., Fromholt, D., Karch, C., Copeland, N. G., Jenkins, N. A. and Borchelt, D. R. (2005) Somatodendritic accumulation of misfolded SOD1-L126Z in motor neurons mediates degeneration: alphaB-crystallin modulates aggregation. Hum.Mol.Genet. 14, 2335.

103. Jonsson, P. A., Ernhill, K., Andersen, P. M., Bergemalm, D., Brannstrom, T., Gredal, O., Nilsson, P. and Marklund, S. L. (2004) Minute quantities of misfolded mutant superoxide dismutase-1 cause amyotrophic lateral sclerosis. Brain. 127, 73.

104. Arrasate, M., Mitra, S., Schweitzer, E. S., Segal, M. R. and Finkbeiner, S. (2004) Inclusion body formation reduces levels of mutant huntingtin and the risk of neuronal death. Nature. 431, 805.

105. Caughey, B. and Lansbury, P. T. (2003) Protofibrils, pores, fibrils, and neurodegeneration: separating the responsible protein aggregates from the innocent bystanders. Annu.Rev.Neurosci. 26, 267.

106. Kirkitadze, M. D., Bitan, G. and Teplow, D. B. (2002) Paradigm shifts in Alzheimer's disease and other neurodegenerative disorders: the emerging role of oligomeric assemblies. J.Neurosci.Res. 69, 567.

107. Ferraiuolo, L., Kirby, J., Grierson, A. J., Sendtner, M., and Shaw, P. J. (2011) Molecular pathways of motor neuron injury in amyotrophic lateral sclerosis. Nat.Rev.Neurol. 7, 616.

108. Andersen, P. M. (2006) Amyotrophic lateral sclerosis associated with mutations in the CuZn superoxide dismutase gene. Curr.Neurol Neurosci.Rep. 6, 37.

109. Esteban, J., Rosen, D. R., Bowling, A. C., Sapp, P., Kenna-Yasek, D., O'Regan, J. P., Beal, M. F., Horvitz, H. R. and Brown, R. H., Jr. (1994) Identification of two novel mutations and a new polymorphism in the gene for Cu/Zn superoxide dismutase in patients with amyotrophic lateral sclerosis. Hum.Mol Genet. 3, 997.

110. Nogales-Gadea, G., Garcia-Arumi, E., Andreu, A. L., Cervera, C. and Gamez, J. (2004) A novel exon 5 mutation (N139H) in the SOD1 gene in a Spanish family associated with incomplete penetrance. J Neurol Sci. 219, 1-6.

111. Prudencio, M., Hart, P. J., Borchelt, D. R. and Andersen, P. M. (2009) Variation in aggregation propensities among ALS-associated variants of SOD1: correlation to human disease. Hum.Mol Genet. 18, 3217.

CHAPTER 2

GLUTATHIONYLATION AT CYS-111 INDUCES DISSOCIATION OF WILD TYPE AND FALS MUTANT SOD1 DIMERS

Introduction

Amyotrophic lateral sclerosis (ALS) is a late-onset neurodegenerative disorder for which effective treatment is extremely limited. The majority of ALS cases have no known genetic cause, but substantial insights into the disease have been gained by the study of Cu/Zn superoxide dismutase (SOD1), mutations of which are linked to inherited, or familial, ALS (FALS). Mutant SOD1 appears to play a prominent role in FALS pathology through an acquired propensity to misfold and aggregate (1-5). Notably, misfolded and/or aggregated wild type SOD1 has also been documented in patients with sporadic ALS (6, 7), suggesting that this enzyme can be induced to adopt toxic conformational states by non-genetic factors. Such a phenomenon was recently demonstrated for wild type SOD1: Bosco *et al*. found that oxidative modification of $SOD1^{WT}$ induced structural rearrangement and conformational similarity to the FALS-associated G93A mutant (6). Oxidative stress may thus represent a factor in the cellular environment that is capable of inducing SOD1 to adopt noxious misfolded conformations.

Oxidative stress is thought to be a factor in the pathogenesis of several neurodegenerative diseases, including Alzheimer's disease, Parkinson's disease and ALS (8, 9). Conditions of oxidative stress produce a shift in the cellular environment that is reflected in altered ratios of various redox couples, notably the tripeptide glutathione. Glutathione is a primary regulator of oxidizing species in the cell and protects against oxidative damage by acting as a reducing agent,

as well as by reversibly modifying proteins to prevent permanent oxidation (10, 11). Mixed protein-glutathione disulfides may later be removed by glutaredoxins, making protein S-glutathionylation an important defense against irreversible oxidative damage to proteins (11). We recently found that SOD1 is heavily glutathionylated at cysteine-111 in human tissue, with the modified enzyme constituting nearly 50% of the pool of SOD1 in freshly-drawn erythrocytes (12).

SOD1 misfolding and aggregation is initiated by dissociation of the native homodimer, leaving monomers more prone to loss of the stabilizing zinc ion (13-15). As such, dimer dissociation is a critical first step in the pathway to SOD1 aggregate formation. In light of our finding that a major fraction of SOD1 in human cells is glutathionylated at cysteine-111, a residue proximal to the dimer interface (12), we considered it pertinent to evaluate the influence of this modification on SOD1 dimer stability. We find that cysteine-111 glutathionylation has a profound effect on the dimer stabilities of wild type SOD1 and the FALS mutant A4V, and that this effect is attributable to decreased association rate (k_{on}). Using Discrete Molecular Dynamics (DMD) simulations, we show that glutathionylation affects specific interface contacts in the SOD1 dimer, offering structural insight into the experimental differences we observe in measurements of dimer stability.

Methods

Expression and purification of SOD1 variants

Wild type and mutant variants of SOD1 were produced in *S. cerevisiae* and isolated as previously described (12). After the final remetallation step, samples were separated by anion-

exchange chromatography using a MonoQ column (GE Healthcare), which resolves two populations of SOD1 isolated from *S. cerevisiae*. μ-ESI-FT-ICR-MS analysis shows that SOD1 eluted at lower ionic strength is primarily unmodified, while the protein eluted at higher ionic strength is enriched >8-fold in the glutathione modification (12). The degree of enrichment is estimated by comparing mass spectrum intensities of modified and unmodified SOD1 in the high- and low-charge populations. By comparing the ratio of intensities for unmodified and modified SOD1, we control for any differences in ionization of these two species. Assuming equal ionization of SOD1 with and without glutathione, approximately 75% of SOD1 monomers in the high-charge population are glutathionylated, and over 90% of SOD1 dimers are expected to be modified on one or both subunits. The glutathione-enriched population eluted at high ionic strength is referred to as glutathionylated SOD1 (GS-SOD1).

Size exclusion chromatography

Purified samples of SOD1 at 88 or 8.8 μM in a buffer containing 20 mM Tris, 150 mM NaCl, pH 7.8 were applied to a Superdex 200 PC 3.2/30 column (GE Healthcare) equilibrated in the sample buffer at 4 °C using a 20 μl sample loop. DTT treatment was administered by dialyzing samples overnight against sample buffer containing 1 mM DTT.

To estimate dissociation constants, A_{280} data from size exclusion chromatography (SEC) was deconvoluted to determine approximate concentrations of monomeric and dimeric SOD1. Diffusion and other band-broadening effects often create significant peak asymmetry in SEC chromatograms, and accurately modeling peak shapes is nontrivial (16). In all chromatograms from the Superdex 200 PC 3.2/30 column, even those of single-subunit standard proteins that do

not self-associate, there is skewness toward the trailing edge of peaks that increases with the quantity of protein loaded (17). To deconvolute peaks corresponding to monomeric and dimeric SOD1 while taking this skewness into account, we assume the A_{280} curve for unmodified wild type SOD1 as the peak shape for completely dimeric SOD1. This assumption is justified since SEC experiments are performed at an SOD1 concentration well above the previously reported value of K_d, which is 10 nM (15). This "standard" dimeric SOD1 curve is subtracted from each data set to be deconvoluted to yield the signal attributable to monomeric SOD1. To control for the band-broadening effects of increased sample load, we subtract the curve for dimeric SOD1 collected at equivalent total protein concentration. The concentrations of monomeric and dimeric SOD1 in each sample are then calculated using:

$$[M] = \frac{A_M}{A_M + A_D} \times [D]_{total} \times 2$$

$$[D] = \frac{A_D}{A_M + A_D} \times [D]_{total}$$

where *[M]* and *[D]* are the concentrations of SOD1 monomer and dimer, respectively in the equilibrated sample; A_M and A_D are the areas under the curves corresponding to monomeric and dimeric SOD1, respectively; and $[D]_{total}$ is the starting concentration of dimeric SOD1 (88 or 8.8 μM). K_d is then calculated using $K_d = \frac{[M]^2}{[D]}$. A K_d of 10 nM for unmodified SOD1 (15) corresponds to monomer concentrations of 0.93 and 0.29 μM at equilibrium when the initial dimer concentrations are 88 and 8.8 μM, respectively, as calculated using:

$$0.01\mu M = \frac{[M]^2}{[D]_{total} - 2[M]}$$

Hence, the maximum contribution of unmodified SOD1 dimer dissociation to the estimated monomer population for GS-SOD1 is less than 5% (see Figure 2.1b).

Determination of dimer dissociation rate constants using surface plasmon resonance

Wild type and mutant SOD1 dimers were biotinylated on a single subunit as previously described (13); briefly, SOD1 was incubated with a primary amine-reactive biotinylating agent (EZ-Link NHS-LC-LC Biotin, Pierce) for 30 minutes at 25°C and brought to 20 mM Tris, 150 mM NaCl, pH 7.8 using a 1 ml Sephadex G-25 medium spin column. Dimer dissociation was monitored by surface plasmon resonance (SPR) using a Biacore 2000 instrument with biotinylated SOD1 dimers immobilized on a streptavidin-coated flow cell (sensor chip SA or Biotin CAPture Kit, GE Healthcare). Biotinylated SOD1 at approximately 40 μM was loaded onto the surface at 5 μl/minute until achieving a signal gain of 1500 – 2500 response units (RU), at which point the dissociation reaction was initiated by flowing SOD1-free buffer over the surface. Biotinylation and SPR measurements were conducted at 25 °C and biotinylated SOD1 was stored at 4 °C until use.

Measuring kinetics of very slow reactions using SPR is complicated by non-covalent interactions of buffer components with the chip surface, resulting in signal drift over time (18). We corrected for this drift by subtracting the signal from a reference streptavidin surface from each data sat, as well as by calculating rate constants using the Guggenheim method (19), which removes the need for an accurate infinite time value. For $SOD1^{WT}$ and $SOD1^{I112T}$, 5000 s of Guggenheim data (dRU/dt) were fit using the equation for double exponential decay, excluding the first 1000 s that were typically noisy. Since the A4V mutant dissociates rapidly, data fitting

was performed for the first 1000 s only. While SOD1 dimer dissociation is a first order process, an additional, fast decay was present in all reactions, evidenced by the comparatively poor fit of a single exponential. We therefore fit SPR data to a double exponential decay, and the rate constant for dimer dissociation was taken to be that of the process that accounted for the majority of signal loss (>70%). The half time of the minor exponential function was invariably between 1 and 15 minutes, and accounted for approximately 5 - 30% of the signal loss during the reaction (Table 2.1). Due to the consistent presence of this process across all reactions, we conclude it to be an instrumental artifact, or perhaps the dissociation of transient noncovalent interactions

	Average fast rate (s^{-1}, n = 3)	**Average contribution of fast rate (%, n = 3)**
WT	$1.60 \times 10^{-3} \pm 3.7 \times 10^{-4}$	3.8 ± 0.7
GS-WT	$2.23 \times 10^{-3} \pm 9.3 \times 10^{-4}$	4.6 ± 2.9
I112T	$1.27 \times 10^{-3} \pm 2.2 \times 10^{-4}$	9.2 ± 2.9
GS-I112T	$1.03 \times 10^{-3} \pm 0.7 \times 10^{-4}$	16.4 ± 1.3
A4V	$1.10 \times 10^{-2} \pm 2.1 \times 10^{-3}$	31.2 ± 3.7
GS-A4V	$1.20 \times 10^{-2} \pm 1.7 \times 10^{-3}$	15.8 ± 10.0

Table 2.1. Average values for the rate and contribution of the artificial fast decay obtained by double exponential fit to Guggenheim data. The derivative of raw SPR data was fit to a double exponential:

$$\frac{dRU}{dt} = A_0 e^{\frac{-t}{A_1}} + A_2 e^{\frac{-t}{A_3}} \qquad (1)$$

Average rates are listed ± S. D. The contribution of each rate is calculated using:

$$\frac{A_0 A_1 e^{-\frac{t_0}{A_1}}}{A_0 A_1 e^{-\frac{t_0}{A_1}} + A_2 A_3 e^{-\frac{t_0}{A_3}}} \times 100 \qquad (2)$$

where t_0 is the initial time value of the data set fit using Eq. 1.

between non-immobilized and immobilized SOD1 dimers following the transition from sample loading to buffer flow. Such observations have been made previously concerning SPR measurements (20).

Comparison of SOD1 monomer stability using thermal denaturation monitored by circular dichroism (CD) spectroscopy

SOD1 variants with and without Cys-111 glutathionylation were analyzed using a Jasco J-815 CD spectrometer (Jasco Inc. Easton, MD). Yeast-expressed SOD1 mutants were dialyzed overnight against 10 mM phosphate buffer and diluted to 0.2 mg/ml for analysis. Sample spectra were taken at 20 °C and 96 °C and the major loss of signal occurred at 230 nm. Upon cooling to 20 °C, the decrease in ellipticity at 230 nm was reversible for all samples to within 65 – 85% of the initial value (Figure 2.4a). All subsequent unfolding experiments were temperature ramps from 20 °C to 96 °C monitored at 230 nm by 1 °C increments with a 5 s dwell time at each. Dialysis buffer was used as a blank. To obtain apparent melting temperature T_m (T_m^*) values, blank-corrected thermal melting data were fit to a modified form of the van't Hoff equation, as previously described in (21). This equation includes parameters for the melting transition as well as the baselines corresponding to the native and denatured states (22):

$$\theta(T) = \frac{a_n T + b_n + (a_d T + b_d)K}{1 + K}$$

where $\Theta(T)$ is the observed ellipticity at a given temperature T; a_n(a_d) and b_n(b_d) are the slopes and intercepts, respectively, of the baselines corresponding to the native (and denatured) states; and K is the equilibrium constant for unfolding:

$$K = e^{\frac{-\Delta G_u}{RT}}$$

where ΔG_u is the difference in Gibbs free energy between the native and denatured states at a given temperature T, and R is the universal gas constant. ΔG_u was calculated according to the Gibbs-Helmholtz equation (23):

$$\Delta G_u = \Delta H_u(1 - \frac{T}{T_m}) - \Delta C_u[(T_m - T) + T\ln(\frac{T}{T_m})]$$

where T_m is the temperature at which ΔG_u=0, and ΔH_u and ΔC_u are the changes in enthalpy and heat capacity, respectively, associated with thermal denaturation. Data were fit with the parameters a_n, a_d, b_n, b_d, ΔH_u, ΔC_u, T_m using non-linear least-squares regression, and T_m values were reported as apparent T_m (T_m^*) due to the incomplete reversibility of the unfolding transition.

All-atom DMD simulations of glutathionylated SOD1 mutants

To obtain the structures of post-translationally modified mutant and wild type SOD1, we use the known X-ray crystallographic structure of wild type SOD1 (PDBID: 1SPD) as a reference structure, and constrain glutathione molecules to their respective SOD1 residues. Mutations are made to these structures using the Eris suite (24), avoiding changes to residues participating in the metal-binding, glutathionylation, or disulfide bond interactions. The overall structure energy was minimized using an all-atom protein model with discrete molecular dynamics (DMD) simulations (25-27).

We perform equilibration and production simulations using DMD. DMD is a molecular dynamics engine that uses discrete potentials in place of continuous potentials, which transforms the simulation into simple calculations of ballistic equations, increasing the speed and efficiency of the simulation and extending sampling of conformational space. Each system is equilibrated for 500 ps at 226 K with a heat exchange occurring every 5 fs. We conduct 50 ns equilibrium simulations of dimeric SOD1 277 K. We perform simulations for each case of mutant or wild type, both the glutathionylated and unmodified structures, resulting in 6 cases total (2 (glutathionylated or unmodified) × 3 (two mutants and wild type)).

Dimer interface contact maps

In our DMD simulations, we define two residues as being in contact in the dimer interface if two C_α atoms of opposing chains are within 10 Å of each other. At each simulation snapshot (5 picoseconds of simulation time), we evaluate the contacts present between the two monomers. We then normalize the count between every pair of residues over the entire simulation.

Calculation of dimer interface area

We sample even intervals of single-temperature simulations for structure snapshots of unmodified and glutathionylated $SOD1^{WT}$, $SOD1^{A4V}$, and $SOD1^{I112T}$ and for each snapshot calculate the solvent accessible surface area (SASA) of each individual monomer and of the dimer. The SASA of the dimer is subtracted from the sum of the SASAs of the monomers,

resulting in the total buried area of both monomers in the respective dimer structure. We divide this resulting total area by two (since two monomers form the interface) to obtain the dimer interface area. All SASAs are calculated using the Gaia suite (28).

Results

SOD1 wild type and mutant dimers are destabilized by glutathionylation under physiological conditions

Size exclusion chromatography (SEC) analysis of GS-SOD1^{WT} reveals the substantial destabilization of dimers by this physiologically prevalent modification (Figure 2.1). GS-SOD1 used in these assays was isolated from the endogenous pool of enzyme expressed in *S. cerevisiae* using ion-exchange chromatography, yielding a population that is heavily (~8-fold) enriched in glutathionylated protein (12). While some unmodified enzyme remains in this sample, we do not perform additional *in vitro* glutathionylation of SOD1, in order to avoid non-physiological modification of cysteine-6 (12). Hence, we report a lower limit for the destabilizing effect of cysteine-111 glutathionylation.

We examined the effect of cysteine-111 glutathionylation on the SOD1 monomer-dimer equilibrium by assaying the oligomeric state of unmodified and glutathionylated SOD1 at physiological pH and concentration (estimated as 50 – 100 μM in neurons (29, 30)). Unmodified wild type SOD1 is completely dimeric under these conditions (thick solid curve, Figure 2.1a), in agreement with the previously reported K_d of 10 nM for wild type SOD1 expressed in *S. cerevisiae* (15). Glutathionylation of SOD1^{WT} results in the appearance of a significant monomeric population (thick dashed curve, Figure 2.1a). To estimate K_d, we must deconvolute

the overlapping peaks for dimeric and monomeric SOD1. We estimate the monomer contribution

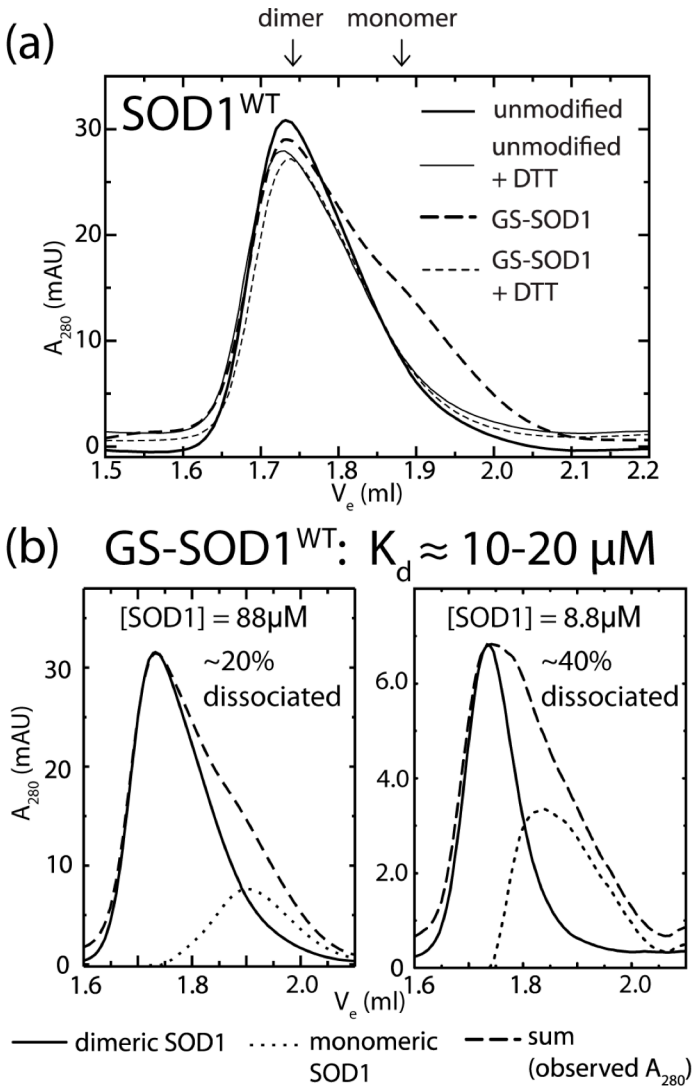

Figure 2.1. Wild type SOD1 dimers are destabilized by Cys-111 glutathionylation. (a) Size exclusion chromatography at physiological [SOD1] (88μM) shows marked destabilization of GS-SOD1^{WT} that is reversed by treatment with DTT to remove the glutathione moeity. Solid lines indicate unmodified SOD1 while dashed lines represent GS-SOD1. Broad and fine lines show these species before and after treatment with DTT, respectively. The elution volumes corresponding to dimeric (~1.74 ml) and monomeric (~1.89 ml) SOD1 are indicated above the panel. Experiments were performed at least in duplicate. (b) Comparison of dimeric and monomeric populations of SOD1 at low and high concentration. Dashed lines show A_{280} data for each species (reproduced from panel (a)), which was deconvoluted as described in Materials and Methods. Solid and dotted lines show curves corresponding to dimeric and monomeric SOD1, respectively.

while accounting for peak skewness (see discussion in Materials and Methods) by assuming the peak shape for unmodified SOD1 (solid curves, Figure 2.1b) to be characteristic of dimeric SOD1. By removing the contribution of this curve from the observed A_{280} (dashed curves, Figures 2.1b and 2.2b), we obtain the signal attributable to monomeric SOD1 (dotted curves, Figures 2.1b and 2.2b). We estimate the K_d of the GS-SOD1^{WT} homodimer to be approximately 10-20 μM, which represents an increase of approximately 1000-fold over that of the extremely stable unmodified enzyme (previously reported as 10 nM (15)). SOD1^{A4V} is also destabilized by glutathionylation, experiencing an approximately 30-fold increase in K_d (Figure 2.2). In contrast, SOD1^{I112T} stability is unaffected by this modification, remaining dimeric when glutathionylated (Figure 2.2a). The mean elution volume for monomeric SOD1^{A4V} is slightly lower (~1.84 ml) compared to that of the wild type (~1.89 ml). This mutation is reported to increase the radius of gyration of monomeric SOD1 (31), accounting for the decrease in mobility in SEC. The differences in oligomeric state between unmodified and glutathionylated SOD1^{A4V} and SOD1^{WT} are observed in replicate experiments and are abrogated by treatment with DTT to remove the glutathione moiety (thin curves, Figures 2.1a and 2.2a), implying that the observed destabilization is due to the presence of the glutathione modification at cysteine-111. All SOD1 species remained dimeric after DTT treatment (Figures 2.1a and 2.2a), demonstrating that only the mixed SOD1-glutathione disulfide was reduced, leaving the native intramolecular disulfide intact. This fact is unsurprising since SOD1 retains this disulfide (between Cys-57 and Cys-146) in the reducing environment of the cytosol.

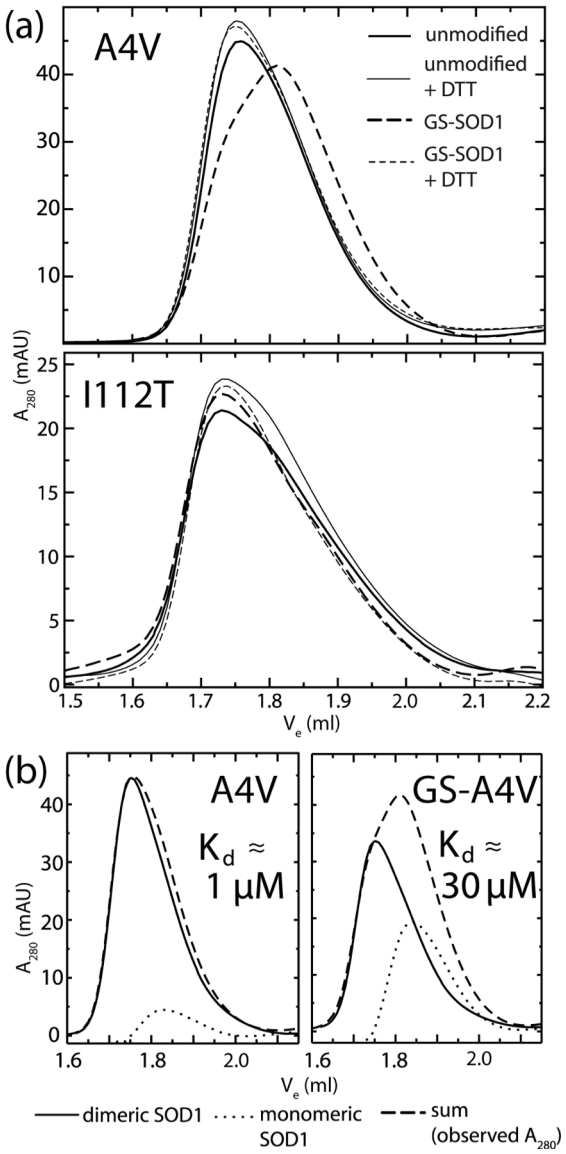

Figure 2.2. Effect of Cys-111 glutathionylation on K_d of selected FALS mutants. (a) Size exclusion chromatography at physiological [SOD1] (88μM) shows destabilization of GS-SOD1^{A4V} that is reversed by treatment with DTT to remove the glutathione moeity. The oligomeric state of SOD1^{I112T} (bottom panel) is relatively unaffected by modification. Solid lines indicate unmodified SOD1 while dashed lines represent GS-SOD1. Broad and fine lines show these species before and after treatment with DTT, respectively. The elution volumes corresponding to dimeric (~1.74 ml) and monomeric (~1.89 ml) SOD1 are indicated above the panel. Experiments were performed at least in duplicate. (b) Comparison of dimeric and monomeric populations of SOD1^{A4V} and GS-SOD1^{A4V}. Dashed lines show A_{280} data for each species (reproduced from panel (a)), which was deconvoluted as described in Materials and Methods. Solid and dotted lines show curves corresponding to dimeric and monomeric SOD1, respectively.

Effects of glutathionylation on dimer dissociation kinetics

To measure the effect of glutathionylation on the rate of SOD1 dimer dissociation, we use surface plasmon resonance (SPR) to monitor the dissociation of biotinylated SOD1 dimers immobilized to a streptavidin-coated sensor chip (13). We observe a clear distinction between the effects of the A4V and I112T mutations on dissociation kinetics. $SOD1^{I12T}$ has an average half time of 1.10 hours, compared to 1.29 hours for the wild type, a difference that is within experimental error (Figure 2.3). $SOD1^{A4V}$ dimers, by contrast, dissociate significantly faster than the wild type, with an average half time of 4.51 minutes (Figure 2.3). This observation is in stark agreement with the common classification of A4V as a mutation that particularly affects dimer

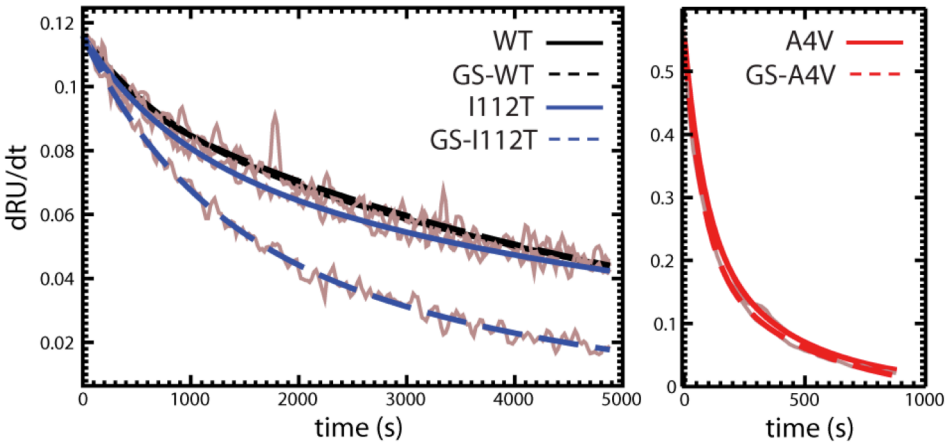

	k_{off} (s^{-1})	$t_{1/2}$
WT	$1.50 \times 10^{-4} \pm 7 \times 10^{-6}$	1.28 ± 0.06 hr
GS-WT	$1.82 \times 10^{-4} \pm 2.9 \times 10^{-5}$	1.08 ± 0.17 hr
A4V	$2.60 \times 10^{-3} \pm 3.7 \times 10^{-4}$	4.51 ± 0.64 min
GS-A4V	$1.78 \times 10^{-3} \pm 6.0 \times 10^{-4}$	7.14 ± 2.94 min
I112T	$1.76 \times 10^{-4} \pm 9 \times 10^{-6}$	1.09 ± 0.06 hr
GS-I112T	$2.17 \times 10^{-4} \pm 8 \times 10^{-6}$	0.89 ± 0.03 hr

Figure 2.3. Dimer dissociation rate constants for unmodified and glutathionylated SOD1. Dissociation of immobilized dimers was monitored by surface plasmon resonance. Guggenheim plots (50 s intervals) of data from representative experiments are shown in grey; colored lines indicate double exponential decay curves fitted to the data. All values are reported as the mean of triplicate experiments ± S. D..

stability (32, 33), with the dimer dissociation rate constant k_{off} for unmodified $SOD1^{A4V}$ nearly 20-fold greater than that of the unmodified wild type. Glutathionylation has a minimal effect on dissociation rate for all SOD1 variants studied: k_{off} values for unmodified and glutathionylated dimers do not differ significantly for the wild type and the A4V mutant. $SOD1^{I112T}$ shows a significant, but small (20%), increase in dimer dissociation rate as a result of glutathionylation. The minimal effect of glutathionylation on the dissociation rate constants (k_{off}) of $SOD1^{WT}$ and $SOD1^{A4V}$ dimers cannot account for the significant destabilization at equilibrium revealed by SEC (Figures 2.1 and 2.2); thus, the effects of this modification on K_d are attributable to decreases in the association rate constant (k_{on}) of modified monomers.

Glutathionylation has little effect on SOD1 monomer stability

We assess the effect of mutations and glutathionylation on SOD1 monomer stability using thermal unfolding experiments monitored by circular dichroism (CD). Because CD primarily reflects protein secondary structure content, we expect that changes in signal upon thermal denaturation of SOD1 are mainly attributable to the loss of β-strand structure as monomers unfold, rather than dissociation of the homodimer. The effect of glutathionylation on monomer unfolding is minimal for the wild type protein, but results in a modest decrease in apparent T_m for $SOD1^{A4V}$ (Figure 2.4). These results, in agreement with a computational study by Proctor *et al.* (34), indicate that glutathionylation primarily exerts effects on dimer stability while leaving monomer stability largely unchanged.

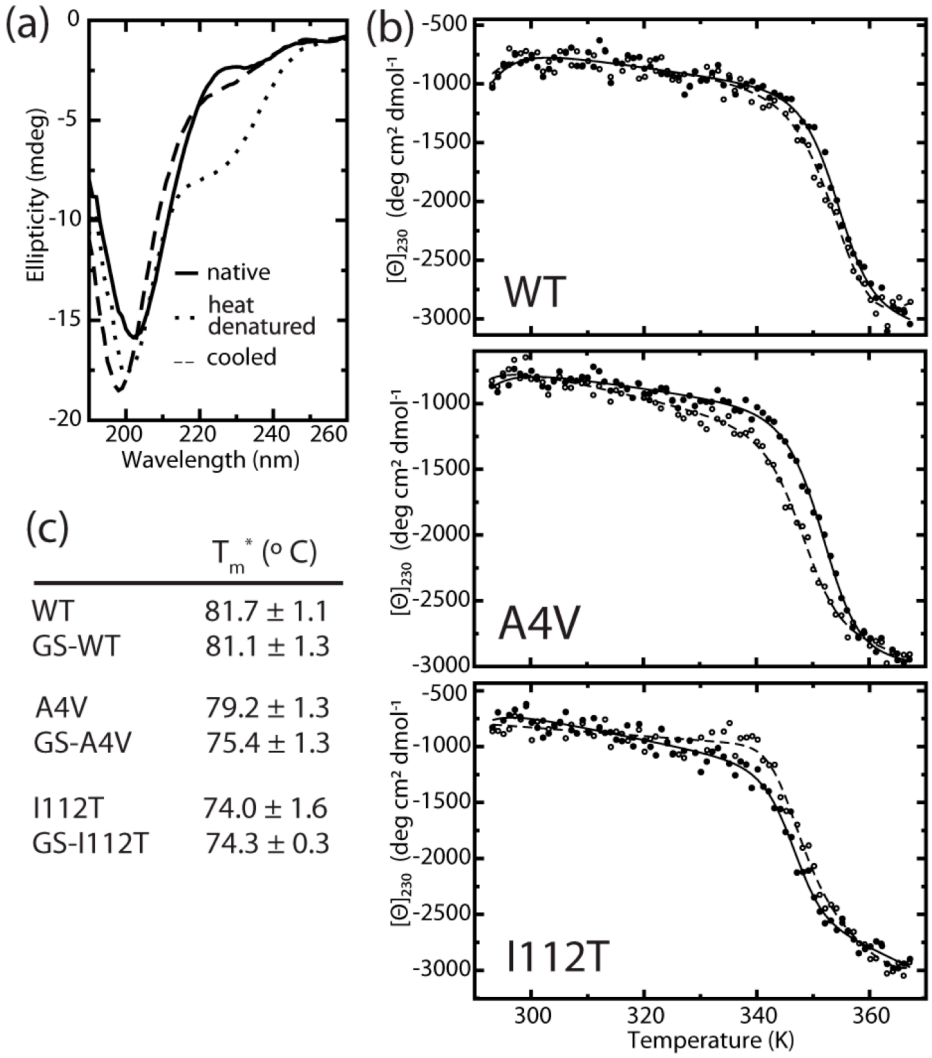

Figure 2.4. Effect of glutathionylation on monomer thermal stability. (a) Representative CD spectra of SOD1 before and after cooling shows reversible decrease in ellipticity at 230 nm. (b) Representative curves for thermally-induced unfolding of unmodified (closed symbols) and glutathionylated (open symbols) wild type and mutant SOD1 monitored by circular dichroism at 230 nm. (c) Apparent T_m (T_m^*) values obtained by fitting blank-corrected thermal melting data as described in Methods. Experiments were performed at least in duplicate; T_m^* values are reported as the mean of all experiments ± S.D..

Structural effects of glutathionylation on SOD1 dimer interface

Using DMD simulations, we show that dimer interface contacts are changed in the glutathionylated versus the unmodified structures. $SOD1^{WT}$ and $SOD1^{A4V}$ exhibit a general loss

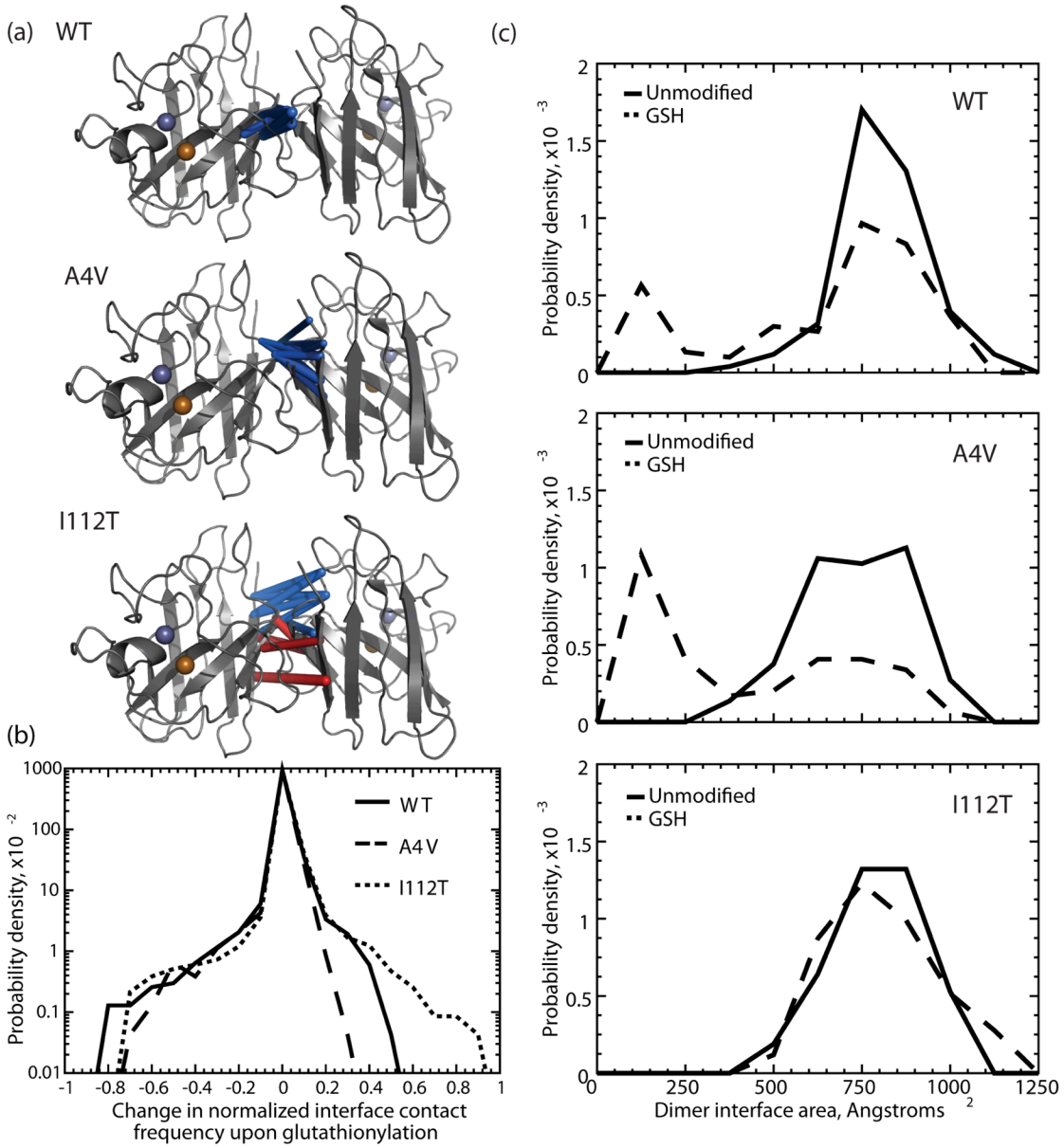

Figure 2.5. Effects of glutathionylation on the SOD1 dimer interface. (a) The top ten most frequently changed Cα interface contacts upon glutathionylation are highlighted with a three-dimensional rod representation for $SOD1^{WT}$, $SOD1^{A4V}$, and $SOD1^{I112T}$. Rod thickness is proportional to the change in frequency of the interaction. Blue rods represent a loss in frequency of the interaction; red rods represent a gain in frequency of the interaction. (b) Distributions of changes in frequency of Cα interface contacts upon Cys-111 glutathionylation for $SOD1^{WT}$, $SOD1^{A4V}$, and $SOD1^{I112T}$. Wild type SOD1 and the A4V mutant have distributions that are skewed towards loss of contacts, while the I112T mutant is balanced in loss and gain of contacts. (c) Distributions of dimer interface areas for unmodified (solid line) and glutathionylated ("GSH", dashed line) $SOD1^{WT}$, $SOD1^{A4V}$, and $SOD1^{I112T}$.

in overall interface C_α contacts, while the I112T mutant experiences a shift in C_α dimer interface contacts upon glutathionylation (Figures 2.5a-b). In $SOD1^{I112T}$, residues that lose interface contacts are balanced by neighboring residues that gain contacts, resulting in an overall change in composition of the interface, without significantly changing the number of interface contacts. Interestingly, in wild type SOD1, we observe that, while the net number of C_α contacts decreases upon glutathionylation, the net number of C_β contacts increases (Figure 2.6). This would indicate rearrangement of the side chains in the dimer interface in order to accommodate the glutathione moiety. We do not observe this effect in the A4V or I112T mutants, which have the same qualitative distribution of losses and gains in contact frequency upon glutathionylation in C_α and C_β contacts.

This phenomenon brings into question the size of the dimer interface in each SOD1 variant. We calculate the area of the dimer interface over the course of single-temperature simulations, and find that all three unmodified SOD1 variants show a single population, featuring an approximately Gaussian distribution around a central value of 750-800 $Å^2$ for the interface area (Figure 2.5c). However, upon glutathionylation, a second population is present in $SOD1^{WT}$ and $SOD1^{A4V}$ near 150 $Å^2$, while the dimer interface area distribution of $SOD1^{I112T}$ is relatively unaffected. This finding agrees with that of decreased C_α (backbone) contacts found in $SOD1^{WT}$ and $SOD1^{A4V}$ upon glutathionylation.

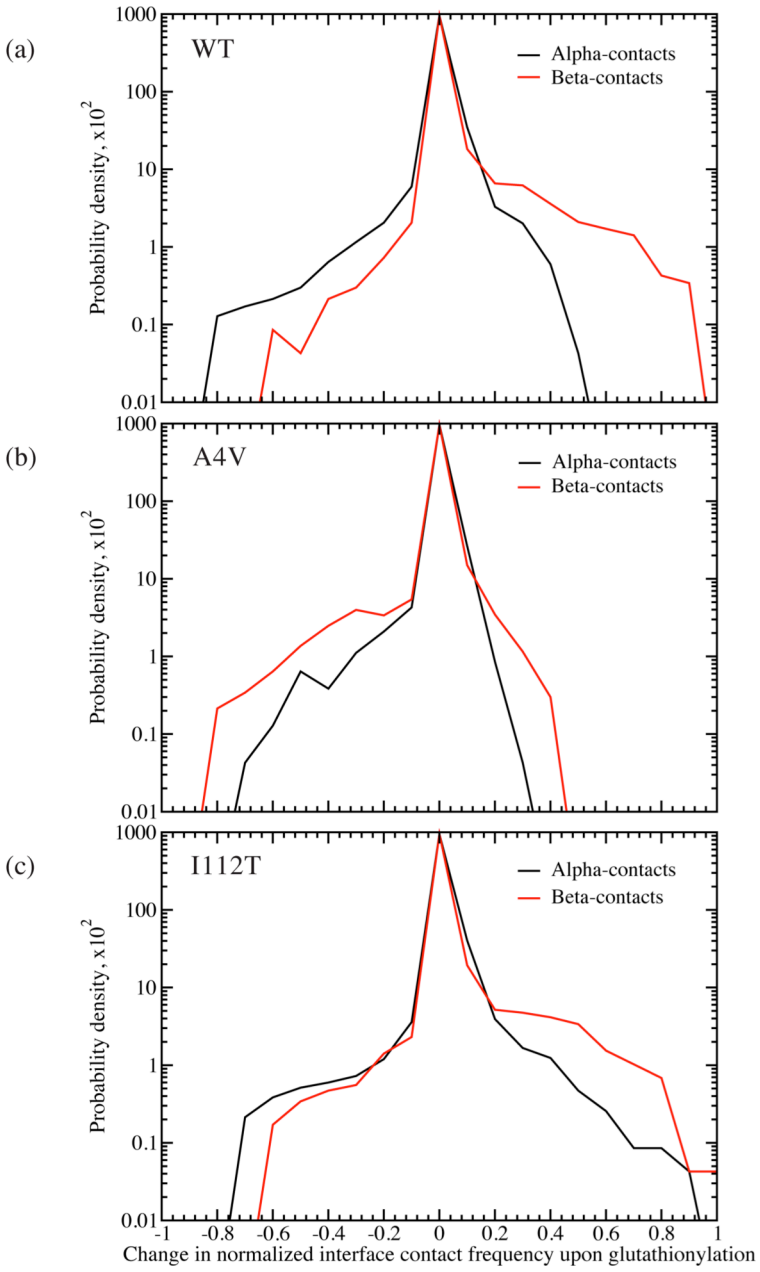

Figure 2.6. Comparison of C_α and C_β dimer interface contacts. Distributions of changes in frequency of both C_α-C_α (backbone) and C_β-C_β (side-chain) dimer interface contacts upon Cys-111 glutathionylation for (a) wild type, (b) A4V, and (c) I112T SOD1. Wild type SOD1 shows a reversal of behavior in the two types of contacts; the interface undergoes an overall loss of backbone contacts, but gains side-chain contacts, indicating the ability of the side-chains to rearrange upon separation of the monomer backbones. This behavior is not observed in A4V or I112T SOD1, whose distributions have similar qualitative behavior between backbone and side-chain contacts.

Discussion

SOD1 is abundantly glutathionylated at cysteine-111 in human tissue (12). Due to the proximity of this tripeptide moiety to the dimer interface, we hypothesized that it introduces steric clashes that favor dimer dissociation and/or hinder association of modified monomers. To distinguish these kinetic effects, we estimate the equilibrium dissociation constant K_d using size exclusion chromatography and measure the rate constant for dimer dissociation (k_{off}) with surface plasmon resonance. Since the equilibrium dissociation constant K_d is equal to the ratio of the rate constants for dissociation and association, we can then deduce effects on dimer formation rate from these two parameters. Dimer dissociation precedes disulfide reduction and

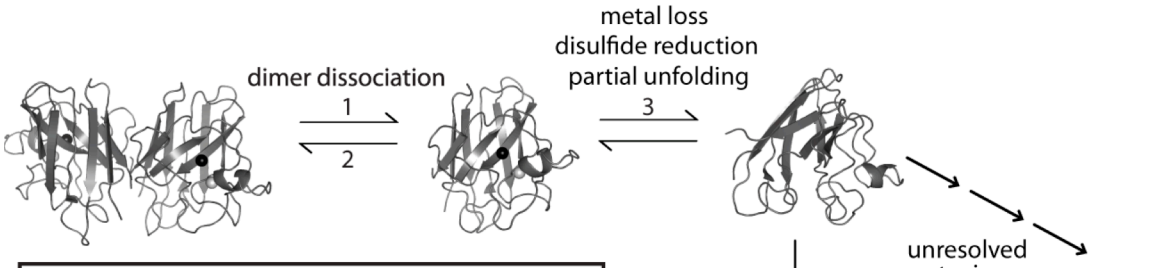

	k_{off} (1)	k_{on} (2)	monomer stability (3)
WT	=	↓	=
I112T	↑	↑	=
A4V	=	↓	↓

Figure 2.7. Summary of effects of Cys-111 glutathionylation on the stabilities of WT SOD1 and the FALS mutants I112T and A4V. Above, general schematic of SOD1 aggregation pathway. Below, effect of glutathionylation on dimer dissociation rate (k_{off} – reaction 1), monomer association rate (k_{on} – reaction 2), and monomer thermal stability (3) for each SOD1 variant. For simplicity of representation, we condense metal loss, intramolecular disulfide reduction, and structural distortion of monomers into a single step (reaction 3). The effect of glutathionylation on k_{on} is inferred from the measured effects on K_d (Figures 2.1 and 2.2) and k_{off} (Figure 2.3) using the relationship $K_d = \frac{k_{off}}{k_{on}}$.

metal loss (13) (Figure 2.7), so the contribution of the latter processes and irreversible aggregation is minimal compared to the dimer dissociation reaction in our SEC (Figures 2.1 and 2.2) and SPR (Figure 2.3) experiments.

Glutathionylation has a dramatic effect on wild type dimer stability at equilibrium. The SOD1 homodimer is exceptionally stable, having low nanomolar binding affinity (12, 15). In agreement with these findings, the unmodified wild type enzyme is dimeric under the conditions of our assay (Figure 2.1a). In contrast, the K_d of GS-SOD1^{WT} is increased by several orders of magnitude, to approximately 10-20 μM, such that there is appreciable (~20%) dissociation at physiological concentration (Figure 2.1b). Although GS-SOD1^{WT} is destabilized at equilibrium relative to the unmodified enzyme, the rate of dimer dissociation does not differ significantly as a result of modification (Figure 2.3). We therefore conclude that glutathionylation destabilizes SOD1^{WT} dimers by decreasing k_{on}, the rate constant for monomer association. These results indicate a much greater destabilizing effect than we initially estimated for the glutathione modification (12). However, we previously estimated K_d using an activity assay to quantify SOD1 dissociation. This method of K_d estimation is predicated on the decreased activity of monomeric SOD1 due to loop disorder (35) and is sensitive enough for use at low protein concentrations that are unobservable by A_{280} (36). However, this method has the disadvantage of being an indirect measure of the oligomerization state, and is susceptible to interference by factors unrelated to monomerization that influence the mobility of active site loops. It may be that altered loop mobilities caused by glutathionylation result in dismutase-active monomeric SOD1, which would cause an underestimation of K_d using this method. SEC analysis, by contrast, is a simple and direct method for assessing the extent of dimer dissociation, and clearly demonstrates the striking destabilization of SOD1^{WT} dimers by Cys-111 glutathionylation.

Glutathionylation also destabilizes $SOD1^{A4V}$ dimers. The K_d of this variant has previously been reported as 3 μM (32), which agrees with our calculated lower limit of 1 μM (Figure 2.2b). Modification by the glutathione moiety results in a significant shift toward monomeric SOD1 and an approximately 10-fold increase in K_d (Figure 2.2). As in the wild type, glutathionylation does not affect dissociation kinetics in $SOD1^{A4V}$, indicating that destabilization of GS-$SOD1^{A4V}$ dimers occurs primarily through effects on k_{on}. Glutathionylation may hinder monomer association in $SOD1^{WT}$ and $SOD1^{A4V}$ by sterically blocking the formation of certain interface contacts. Alternatively, glutathionylation at cysteine-111 may promote local structural rearrangements in these monomers that impede formation of interface contacts. The ~3.8°C decrease in apparent melting temperature of GS-$SOD1^{A4V}$ monomers (Figure 2.4) may provide evidence for this; however, it is also possible that structural differences exist that do not significantly alter secondary structural elements.

To our knowledge, the stability of the I112T mutant of SOD1 has not previously been studied experimentally. Although SEC peaks for $SOD1^{I112T}$ show increased skewness compared to those of unmodified $SOD1^{WT}$, all appear to be unimodal and centered at the elution volume of dimeric SOD1 (Figure 2.2a). This difference in peak shape may reflect increased conformational flexibility of $SOD1^{I112T}$, resulting in a broader distribution of radii of gyration for the dimer. Alternatively, if this mutant has micromolar rather than nanomolar binding affinity, the peak could be skewed by the contribution of monomeric SOD1. Computational analysis of $SOD1^{I112T}$ thermodynamics showed that this mutation has increased dimer stability compared to the wild type (1), supporting the interpretation that this variant is solely dimeric under the conditions of our assay. Regardless of the effect of the I112T mutation itself, changes in dimer stability resulting from glutathionylation are clearly minimal (Figure 2.2a). In contrast to wild type SOD1

and the A4V mutant, glutathionylation of $SOD1^{I112T}$ dimers results in little to no effect on K_d despite a modest but statistically significant increase in the dissociation rate constant (Figure 2.3). Modification may exert opposing effects on this SOD1 mutant, destabilizing the dimer but facilitating the re-association of modified monomers.

DMD simulations reveal a structural basis for the distinct effects of cysteine-111 glutathionylation on wild type and FALS mutant SOD1. $SOD1^{WT}$ and $SOD1^{A4V}$ experience a net loss of both dimer interface area and C_α interface contacts as a result of glutathionylation (Figure 2.5), and these dimers are both destabilized exclusively by decreased k_{on}. Therefore, some losses in interface C_α contacts may be indicative of structural changes that hinder monomer association (k_{on}) rather than directly impacting the rate constant for dissociation (k_{off}). In particular, a net loss of C_α contacts specifically indicates backbone movements that separate the two monomers, rather than simple rearrangement of the residue side-chains. The appearance of a significant smaller-interface population in the glutathionylated species of $SOD1^{WT}$ and $SOD1^{A4V}$ during simulations (Figure 2.5c) further indicates that this modification stabilizes a partially dissociated intermediate, as seen in (34). In the $SOD1^{I112T}$ dimer interface, glutathionylation results in a shift in interface composition rather than a net loss of C_α contacts (Figure 2.5a-b); likewise, no smaller-interface population is observed for GS-$SOD1^{I112T}$ (Figure 2.5c). For this variant, change in the dissociation constant K_d is minimal even though k_{off} is increased. These trends raise the possibility that the identity, not quantity, of the residues participating in the dimer interface affects dissociation kinetics.

The late-onset nature of ALS suggests a connection to a natural process of aging that either allows the initiation of a previously suppressed pathology (e.g. SOD1 aggregation) or renders the organism less able to cope with an ongoing threat that was previously tightly

regulated. While symptom onset occurs in mid-life (>45 years) or later for the vast majority of ALS patients, disease duration is variable, even amongst patients with identical SOD1 mutations (2). Patients with the A4V mutation experience particularly aggressive motor function loss (< 2 years average disease duration (2)) while I112T is apparently incompletely penetrant (not all individuals with this allele develop ALS (37)). The phenotypic heterogeneity of disease duration amongst those with identical SOD1 genotype implies that non-genetic environmental factors contribute significantly to mutant SOD1 pathogenicity.

Oxidative stress, manifested as a dysregulation of reactive oxygen species (ROS) or reactive nitrogen species (RNS), is one such process. The levels of ROS and RNS are normally tightly regulated by a variety of enzymes, such as SOD1, and small molecule or peptide redox couples. Glutathione, one such redox couple, is present at a high concentration in the cytosol (up to 12 mM (38)) and protects against oxidative damage by acting as a reducing agent, as well as by reversibly modifying proteins to prevent permanent oxidation (10, 11). Protein S-glutathionylation occurs more frequently under conditions of oxidative stress as a result of two mechanisms. In the first, thiyl radicals generated by oxidizing species react with reduced glutathione (GSH). Under oxidizing conditions, there also exists a greater proportion of cellular glutathione in the disulfide-linked oxidized form (GSSG), which modifies free cysteine residues by disulfide exchange.

SOD1 is an enzyme that directly interacts with oxidizing species, converting superoxide to hydrogen peroxide, and glutathionylation is a common modification of SOD1 in human tissue, including that of ALS patients (12, 39). SOD1 is glutathionylated at a steady state level that likely reflects the immediate degree of oxidative stress occurring in the individual organism, rather than accumulating over the entire lifespan (discussed in (12)). Because a large fraction of

SOD1 from a variety of healthy human donors is glutathionylated (12), SOD1 glutathionylation alone is unlikely to cause ALS. The substantial drop in glutathionylated wild type dimer stability to micromolar affinity (Figure 2.1b), has not previously been observed even though this modification is prevalent in SOD1 from both human tissue and recombinant sources (12, 39, 40). Since enrichment of the glutathionylated protein by ion exchange is necessary to observe this destabilizing effect, it may be that the decreased k_{on} we report is only associated with formation of dimers of two modified subunits.

Given the central importance of dimer dissociation in the initiation of SOD1 aggregation (13, 14), the high levels of glutathionylated SOD1 expected to be present in an oxidatively stressed motor neuron could trigger or exacerbate dysfunction by substantially increasing the monomer population. A prolonged shift in the monomer-dimer equilibrium, especially in harsh conditions, would result in increased populations of metal-free, misfolded, and aggregated SOD1 (Figure 2.6). It has been observed that Cys-111 mediates mutant SOD1 aggregation in a cell culture model of ALS and that overexpression of glutaredoxin-1 (which reduces both protein-protein and protein-glutathione disulfides) or mutation of Cys-111 attenuate this toxic process (41). While initially interpreted as further evidence of the involvement of intermolecular disulfide bonds in aggregate formation (30, 42), these data also support the hypothesis that destabilization caused by Cys-111 glutathionylation promotes aggregation and cell death in ALS. The A4V and I112T mutant SODs are affected differently by glutathionylation, suggesting differing sensitivities of these SOD1 variants to an oxidizing intracellular environment. These differences could explain some of the variability in disease progression among the over 140 mutations implicated in the familial form of the disease. Furthermore, the significant destabilization of both wild type SOD1 and the FALS mutant A4V by glutathione suggests that

this modification could promote formation of non-native SOD1 oligomers in both sporadic and familial ALS cases. The modulation of SOD1 dimer stability by cysteine-111 glutathionylation, a post-translational modification linked to redox status, suggests a novel mechanism by which oxidative stress and SOD1 aggregation are interconnected in ALS pathology.

REFERENCES

1. Khare, S., Caplow, M., and Dokholyan, N. (2006) FALS mutations in Cu, Zn superoxide dismutase destabilize the dimer and increase dimer dissociation propensity: a large-scale thermodynamic analysis, *Amyloid 13*, 226-235.

2. Wang, Q., Johnson, J., Agar, N., and Agar, J. (2008) Protein aggregation and protein instability govern familial amyotrophic lateral sclerosis patient survival, *PLoS Biol 6*, e170.

3. Sandelin, E., Nordlund, A., Andersen, P. M., Marklund, S. S. L., and Oliveberg, M. (2007) Amyotrophic Lateral Sclerosis-associated Copper/Zinc Superoxide Dismutase Mutations Preferentially Reduce the Repulsive Charge of the Proteins, *Journal of Biological Chemistry 282*, 21230 -21236.

4. Bystrom, R., Andersen, P., Grobner, G., and Oliveberg, M. (2010) SOD1 mutations targeting surface hydrogen bonds promote amyotrophic lateral sclerosis without reducing apo-state stability, *J.Biol.Chem. 285*, 19544-19552.

5. Lindberg, M. J., Byström, R., Boknäs, N., Andersen, P. M., and Oliveberg, M. (2005) Systematically perturbed folding patterns of amyotrophic lateral sclerosis (ALS)-associated SOD1 mutants, *Proceedings of the National Academy of Sciences of the United States of America 102*, 9754 -9759.

6. Bosco, D. A., Morfini, G., Karabacak, N. M., Song, Y., Gros-Louis, F., Pasinelli, P., Goolsby, H., Fontaine, B. A., Lemay, N., McKenna-Yasek, D., Frosch, M. P., Agar, J. N., Julien, J., Brady, S. T., and Brown, R. H. (2010) Wild-type and mutant SOD1 share an aberrant conformation and a common pathogenic pathway in ALS, *Nat Neurosci 13*, 1396-1403.

7. Forsberg, K., Jonsson, P. A., Andersen, P. M., Bergemalm, D., Graffmo, K. S., Hultdin, M., Jacobsson, J., Rosquist, R., Marklund, S. L., and Brännström, T. (2010) Novel Antibodies Reveal Inclusions Containing Non-Native SOD1 in Sporadic ALS Patients, *PLoS ONE 5*, e11552.

8. Higgins, G., Beart, P., Shin, Y., Chen, M., Cheung, N., and Nagley, P. (2010) Oxidative stress: emerging mitochondrial and cellular themes and variations in neuronal injury, *J Alzheimers.Dis. 20 Suppl 2*, S453-S473.

9. Jellinger, K. (2010) Basic mechanisms of neurodegeneration: a critical update, *J Cell Mol Med. 14*, 457-487.

10. le-Donne, I., Rossi, R., Colombo, G., Giustarini, D., and Milzani, A. (2009) Protein S-

glutathionylation: a regulatory device from bacteria to humans, *Trends Biochem Sci 34*, 85-96.

11. Townsend, D. (2007) S-glutathionylation: indicator of cell stress and regulator of the unfolded protein response, *Mol Interv. 7*, 313-324.

12. Wilcox, K., Zhou, L., Jordon, J., Huang, Y., Yu, Y., Redler, R., Chen, X., Caplow, M., and Dokholyan, N. (2009) Modifications of superoxide dismutase (SOD1) in human erythrocytes: a possible role in amyotrophic lateral sclerosis, *J Biol Chem 284*, 13940-13947.

13. Khare, S., Caplow, M., and Dokholyan, N. (2004) The rate and equilibrium constants for a multistep reaction sequence for the aggregation of superoxide dismutase in amyotrophic lateral sclerosis, *Proc Natl Acad Sci U S A 101*, 15094-15099.

14. Rakhit, R., Crow, J., Lepock, J., Kondejewski, L., Cashman, N., and Chakrabartty, A. (2004) Monomeric Cu,Zn-superoxide dismutase is a common misfolding intermediate in the oxidation models of sporadic and familial amyotrophic lateral sclerosis, *J Biol Chem 279*, 15499-15504.

15. Doucette, P., Whitson, L., Cao, X., Schirf, V., Demeler, B., Valentine, J., Hansen, J., and Hart, P. (2004) Dissociation of human copper-zinc superoxide dismutase dimers using chaotrope and reductant. Insights into the molecular basis for dimer stability, *J Biol Chem 279*, 54558-54566.

16. Felinger, A., Pasti, L., Dondi, F., van, H. M., Schoenmakers, P., and Martin, M. (2005) Stochastic theory of size exclusion chromatography: peak shape analysis on single columns, *Anal.Chem 77*, 3138-3148.

17. Janson, J., and Rydén, L. (1998) Protein purification: principles, high-resolution methods, and applications. Wiley-VCH.

18. Caplow, M., and Fee, L. (2002) Dissociation of the tubulin dimer is extremely slow, thermodynamically very unfavorable, and reversible in the absence of an energy source, *Mol Biol Cell 13*, 2120-2131.

19. Niebergall, P., and Sugita, E. (1968) Utilization of the Guggenheim method in kinetics, *J Pharm.Sci 57*, 1805-1808.

20. Schuck, P. (1997) Reliable determination of binding affinity and kinetics using surface plasmon resonance biosensors, *Current Opinion in Biotechnology 8*, 498-502.

21. Wang, Y., He, H., and Li, S. (2010) Effect of Ficoll 70 on thermal stability and structure of

creatine kinase, *Biochemistry (Mosc.) 75*, 648-654.

22. Ramsay, G. D., and Eftink, M. R. (1994) [27] Analysis of multidimensional spectroscopic data to monitor unfolding of proteins, in *Part B: Numerical Computer Methods*, pp 615-645. Academic Press.

23. Becktel, W. J., and Schellman, J. A. (1987) Protein stability curves, *Biopolymers 26*, 1859-1877.

24. Yin, S., Ding, F., and Dokholyan, N. (2007) Eris: an automated estimator of protein stability, *Nat.Methods 4*, 466-467.

25. Ding, F., and Dokholyan, N. (2006) Emergence of protein fold families through rational design, *PLoS Comput.Biol 2*, e85.

26. Ding, F., Tsao, D., Nie, H., and Dokholyan, N. (2008) Ab initio folding of proteins with all-atom discrete molecular dynamics, *Structure 16*, 1010-1018.

27. Dokholyan, N., Buldyrev, S., Stanley, H., and Shakhnovich, E. (1998) Discrete molecular dynamics studies of the folding of a protein-like model, *Fold.Des 3*, 577-587.

28. Kota, P., Ding, F., Ramachandran, S., and Dokholyan, N. V. (2011) Gaia: Automated Quality Assessment of Protein Structure Models, *Bioinformatics*.

29. DiDonato, M., Craig, L., Huff, M., Thayer, M., Cardoso, R., Kassmann, C., Lo, T., Bruns, C., Powers, E., Kelly, J., Getzoff, E., and Tainer, J. (2003) ALS mutants of human superoxide dismutase form fibrous aggregates via framework destabilization, *J Mol Biol 332*, 601-615.

30. Banci, L., Bertini, I., Durazo, A., Girotto, S., Gralla, E., Martinelli, M., Valentine, J., Vieru, M., and Whitelegge, J. (2007) Metal-free superoxide dismutase forms soluble oligomers under physiological conditions: a possible general mechanism for familial ALS, *Proc Natl Acad Sci U S A 104*, 11263-11267.

31. Schmidlin, T., Kennedy, B., and Daggett, V. (2009) Structural changes to monomeric CuZn superoxide dismutase caused by the familial amyotrophic lateral sclerosis-associated mutation A4V, *Biophys J 97*, 1709-1718.

32. Ray, S., Nowak, R., Strokovich, K., Brown, R., Walz, T., and Lansbury, P. (2004) An intersubunit disulfide bond prevents in vitro aggregation of a superoxide dismutase-1 mutant linked to familial amytrophic lateral sclerosis, *Biochemistry 43*, 4899-4905.

33. Hough, M., Grossmann, J., Antonyuk, S., Strange, R., Doucette, P., Rodriguez, J., Whitson, L., Hart, P., Hayward, L., Valentine, J., and Hasnain, S. (2004) Dimer destabilization in superoxide dismutase may result in disease-causing properties: structures of motor neuron disease mutants, *Proc Natl Acad Sci U S A 101*, 5976-5981.

34. Proctor, E. A., Ding, F., and Dokholyan, N. V. (2011) Structural and Thermodynamic Effects of Post-translational Modifications in Mutant and Wild Type Cu, Zn Superoxide Dismutase, *Journal of Molecular Biology 408*, 555-567.

35. Ferraroni, M., Rypniewski, W., Wilson, K., Viezzoli, M., Banci, L., Bertini, I., and Mangani, S. (1999) The crystal structure of the monomeric human SOD mutant F50E/G51E/E133Q at atomic resolution. The enzyme mechanism revisited, *J Mol Biol 288*, 413-426.

36. Heikkila, R. E., and Cabbat, F. (1976) A sensitive assay for superoxide dismutase based on the autoxidation of 6-hydroxydopamine, *Analytical Biochemistry 75*, 356-362.

37. Esteban, J., Rosen, D., Bowling, A., Sapp, P., Kenna-Yasek, D., O'Regan, J., Beal, M., Horvitz, H., and Brown, R. (1994) Identification of two novel mutations and a new polymorphism in the gene for Cu/Zn superoxide dismutase in patients with amyotrophic lateral sclerosis, *Hum.Mol Genet. 3*, 997-998.

38. Dringen, R. (2000) Metabolism and functions of glutathione in brain, *Prog.Neurobiol. 62*, 649-671.

39. Nakanishi, T., Kishikawa, M., Miyazaki, A., Shimizu, A., Ogawa, Y., Sakoda, S., Ohi, T., and Shoji, H. (1998) Simple and defined method to detect the SOD-1 mutants from patients with familial amyotrophic lateral sclerosis by mass spectrometry, *J Neurosci.Methods 81*, 41-44.

40. Marklund, S., Andersen, P., Forsgren, L., Nilsson, P., Ohlsson, P., Wikander, G., and Oberg, A. (1997) Normal binding and reactivity of copper in mutant superoxide dismutase isolated from amyotrophic lateral sclerosis patients, *J Neurochem. 69*, 675-681.

41. Cozzolino, M., Amori, I., Pesaresi, M., Ferri, A., Nencini, M., and Carri, M. (2008) Cysteine 111 affects aggregation and cytotoxicity of mutant Cu,Zn-superoxide dismutase associated with familial amyotrophic lateral sclerosis, *J.Biol.Chem. 283*, 866-874.

42. Karch, C., Prudencio, M., Winkler, D., Hart, P., and Borchelt, D. (2009) Role of mutant SOD1 disulfide oxidation and aggregation in the pathogenesis of familial ALS, *Proc.Natl.Acad.Sci.U.S.A 106*, 7774-7779.

CHAPTER THREE

NON-NATIVE SOLUBLE SOD1 OLIGOMERS CONTAIN A CONFORMATIONAL EPITOPE LINKED TO CYTOTOXICITY IN ALS

Introduction

Accumulating evidence supports a prominent contribution of misfolding and aggregation of SOD1 to the dysfunction and progressive death of motor neurons in ALS. Over 140 mutations (mostly missense) in the *SOD1* gene have been identified in patients with familial ALS (FALS), most of which destabilize the native SOD1 homodimer and/or increase aggregation propensity (1, 2). Current evidence supports the pathogenic capacity of soluble misfolded SOD1, rather than the large insoluble aggregates that appear only near the onset of paralysis in ALS mouse models (3–7). However, little is known about the structural features of soluble non-native SOD1 conformers or the factors in the cellular environment that influence misfolding and aggregation. Soluble misfolded WT SOD1 has been found in spinal cord from sporadic ALS patients that do not carry mutations in *SOD1* (8, 9), demonstrating the sufficiency of non-genetic factors to induce formation of potentially toxic oligomers by SOD1.

To identify misfolded SOD1 conformers with greatest relevance to ALS pathology, we probed isolated oligomeric species with a conformation-specific antibody (C4F6) to identify those with potential cytotoxicity. In FALS patients and mouse models, C4F6 specifically recognizes soluble SOD1 found only in disease-affected tissue, suggesting a connection between

FALS pathology and the as-yet unidentified epitope bound by C4F6 (7). Here we show that higher-order non-native oligomers of mutant SOD1, but not dimers or monomers, contain the epitope recognized by the C4F6 antibody. To assess the impact of the cellular redox environment on formation of potentially toxic soluble oligomers, we determine the effect of a physiologically prevalent oxidative modification (glutathionylation at Cys-111) on oligomerization. Cys-111 glutathionylation increases both abundance of soluble oligomers and exposure of the disease-specific epitope recognized by C4F6, revealing a novel mechanism by which oxidative stress modulates potentially toxic SOD1 aggregation. Our results suggest that SOD1 acquires pathogenic features upon formation of soluble non-native oligomeric assemblies, indicating a particular relevance of these species to neuronal dysfunction in ALS.

Methods

Cloning, expression and purification of recombinant SOD1 from S. cerevisiae

Mutagenesis of constructs for expression of human SOD1, expression in *S. cerevisiae*, and SOD1 purification were performed according to previously published methods (10, 11). The final step of purification of recombinant SOD1 is anion-exchange chromatographic separation using a MonoQ HR 10/10 column connected to an AKTA purifier system (GE Healthcare), which separates a population of predominantly unmodified SOD1 from one enriched in SOD1 that is glutathionylated at Cys-111 (10). Samples were stored at -80°C in 20 mM Tris, 150 mM NaCl, pH 7.4 until use.

High-resolution mass determination of intact recombinant SOD1

SOD1 sample buffer was exchanged with 10 mM ammonium acetate using 2 KDa VIVACON 500 filtration devices (Sartorius Stedim Biotech GmbH), after which samples were collected by centrifugation of the inverted concentrator body within a fresh tube. These samples were then diluted 1:10 in a 50% acetonitrile/49% water/1% formic acid mixture and directly infused into the LTQ Orbitrap Velos (Thermo Fisher Scientific) using a Picoview nanoelectrospray source (New Objective). Spectra were collected with the Orbitrap analyzer in positive ion mode at a resolution of 30,000 (at 400 m/z), with maximum ion injection time of 200 ms, spray voltage of 5KV, and the automatic gain control (AGC) set to 2×10^5. Spectra were deconvoluted using Promass for Xcalibur, Ver. 2.5 SR-1 (Thermo Fisher Scientific).

Time-resolved analytical size exclusion chromatography (SEC)

Cu^{2+} and Zn^{2+} were removed from as-isolated remetallated SOD1 by dialysis against 50 mM sodium acetate, 10 mM EDTA, pH 3.8 for 1.5 hours in the case of mutant SOD1 and 2 hours in the case of the WT enzyme. Complete removal of copper and zinc was confirmed by inductively coupled plasma mass spectrometry (data not shown). Removal of EDTA and return to physiological pH were achieved by overnight dialysis against 20 mM Tris, 150 mM NaCl, pH 7.4. All dialysis was performed at 4°C. Demetallated ("apo") SOD1 was brought to a concentration of 100 μM in 20 mM Tris, 150 mM NaCl, pH 7.4 and incubated in a 37°C water bath. At each indicated time point, an aliquot containing 64 μg of apo-SOD1 was removed, filtered using a 0.22 μm centrifugal filter and injected onto a Superdex 200 10/300 GL column (GE Healthcare) at 4°C equilibrated in 20 mM Tris, 150 mM NaCl, pH 7.4.

Estimation of molecular weight of oligomers using size exclusion chromatography combined with multi-angle light scattering (SEC-MALS)

Apo-SOD1 incubated for 1 week under the pH, temperature, and ionic strength conditions listed above was analyzed using a DAWN HELEOS II light scattering instrument (Wyatt Technology), which detects scattered light at 18 angles with respect to the incident beam. The light scattering instrument is interfaced to an Agilent FPLC System with a connected Superdex 200 10/300 GL column (GE Healthcare), a T-rEX refractometer, and a dynamic light scattering module (Wyatt Technology). SEC separation and detection by MALS were performed at room temperature. Data were analyzed and weight average molar masses as a function of elution volume were determined using ASTRA software (Wyatt Technology) with the Zimm fit method, which assumes weak protein-solvent interactions (38).

Measurement of C4F6 epitope exposure of isolated apo-SOD1 oligomer populations

Apo-SOD1 oligomers were prepared by incubation at 100 μM in 20 mM Tris, 150 mM NaCl, pH 7.4 at 37°C for 1 week. Samples containing 640 μg of apo-SOD1 were filtered and separated by SEC as described above. Immediately following elution, individual oligomeric populations were collected and individually loaded onto PVDF membranes equilibrated in 20 mM Tris pH 7.4 using a chilled Minifold I dot-blot system (S&S). Samples were blotted in duplicate simultaneously; one blot was immediately incubated with monoclonal antibody to misfolded SOD1 (C4F6, MediMabs) diluted 1:250 in blocking buffer (TBS-T with 5% (w/v) nonfat dry milk); the duplicate blot was stained with Ponceau S in 5% acetic acid to visualize

total protein loaded onto the membrane. Duplicate blotting was carried out in lieu of fixation with Ponceau S prior to incubation with primary antibody due to our observation of increased C4F6 reactivity following Ponceau S staining and destaining, as well as to minimize the time elapsed between isolation of oligomers by SEC and probing with C4F6. Blots were incubated with C4F6 overnight at 4°C and C4F6 binding was visualized using HRP-conjugated anti-mouse antibodies (GE Healthcare, Pierce, Millipore).

To quantify abundance of individual oligomeric populations represented in SEC chromatograms, A_{280} data from V_e = 7.5 – 19 ml were deconvoluted into multiple single Gaussian distributions using Matlab (Mathworks), and the area under each Gaussian curve was calculated as a percentage of the total area under all Gaussian curves in the deconvoluted chromatogram. For comparison of oligomeric populations in glutathionylated and unmodified apo-SOD1, oligomers were grouped based on V_e at the center of the Gaussian curve obtained by deconvolution: O1 consists of oligomers eluting between 14 and 15 ml, O2 consists of oligomers eluting between 11.3 and 13.5 ml, O3 consists of oligomers eluting between 9.2 and 11.2 ml, and V_o consists of oligomers eluting between 8.0 and 9.0 ml (corresponding to the approximate void volume of the column).

Effect of reducing agent treatment on apo-SOD1 oligomer stability

Oligomers of apo-SOD1 were prepared as described above and DTT was added to a final concentration of 1 mM to the sample and SEC running buffer. Aliquots from the mixture of oligomers were separated by SEC as described above immediately following addition of DTT and after two hours and overnight incubation at room temperature.

Results

Formation of metastable soluble oligomers by apo-SOD1 with FALS-linked substitutions

To identify potentially disease-relevant metastable SOD1 oligomers, we incubated apo-SOD1 at physiological pH, temperature, ionic strength, and SOD1 concentration for up to one week, separating the reaction mixture by SEC at multiple time points. We use recombinant protein in which SOD1's native free cysteines (Cys-6 and Cys-111) are retained, as they have

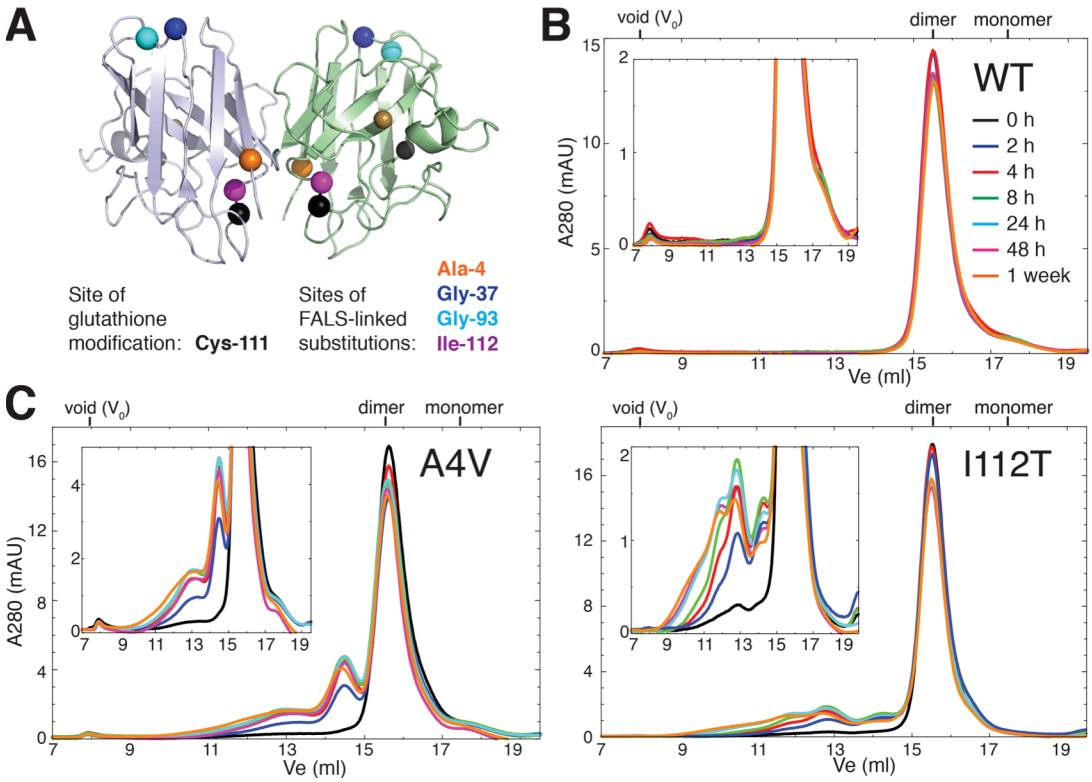

Figure 3.1. Formation of metastable soluble non-native oligomers of metal-free SOD1. (A) Positions of the glutathione modification and of the FALS-linked amino acid substitutions included in the current study; residue positions are indicated by colored spheres on the background of the WT SOD1 crystal structure (PDB ID: 1spd). (B) SEC chromatograms showing aggregation of 100 μM apo-WT SOD1 at 37°C in 20 mM Tris, 150 mM NaCl, pH 7.4 for up to 1 week. (C) Aggregation of 100 μM apo-SOD1 with the indicated FALS-linked amino acid substitutions under identical conditions as described for (B). Insets show chromatograms with expanded y-axes.

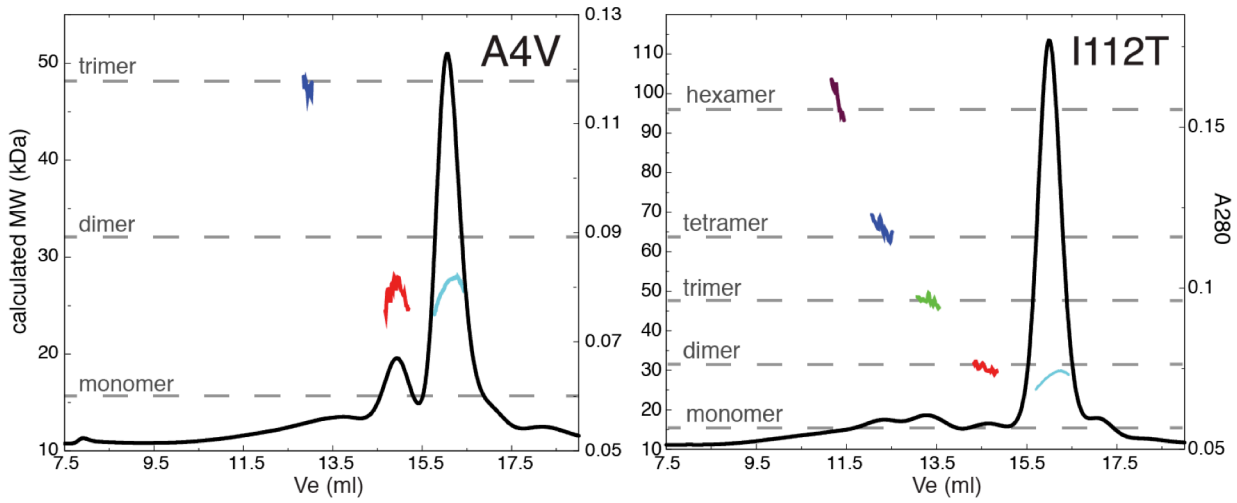

Figure 3.2. Estimation of apoSOD1 oligomer size by SEC-MALS. Weight average molar masses of metastable soluble SOD1 oligomers separated by SEC, as determined by multi-angle light scattering (SEC-MALS). Black curves: Absorbance at 280 nm (A280) vs. elution volume (V_e); colored curves: molecular weight (MW) calculated at each V_e from the intensities of scattered light at multiple fixed detectors. Dashed grey lines indicate approximate theoretical molecular masses for SOD1 oligomers.

been demonstrated to play crucial roles in oligomerization (12, 13). Metal-free ("apo") SOD1 is utilized in all experiments since it is widely considered to be the common precursor to misfolded and aggregated species (4, 14, 15). We analyze soluble oligomers because of their particular relevance to ALS pathology; apo-SOD1 remains soluble throughout the 1-week incubation period, as evidenced by the minimal changes in total A_{280} from SEC chromatograms (Figures 3.1B, 3.1C). WT SOD1 (Figure 3.1B) and SOD1 containing the FALS-linked G93A and G37R substitutions (black curves, Figure 2B) have low propensities to form soluble oligomers under these conditions, whereas SOD1 with the A4V or I112T substitutions shows substantial oligomerization (Figure 3.1C). Analysis of SEC-separated oligomers with multi-angle light scattering is consistent with the presence of native-like dimers, non-native-like expanded dimers, trimers, tetramers, and hexamers (Figure 3.2). The presence of an expanded dimer is inferred from the SEC-MALS data based on the presence of a peak eluting before the native-like dimer (indicating its larger hydrodynamic radius), yet having a calculated molecular weight equivalent

to that of the native-like dimer (red vs. cyan curves, Figure 3.2). In the case of the aggregation-prone A4V and I112T variants, small soluble oligomers are apparent by 2 hours of incubation at 37°C (Figure 3.1C) and remain detectable throughout the 1-week incubation period. The smallest non-native oligomers (those eluting near 13 ml and 14.5 ml following injection onto the gel filtration column) increase in abundance for the first 8-24 hours, after which their populations decline concomitant with the appearance of higher-order species (Figure 3.1C).

Glutathionylation at Cys-111 induces monomerization of apo-SOD1 and increases propensity to form non-native oligomers

Protein S-glutathionylation is a reversible post-translational modification that serves, in addition to regulatory and signaling functions, as a protective measure against irreversible oxidation of cysteines (16). SOD1 glutathionylated at Cys-111 is abundant in SOD1 isolated from human tissue or expressed in *S. cerevisiae*, can be partially resolved from the unmodified enzyme by ion-exchange chromatography, and destabilizes the holo-SOD1 dimer (10, 17–19). To assess the effects of Cys-111 glutathionylation on assembly of soluble SOD1 oligomers, we analyzed the impact of this modification on the oligomeric distributions of soluble WT and mutant apo-SOD1. For each SOD1 variant studied, a predominantly unmodified SOD1 population and one enriched in glutathionylated SOD1 (GS-SOD1) (Figure 3.3A) were incubated at physiological pH, temperature, ionic strength, and SOD1 concentration. We assess the effect

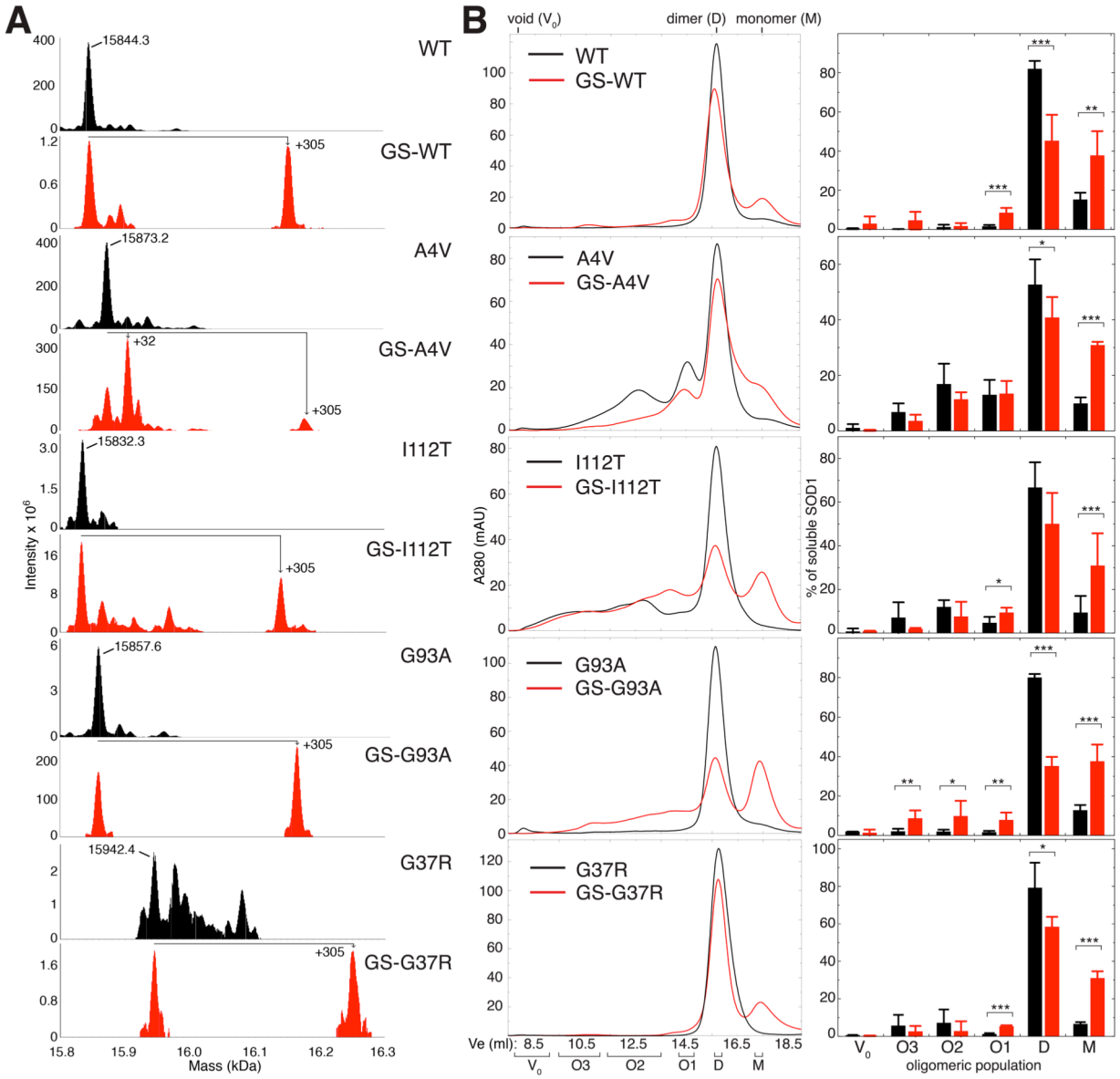

Figure 3.3. Cys-111 glutathionylation promotes the formation of non-native apo-SOD1 oligomers. (A) Analysis of full-length SOD1 by mass spectrometry. For each SOD1 variant studied, deconvoluted mass spectra are shown for two populations separated by ion exchange chromatography: one in which unmodified SOD1 is the predominant species (black spectra), and one enriched in post-translationally modified SOD1 (red spectra). Labeled masses correspond to the average masses obtained by deconvolution of spectra using ProMass for Xcalibur software. (B) Left, SEC chromatograms showing populations of soluble metastable oligomers of unmodified (black) and glutathionylated (red) apo-SOD1 incubated at 100 μM (initial dimeric concentration) for 1 week at 37°C in 20 mM Tris, 150 mM NaCl, pH 7.4. Right, oligomeric populations quantified by deconvolution of SEC data and integration of Gaussian curves corresponding to individual oligomeric populations. Bar heights represent average values and error bars represent S. D. from at least 3 independent experiments. Student's t-test was used to compare the abundance of oligomers in the presence and absence of Cys-111 glutathionylation. * = $p \leq 0.05$; ** = $p \leq 0.01$; *** = $p \leq 0.001$.

of glutathionylation on oligomer formation by comparing these two populations of recombinant human SOD1, which are modified endogenously as the protein is expressed in *S. cerevisiae*. The GS-SOD1 population is not subjected to further *in vitro* glutathionylation in order to avoid modification of Cys-6, which is not glutathionylated in SOD1 isolated from human tissue (10).

For the wild type as well as all FALS mutants studied, glutathionylation of apo-SOD1 results in a significant increase in the proportion of soluble protein present as monomers (Figure 3.3B). Glutathionylation also significantly increases the abundance of several non-native higher-order species, especially in G93A SOD1 (Figure 3.3B). In all variants except A4V SOD1, glutathionylation significantly increases formation of the oligomeric population eluting just prior to the native-like dimer: O1, the putative expanded dimer (Figures 3.3B, 3.2).

Metastable oligomers show enhanced exposure of an epitope common to SOD1 found in ALS patients

Though soluble misfolded SOD1 (as opposed to that which is present in insoluble aggregates) is increasingly implicated in motor neuron dysfunction (4, 5, 20, 21), the potential cytotoxicities of individual oligomeric species have not been evaluated. Direct determination of the effects of specific oligomers on motor neuron viability is complicated by the difficulty of delivering metastable protein assemblies to the cytoplasm of living cells. To begin to evaluate the cytotoxic potential of the apo-SOD1 oligomers we isolate by SEC, we probed for exposure of an epitope known to be exposed on misfolded SOD1 in disease-affected cell populations of ALS patients (7, 8). The various apo-SOD1 oligomeric populations isolated by SEC and dimeric holo-SOD1 were bound to PVDF membranes and probed with the C4F6 conformation-specific

antibody (Figure 3.4). The species with greatest reactivity to C4F6 are higher-order non-native oligomers, those eluting at post-injection volumes ranging from the column void to ~14.5 ml, just prior to elution of native-like SOD1 dimer (Figure 3.4). Monomeric apo-SOD1 is not C4F6-reactive in any of the SOD1 variants studied, while dimeric holo- and apo-SOD1 is faintly reactive in some cases. Oligomers of glutathionylated apo-SOD1 were also probed with C4F6 to determine whether this modification induces structural rearrangements that enhance exposure of the disease-specific epitope. In the case of SOD1 with the FALS-linked A4V or I112T substitutions, glutathionylation enhances exposure of the C4F6-recognized epitope in higher-order soluble oligomers (Figure 3.4), suggesting that glutathionylation

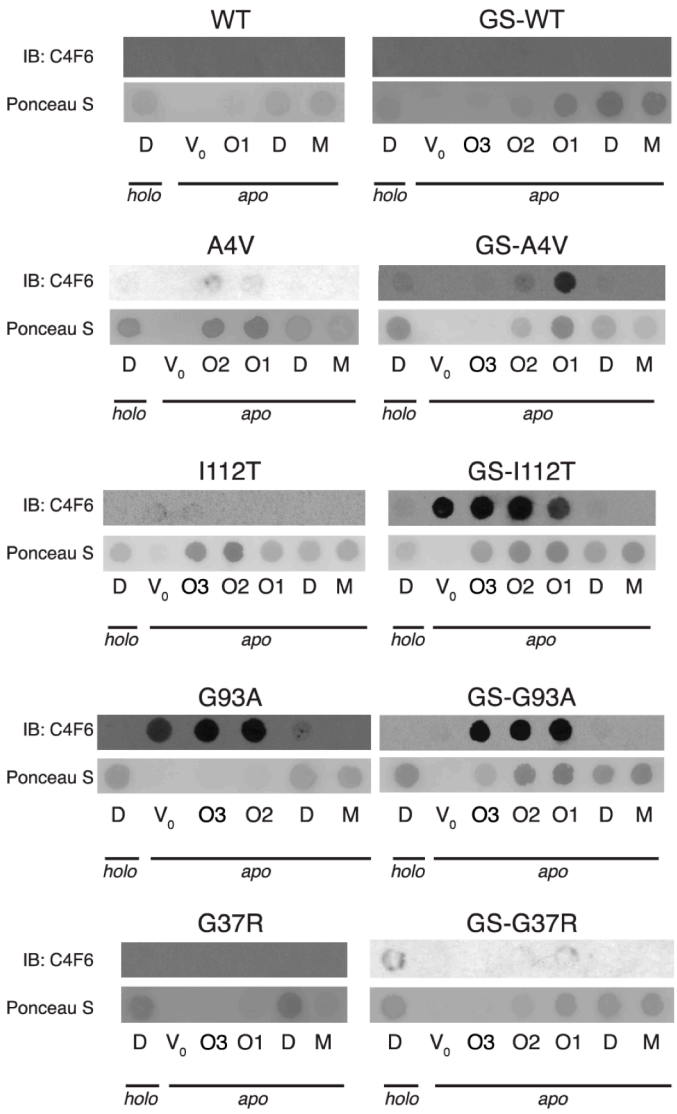

Figure 3.4. Non-native oligomers of SOD1 are potentially toxic in ALS. Dot blots of apo-SOD1 oligomers isolated by SEC and probed with the C4F6 monoclonal conformation-specific antibody, which has been proposed to recognize a toxic subset of misfolded SOD1 (Brotherton et al., 2012). Dimeric SOD1 isolated from *S. cerevisiae* and remetallated ("holo") was also probed to determine initial C4F6 reactivity prior to removal of metals and oligomerization. The amounts of each oligomeric population bound to the membrane were visualized by Ponceau S staining.

substantially alters the conformations of oligomers formed by these disease-associated mutant proteins.

Cys-111 modulates soluble oligomer formation through mechanism(s) independent of intermolecular disulfide bonding

The two free cysteines of SOD1, especially Cys-111, have been recognized to modulate its aggregation propensity (12, 13). The most commonly assumed mechanism by which free cysteines affect aggregation is their participation in intermolecular disulfide bonds that stabilize oligomers (22). However, our findings of decreased dimer stability ((17), Figure 3.3B), altered aggregation propensity (Figure 3.3B), and altered oligomer conformation (Figure 3.4) in GS-SOD1 suggest that glutathionylation affects SOD1 aggregation through complex mechanisms not limited to intermolecular cross-linking through Cys-111. We therefore sought to determine whether intermolecular disulfide bonds are required for stability of the apo-SOD1 oligomers we observe *in vitro*. Oligomers of A4V and I112T SOD1 generated by incubation at physiological pH, temperature, ionic strength, and SOD1 concentration for one week (WT, G93A, and G37R SOD1 form few oligomers under these conditions (Figure 3.3B)) were incubated at room temperature with the reducing agent DTT, and aliquots were removed at various time points for SEC analysis. The largest oligomers, those eluting from the void volume to ~13.5 ml post-injection on the Superdex 200 10/300 GL column, are most sensitive to dissociation by treatment with reducing agent (Figure 3.5). The oligomeric population eluting at ~14.5 ml (O1) is relatively resistant to DTT treatment, exhibiting little decrease in abundance or continuing to accumulate throughout the course of incubation with DTT (Figure 3.5).

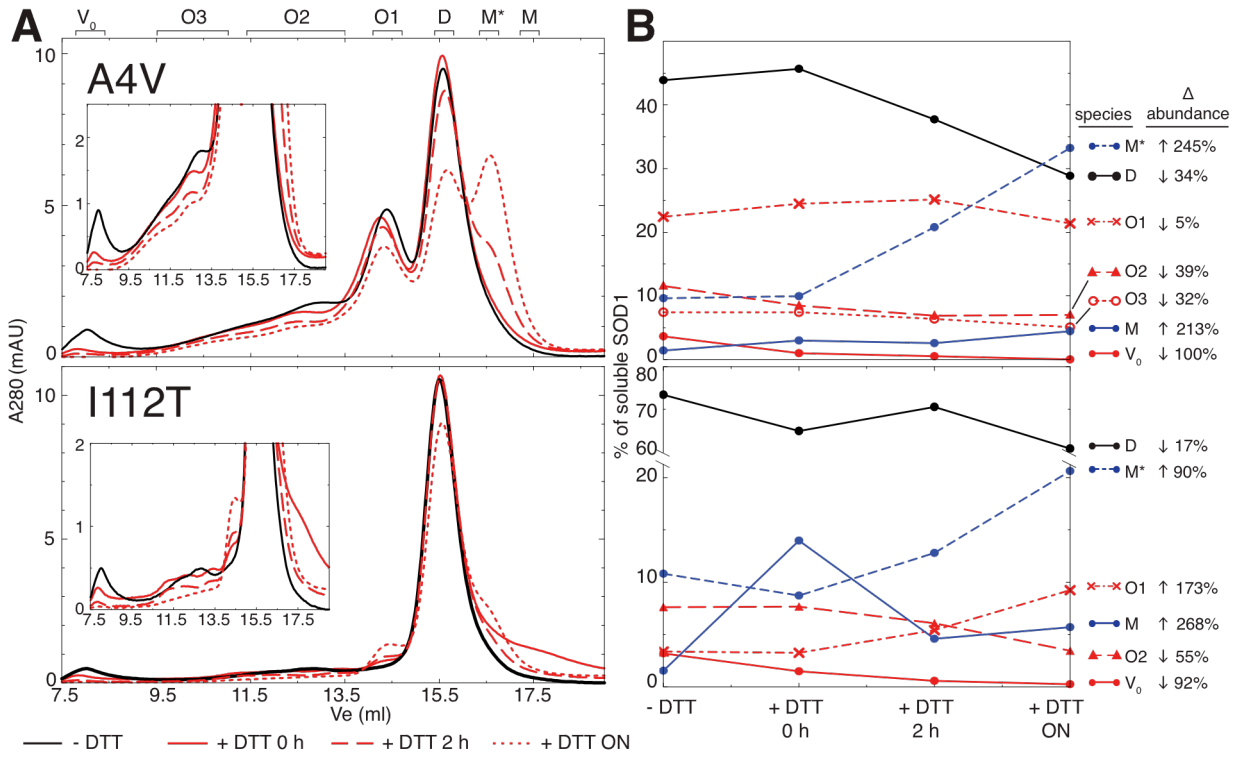

Figure 3.5. Intermolecular disulfide bonding is not universally required for the persistence of metastable non-native oligomers *in vitro*. (A) Apo-SOD1 oligomers generated by incubation for 1 week at 37°C in 20 mM Tris, 150 mM NaCl, pH 7.4 were separated by SEC in the absence (black curves) of DTT and in the presence of 1 mM DTT following incubation at room temperature (red curves). Designations of oligomeric populations (D, M, O1, O2, O3, and V_0) correspond to those in Figure 2A, while M* denotes a species that that appears subsequent to DTT treatment and whose elution volume is consistent with an expanded monomer. (B) Quantification of oligomeric populations prior to DTT treatment and after room temperature incubation with 1 mM DTT for the indicated time periods. ON = overnight incubation.

Discussion

Relevance of the in vitro *system to pathological SOD1 aggregation in ALS*

Although misfolding and aggregation of SOD1 is believed to be a major contributor to ALS pathology, little is known about the potential toxicities of individual aggregate species or

the cellular determinants of their formation. Here we examine the propensities of WT and FALS mutant SOD1 to form metastable soluble oligomers with an epitope linked to toxicity in ALS, and explore the effects of oxidative modification of Cys-111, a residue known to modulate SOD1 aggregation. We assess oligomerization of SOD1 under conditions approximating physiological pH (7.4), temperature (37°C), and SOD1 concentration (100 μM, (22)), without agitation. The degrees to which the various FALS-linked mutations increase SOD1 destabilization and aggregation propensity have been shown to be correlated with disease severity (2). Although this correlation was recently challenged (23), this latter study employed the use of SOD1 in which both free cysteines (at positions 6 and 111) are mutated to alanine and serine, respectively, potentially restricting the applicability to physiological SOD1 aggregation. We find that the A4V and I112T substitutions, which are found in patients with rapidly-progressing FALS (2), exhibit the highest propensities to form soluble oligomers (Figures 3.1C, 3.3B). These results would be predicted by the correlation of aggregation propensity with disease severity, as would the minimal aggregation of SOD1 containing the G37R substitution (black curve, Figure 3.3B), which causes relatively slowly-progressing paralysis in ALS patients and mouse models (2, 24). The higher oligomerization propensity we observe for the A4V and I112T variants may stem from the proximity of these substitutions to the native homodimeric interface. The average disease duration (taken from the meta-analysis by Wang *et al*. (2)) for patients harboring the G93A mutation (3.1 years, n = 16) is closer to that of patients with A4V (1.2 years, n = 205) or I112T (0.9 years, n = 2) substitutions than to that associated with the G37R mutation (17 years, n = 27). Despite causing relatively rapidly-progressing FALS, the G93A substitution was linked to very minimal aggregation of apo-SOD1 under the conditions of our assay (black curve, Figure 3.3B), making it the only SOD1 variant in our study whose propensity to form

soluble oligomers was not consistent with the previously-reported correlation between SOD1 aggregation propensity and disease severity in FALS (2).

Identification of species with potential toxicity in ALS

While we observe differences in aggregation propensities among the SOD1 variants studied, the formation of certain metastable non-native oligomers (such as those eluting at 14.5 ml) by both wild type and FALS mutant SOD1 suggests that some common mechanism(s) underlie SOD1 oligomerization. To explore potentially unifying conformational changes that occur as apo-SOD1 transitions from dimeric to monomeric and higher-order oligomeric species, we analyzed exposure of a putatively disease-relevant epitope. The epitope recognized by C4F6 is not known, but this antibody binds to soluble misfolded SOD1 in disease-affected motor neuron populations in ALS patient spinal cord (7, 8), For this reason, the C4F6 monoclonal antibody has been proposed to recognize an epitope present specifically in toxic conformers of SOD1 (7). We find that the C4F6 antibody binds to several higher-order oligomers of apo-SOD1, but not to monomers and rarely to native-like dimers (Figure 3.4). The C4F6 antibody was raised against apo-G93A, and has been shown to have specific reactivity to this sequence element (WT SOD1, FALS mutants other than G93A, and SOD1 with other substitutions other than alanine at position 93 show little reactivity to C4F6 when denatured) (8, 24). However, C4F6 also exhibits conformation-specific reactivity, which is not restricted to G93A under nondenaturing conditions (8). We probe apo-SOD1 oligomers under nondenaturing conditions in order to detect species with the conformation-specific epitope recognized by C4F6 in ALS-affected motor neurons. The strong C4F6 reactivity of unmodified apo-G93A oligomers may owe partially to recognition of

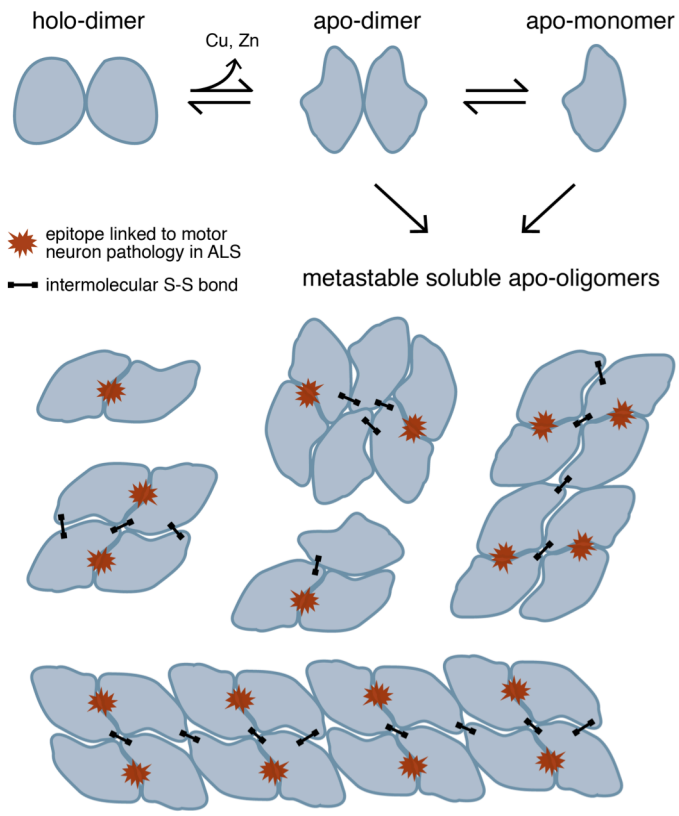

Figure 3.6. Model of early SOD1 oligomerization. Following loss of metals and dimer dissociation, apoSOD1 acquires potentially pathogenic conformational features upon assembly into soluble higher-order oligomers. Red stars represent the epitope recognized by the C4F6 conformation-specific antibody. Intermolecular disulfide bonds stabilize some, but not all, of these non-native oligomers.

the G93A sequence epitope. Interestingly, non-native oligomers of unmodified G93A still exhibit robust C4F6 reactivity relative to that of dimers and monomers, despite their very low abundance. Previous work has implicated soluble misfolded SOD1 in a range of oligomeric states in specific cytotoxic phenomena (5, 20, 21). Our findings suggest that, of the pool of soluble species formed by apo-SOD1 *in vitro*, metastable oligomers larger than the native dimer are the most likely toxic culprits (modeled in Figure 3.6).

Oxidative modification of Cys-111 induces conformational changes that promote oligomer assembly and exposure of the disease-linked C4F6 epitope

Oxidation of SOD1 has been shown to induce its misfolding and aggregation (8, 25, 26), and various oxidized forms of SOD1 have been linked to toxicity in cultured neurons (27), a mouse model of FALS (28), and a subset of sporadic ALS cases (29). In particular, the presence

of an oxidizable cysteine at position 111 has been shown to promote SOD1 aggregation (12, 26), an effect that has been widely attributed to stabilization of insoluble aggregates and soluble oligomers by intermolecular disulfide bonds involving Cys-111 (13, 22, 28, 30). However, others have suggested that intermolecular disulfide cross-linking is a secondary event to non-native oligomer assembly and is not universally present in SOD1 oligomers (31, 32).

We find that glutathionylation of Cys-111, a reversible oxidative modification present extensively on SOD1 from human tissue (10, 19, 33), increases the proportion of monomeric apo-SOD1 in all studied variants and enhances the formation of several soluble non-native oligomers (Figure 3.3B). This observation, as well as the increased C4F6 reactivity of GS-I112T-SOD1 and GS-A4V-SOD1 oligomers (Figure 3.4), suggests that conformational changes in SOD1 induced by Cys-111 glutathionylation (17, 18) have significant effects on the abundance and morphologies of SOD1 oligomers. We also find that while intermolecular disulfide bonds stabilize higher-order soluble SOD1 oligomers, these bonds are absent or not essential for stability in the smallest and earliest-appearing non-native oligomers (the O1 population, Figure 3.5).

Taken together, these results suggest that intermolecular disulfide cross-linking represents just one mechanism by which Cys-111 facilitates oligomerization. At the earliest stages of SOD1 misfolding and aggregation, oxidative modification of Cys-111 induces conformational changes that destabilize the dimer (17, 18) and favor assembly into potentially toxic non-native oligomers (Figures 3.3B, 3.4). Given the central role of Cys-111 in SOD1 aggregation (12) and the abundance of glutathionylated SOD1 in human tissue (10), we hypothesize that Cys-111 glutathionylation is a physiologically relevant mechanism by which oxidative stress induces aberrant oligomerization of SOD1.

Overall, our results highlight the toxic potential of soluble oligomers of apo-SOD1 and demonstrate the ability of Cys-111 oxidation to promote formation of oligomers with the disease-linked epitope. The latter finding implicates oxidative stress as a factor in the cellular environment that can induce formation of potentially toxic SOD1 oligomers. Our use of C4F6 binding as a proxy for disease relevance is, to the best of our knowledge, the first evaluation of the potential toxicities of SOD1 oligomers isolated *in vitro*. Enhanced exposure of the disease-linked epitope in non-native SOD1 oligomers supports a cytotoxic role for these assemblies, in parallel with previous findings directly demonstrating toxicity of small oligomers of Aβ and α-synuclein in models of Alzheimer's disease and Parkinson's disease, respectively (34, 35). A pattern is thus emerging among numerous neurodegenerative disorders in which small oligomers exert neurotoxic effects that are mitigated by assembly into large, insoluble species such as amyloid fibrils (36, 37). Inhibition of small oligomer formation of disease-linked proteins therefore represents a therapeutic approach with potentially broad applicability to many neurodegenerative disorders. Knowledge of atomic-level structural features of putatively toxic soluble SOD1 oligomers and identification of factors modulating their formation would facilitate the direct determination of their contribution(s) to cellular pathology, as well as provide an avenue for development of anti-oligomerization therapeutics for ALS.

REFERENCES

1. Khare SD, Caplow M, Dokholyan NV (2006) FALS mutations in Cu, Zn superoxide dismutase destabilize the dimer and increase dimer dissociation propensity: a large-scale thermodynamic analysis. *Amyloid* 13:226–235.

2. Wang Q, Johnson JL, Agar NY., Agar JN (2008) Protein Aggregation and Protein Instability Govern Familial Amyotrophic Lateral Sclerosis Patient Survival. *PLoS Biol* 6:e170.

3. Wang J, Xu G, Borchelt DR (2002) High Molecular Weight Complexes of Mutant Superoxide Dismutase 1: Age-Dependent and Tissue-Specific Accumulation. *Neurobiology of Disease* 9:139–148.

4. Zetterström P et al. (2007) Soluble misfolded subfractions of mutant superoxide dismutase-1s are enriched in spinal cords throughout life in murine ALS models. *Proc Natl Acad Sci USA* 104:14157–14162.

5. Nishitoh H et al. (2008) ALS-linked mutant SOD1 induces ER stress- and ASK1-dependent motor neuron death by targeting Derlin-1. *Genes Dev* 22:1451–1464.

6. Prudencio M, Durazo A, Whitelegge JP, Borchelt DR (2010) An examination of wild-type SOD1 in modulating the toxicity and aggregation of ALS-associated mutant SOD1. *Hum Mol Genet* 19:4774–4789.

7. Brotherton TE et al. (2012) Localization of a toxic form of superoxide dismutase 1 protein to pathologically affected tissues in familial ALS. *Proc Natl Acad Sci USA* 109:5505–5510.

8. Bosco DA et al. (2010) Wild-type and mutant SOD1 share an aberrant conformation and a common pathogenic pathway in ALS. *Nat Neurosci* 13:1396–1403.

9. Forsberg K, Andersen PM, Marklund SL, Brännström T (2011) Glial nuclear aggregates of superoxide dismutase-1 are regularly present in patients with amyotrophic lateral sclerosis. *Acta Neuropathol* 121:623–634.

10. Wilcox KC et al. (2009) Modifications of superoxide dismutase (SOD1) in human erythrocytes: a possible role in amyotrophic lateral sclerosis. *J Biol Chem* 284:13940–13947.

11. Goscin SA, Fridovich I (1972) The purification and properties of superoxide dismutase from Saccharomyces cerevisiae. *Biochim Biophys Acta* 289:276–283.

12. Cozzolino M et al. (2008) Cysteine 111 Affects Aggregation and Cytotoxicity of Mutant Cu,Zn-superoxide Dismutase Associated with Familial Amyotrophic Lateral Sclerosis. *J Biol Chem* 283:866–874.

13. Ferri A et al. (2010) Glutaredoxin 2 prevents aggregation of mutant SOD1 in mitochondria and abolishes its toxicity. *Hum Mol Genet* 19:4529–4542.

14. Khare SD, Caplow M, Dokholyan NV (2004) The rate and equilibrium constants for a multistep reaction sequence for the aggregation of superoxide dismutase in amyotrophic lateral sclerosis. *Proc Natl Acad Sci USA* 101:15094–15099.

15. Ding F, Dokholyan NV (2008) Dynamical roles of metal ions and the disulfide bond in Cu, Zn superoxide dismutase folding and aggregation. *Proc Natl Acad Sci USA* 105:19696–19701.

16. Dalle-Donne I, Rossi R, Colombo G, Giustarini D, Milzani A (2009) Protein S-glutathionylation: a regulatory device from bacteria to humans. *Trends in Biochemical Sciences* 34:85–96.

17. Redler RL et al. (2011) Glutathionylation at Cys-111 induces dissociation of wild type and FALS mutant SOD1 dimers. *Biochemistry* 50:7057–7066.

18. Proctor EA, Ding F, Dokholyan NV (2011) Structural and thermodynamic effects of post-translational modifications in mutant and wild type Cu, Zn superoxide dismutase. *J Mol Biol* 408:555–567.

19. Marklund SL et al. (1997) Normal Binding and Reactivity of Copper in Mutant Superoxide Dismutase Isolated from Amyotrophic Lateral Sclerosis Patients. *Journal of Neurochemistry* 69:675–681.

20. Kikuchi H et al. (2006) Spinal cord endoplasmic reticulum stress associated with a microsomal accumulation of mutant superoxide dismutase-1 in an ALS model. *Proc Natl Acad Sci USA* 103:6025–6030.

21. Urushitani M, Kurisu J, Tsukita K, Takahashi R (2002) Proteasomal inhibition by misfolded mutant superoxide dismutase 1 induces selective motor neuron death in familial amyotrophic lateral sclerosis. *Journal of Neurochemistry* 83:1030–1042.

22. Banci L et al. (2007) Metal-free superoxide dismutase forms soluble oligomers under physiological conditions: A possible general mechanism for familial ALS. *Proc Natl Acad Sci USA* 104:11263–11267.

23. Vassall KA et al. (2011) Decreased stability and increased formation of soluble aggregates by immature superoxide dismutase do not account for disease severity in ALS. *Proc Natl Acad Sci USA* 108:2210–2215.

24. Urushitani M, Ezzi SA, Julien J-P (2007) Therapeutic effects of immunization with mutant superoxide dismutase in mice models of amyotrophic lateral sclerosis. *Proc Natl Acad Sci USA* 104:2495–2500.

25. Rakhit R et al. (2002) Oxidation-induced Misfolding and Aggregation of Superoxide Dismutase and Its Implications for Amyotrophic Lateral Sclerosis. *J Biol Chem* 277:47551–47556.

26. Fujiwara N et al. (2007) Oxidative Modification to Cysteine Sulfonic Acid of Cys111 in Human Copper-Zinc Superoxide Dismutase. *J Biol Chem* 282:35933–35944.

27. Ezzi SA, Urushitani M, Julien J-P (2007) Wild-type superoxide dismutase acquires binding and toxic properties of ALS-linked mutant forms through oxidation. *J Neurochem* 102:170–178.

28. Furukawa Y, Fu R, Deng H-X, Siddique T, O'Halloran TV (2006) Disulfide cross-linked protein represents a significant fraction of ALS-associated Cu, Zn-superoxide dismutase aggregates in spinal cords of model mice. *Proc Natl Acad Sci USA* 103:7148–7153.

29. Guareschi S et al. (2012) An over-oxidized form of superoxide dismutase found in sporadic amyotrophic lateral sclerosis with bulbar onset shares a toxic mechanism with mutant SOD1. *Proc Natl Acad Sci USA* 109:5074-5079.

30. Furukawa Y, O'Halloran TV (2005) Amyotrophic lateral sclerosis mutations have the greatest destabilizing effect on the apo- and reduced form of SOD1, leading to unfolding and oxidative aggregation. *J Biol Chem* 280:17266–17274.

31. Karch CM, Borchelt DR (2008) A limited role for disulfide cross-linking in the aggregation of mutant SOD1 linked to familial amyotrophic lateral sclerosis. *J Biol Chem* 283:13528–13537.

32. Chen X et al. (2012) Oxidative Modification of Cysteine 111 Promotes Disulfide Bond-Independent Aggregation of SOD1. *Neurochem Res* 37:835–845.

33. Nakanishi T et al. (1998) Simple and defined method to detect the SOD-1 mutants from patients with familial amyotrophic lateral sclerosis by mass spectrometry. *J Neurosci Methods* 81:41–44.

34. Walsh DM et al. (2002) Naturally secreted oligomers of amyloid β protein potently inhibit hippocampal long-term potentiation in vivo. *Nature* 416:535–539.

35. Winner B et al. (2011) In vivo demonstration that α-synuclein oligomers are toxic. *Proc Natl Acad Sci USA* 108:4194–4199.

36. Kirkitadze MD, Bitan G, Teplow DB (2002) Paradigm shifts in Alzheimer's disease and other neurodegenerative disorders: the emerging role of oligomeric assemblies. *J Neurosci Res* 69:567–577.

37. Haass C, Selkoe DJ (2007) Soluble protein oligomers in neurodegeneration: lessons from the Alzheimer's amyloid beta-peptide. *Nat Rev Mol Cell Biol* 8:101–112.

38. Sahin E, Roberts CJ (2012) Size-Exclusion Chromatography with Multi-angle Light Scattering for Elucidating Protein Aggregation Mechanisms. In: Therapeutic Proteins (Voynov V, Caravella JA, eds), pp 403–423 Methods in Molecular Biology. Humana Press.

CHAPTER FOUR: DISCUSSION AND FUTURE DIRECTIONS

Vulnerability of SOD1 to destabilizing post-translational modifications

An abundance of recent work has documented the presence of a wide spectrum of posttranslational modifications of SOD1 from human tissue, including numerous oxidative modifications of cysteines and histidines (1-3), phosphorylation (1), sumoylation (4), succinylation (5), palmitoylation (6), and cysteinylation (7). The effects of many of these modifications on stability and enzymatic activity of WT and FALS mutant SOD1 have not yet been fully delineated, including the question of whether they serve any functional regulatory purposes. A great deal of interest in the field has focused on oxidative modifications of SOD1's free cysteines, as these residues have been shown to modulate SOD1 aggregation propensity (8) and since oxidative stress increases concomitant with ALS disease progression (9). Our work shows that an oxidative modification prevalent on SOD1 from human tissue, Cys-111 glutathionylation, promotes loss of SOD1's native quaternary structure. In addition to promoting the first step in SOD1 misfolding, dimer dissociation (10,11), this modification induces conformational changes that favor assembly into non-native oligomers that contain an epitope characteristic of disease-implicated misfolded SOD1 (12).

This work motivates further inquiry into the prevalence of glutathionylated SOD1 (GS-SOD1) in ALS patients. Enrichment of GS-SOD1 in tissue of ALS patients vs. healthy age-matched controls, or in disease-affected vs. disease-resistant cell populations in ALS patients,

would further support a role for this modification in onset and/or progression of motor neuron degeneration. A correlation between abundance of SOD1 containing oxidative modifications (including glutathionylation) and ALS risk would also allow the evaluation of modified forms of SOD1 as potential biomarkers. As SOD1 isolated from blood of healthy human donors contains substantial amounts of GS-SOD1, this modification alone is unlikely to cause ALS; however, in the context of prolonged oxidative stress or impaired proteostasis due to aging, genetic variability, and/or exposure to toxins, misfolding and aggregation of SOD1 induced by glutathionylation could cross a pathogenic threshold. In addition, destabilizing post-translational modifications of SOD1 may be especially deleterious to motor neurons innervating the lower extremities; since SOD1 must be transported from the cell body to the distal axon (involving distances in excess of one meter), the lifetime of this protein (> 1 year) is longer than in other cell types by multiple orders of magnitude (13). The slow turnover of SOD1 in the largest motor neurons could lead to the enrichment of post-translationally modified SOD1 at axon termini, which is also the location at which abnormalities are detected earliest in mouse models of ALS (14). Modifications of SOD1 (and other proteins implicated in ALS, such as TDP-43 (15)) merit further investigation as factors through which an altered cellular environment modulates protein misfolding and aggregation.

Relative cytotoxicities of misfolded SOD1 species

As for several other neurodegenerative diseases involving protein aggregation, existing evidence supports the idea that soluble misfolded SOD1, rather than larger insoluble aggregates, are most toxic (16). In Chapter 3, we provide evidence that higher-order soluble non-native

oligomers of SOD1 (as opposed to native-like dimers or monomers) are toxic, on the basis that these assemblies expose an epitope present on misfolded SOD1 found only in pathologically-affected cell populations in ALS patient spinal cord (12). Directly testing the toxicities of various non-native SOD1 oligomers is desirable but technically challenging; these metastable assemblies are likely to be present predominantly or exclusively intracellularly and no details regarding their structures are yet known.

Studies assessing toxicity of various $A\beta_{40}$ and $A\beta_{42}$ oligomers (e.g., Ladiwala *et al*. (17)) often involve addition of these assemblies to cell culture media, which is physiologically relevant since these peptides are generated extracellularly. SOD1, by contrast, is a cytosolic protein, so extracellular application of oligomers would not allow observation of toxic character that is most relevant to ALS. Delivering oligomers isolated *in vitro* by protein transfection or microinjection is possible for some cultured neurons, but oligomers may not remain in their initial conformations upon association with transfection reagents or dilution into the cytosol. Stabilization of oligomers using covalent cross-linking for delivery to cells via microinjection or protein transfection may be a feasible strategy; however, this approach will require extensive optimization of cross-linking reaction conditions (such as linker length) and validation that such derivatization does not substantially alter oligomer conformations. Such validation also requires some degree of knowledge of the original structural features of oligomers. Cytosolic α-synuclein oligomers were demonstrated to be toxic through rational manipulation of oligomerization propensity by mutagenesis (18). However, to employ this strategy for soluble SOD1 oligomers would require atomic-level structural information from which to propose mutations to preferentially stabilize non-native oligomers. Further characterization of potentially toxic non-native SOD1 oligomers (such as those that we identify in Chapter 3) may eventually reveal

strategies for direct experimental assessment of their toxicities. A combined experimental and computational approach for characterizing structural features and cytotoxicity of soluble SOD1 oligomers is currently being developed by the Dokholyan lab and is described briefly at the end of this chapter.

Future directions

Effects of Cys-111 glutathionylation and Thr-2 phosphorylation on SOD1 dimer structure

While we have demonstrated experimentally and in simulations that glutathionylation of Cys-111 destabilizes the native SOD1 homodimer, a high-resolution experimental structure of GS-SOD1 would be invaluable for understanding the effect of this modification on SOD1 folding and stability. SOD1 purified from human erythrocytes is glutathionylated in sub-stoichiometric amounts (typically 40-60% of the total pool of isolated SOD1) and is also phosphorylated (1). Crystallization of a GS-SOD1 enriched fraction of SOD1 from erythrocytes (isolated by ion-exchange chromatography as described in Chapter 3 Methods) yields crystals with high mosaicity (Figure 4.1B), most likely due to the inhomogeneity of the starting material. To improve the purity of GS-SOD1 used for crystallization, we treated this GS-SOD1 enriched fraction sequentially with alkaline phosphatase and oxidized glutathione (GSSG) to dephosphorylate and glutathionylate SOD1, respectively. Separation by anion-exchange chromatography yielded a fraction of protein that was confirmed by mass spectrometry to lack phosphorylation and contain at least 95% GS-SOD1. Crystallization of this purified GS-SOD1 yielded improved crystals (Figure 4.1B), but none of sufficient quality for structure determination. Continued efforts to crystallize GS-SOD1 are ongoing.

We also seek detailed structural information for phosphorylated SOD1 (p-SOD1), but isolation of p-SOD1 from the pool of enzyme purified from human erythrocytes is infeasible due to the low prevalence (1) and small differences in mass and charge associated with this modification. Therefore, we have introduced mutations at Thr-2, a position identified by MS/MS to be a site of phosphorylation in SOD1 from human erythrocytes (1), that correspond to aspartic acid and glutamic acid substitutions. Such substitutions are often used to mimic phosphorylation at serine and threonine residues due to the similar steric and electrostatic changes introduced (19-21, Figure 4.1A).

SOD1-T2D and SOD1-T2E were expressed in *S. cerevisiae,* purified as described in Chapter 2 Methods, and crystallized using the hanging drop method of vapor diffusion.

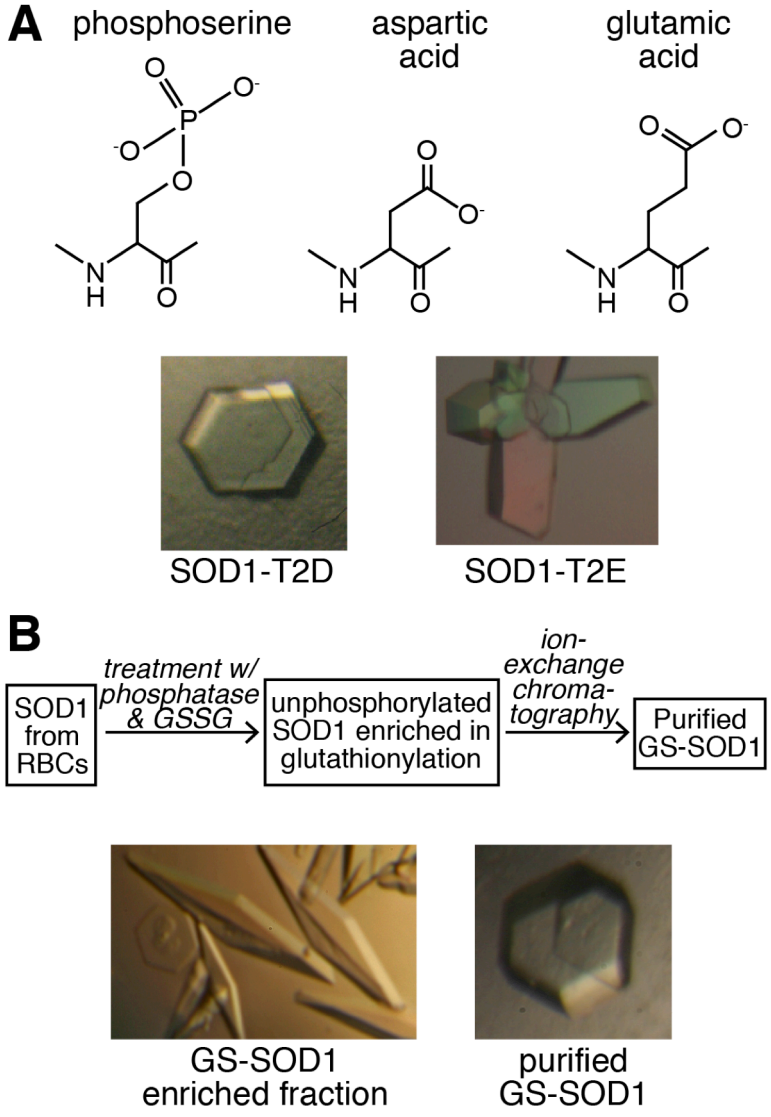

Figure 4.1. Strategies for crystallization of post-translationally modified SOD1. (A) Crystals of SOD1 containing phosphomimetic aspartic acid and glutamic acid substitutions at Thr-2. (B) Crystals of a GS-SOD1 enriched fraction of SOD1 as purified from human erythrocytes, and following enrichment and purification of GS-SOD1.

After an initial screen of crystallization buffers using a version of the "sparse matrix" method (22) modified by Dr. Hengming Ke, conditions supporting crystal growth were optimized until crystals of sufficient size and apparent quality were produced. Crystals were harvested and preliminary studies of X-ray diffraction were performed at the UNC Macromolecular X-Ray Crystallography Core Facility. Diffraction data for crystals deemed to be of high quality based on this initial screen were obtained using a synchrotron source (Brookhaven National

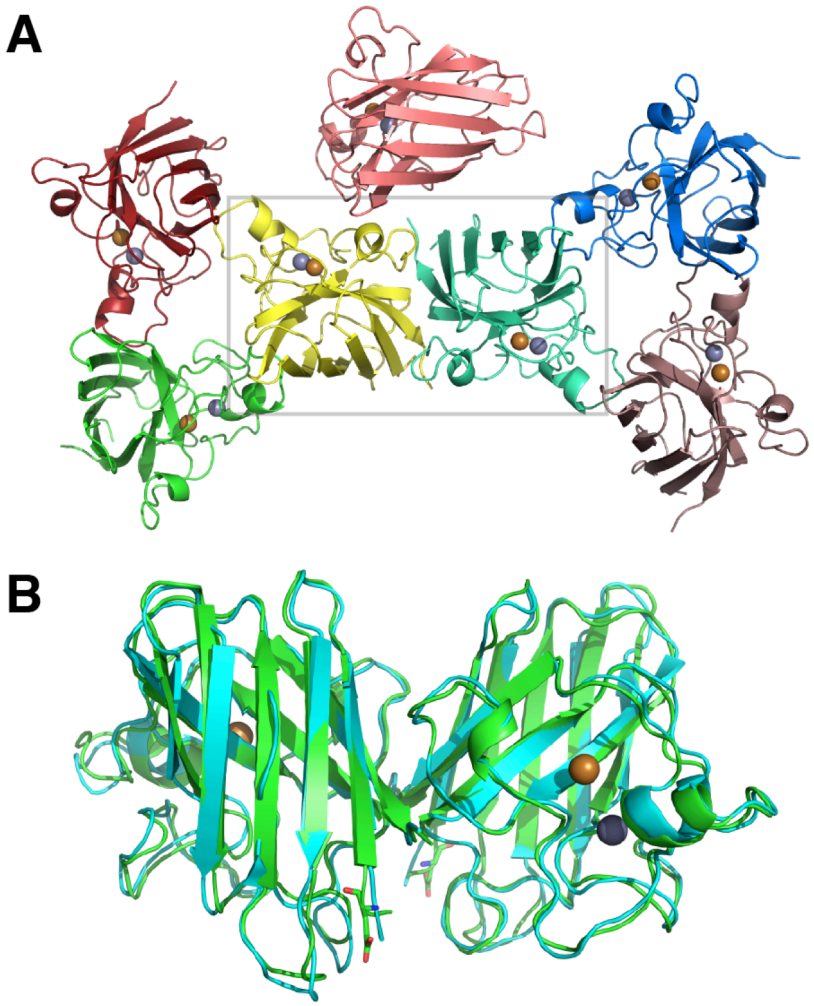

Figure 4.2. Crystal structure of SOD1-T2E. (A) Asymmetric unit of the SOD1-T2E crystal structure. The grey box indicates the physiological dimer. (B) Alignment of SOD1-T2E (green) and SOD1-WT (cyan, PDB ID: 1spd) structures. Glutamic acid residues at position 2 are represented as sticks; Cu^{2+} and Zn^{2+} ions are represented as spheres.

Laboratory). Diffraction data were processed using the program HKL (23). Structures were solved using molecular replacement using SOD1-WT (PDB ID: 1spd) as a starting structure (24), and structural models were built using O (25) cycled with refinement by CNS (26).

SOD1-T2E crystallized in the C121 space group and the structure was solved to 2Å

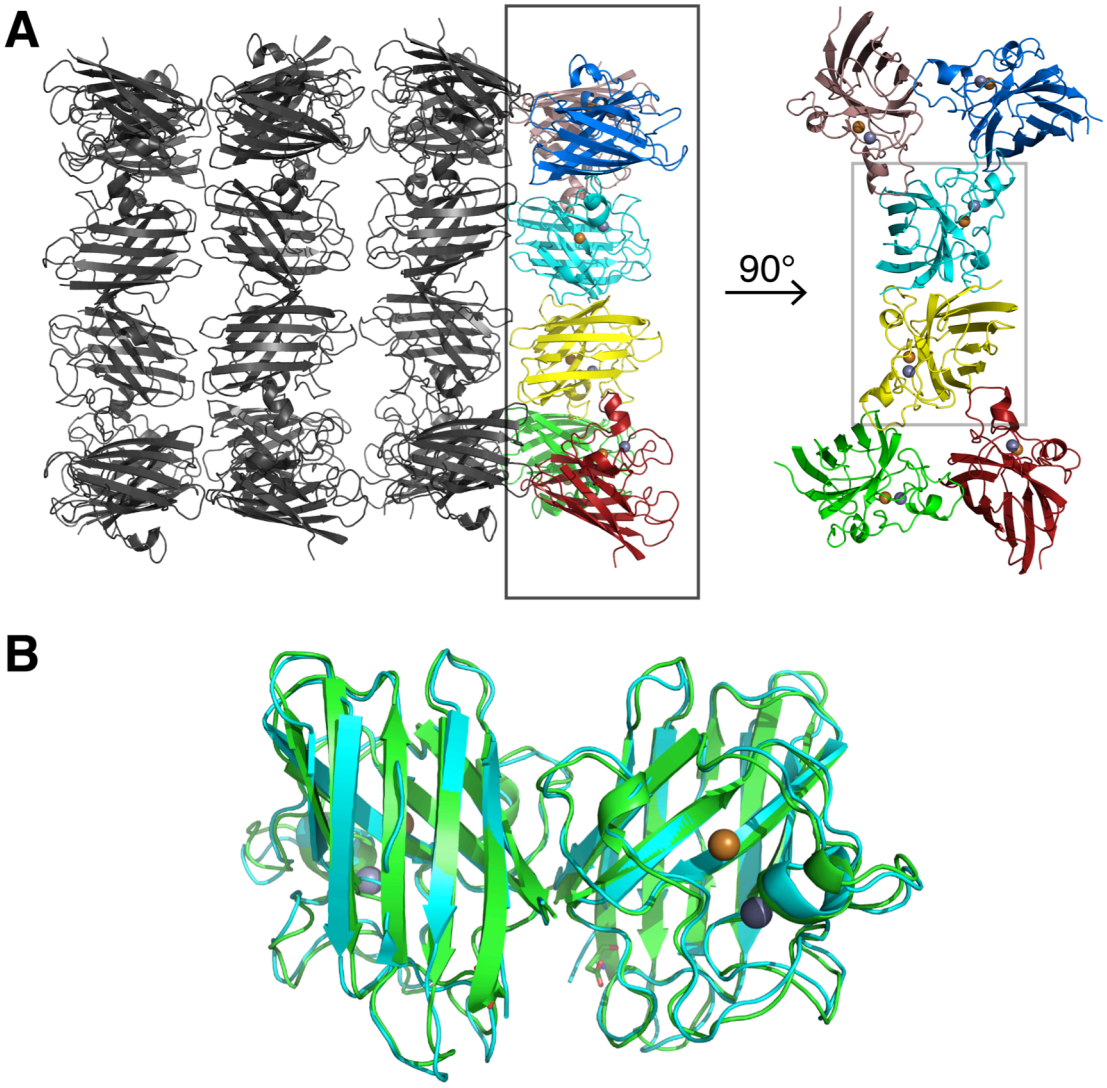

Figure 4.3. Crystal structure of SOD1-T2D. (A) Asymmetric unit of the SOD1-T2D crystal structure. The grey box indicates the physiological dimer. (B) Alignment of SOD1-T2D (green) and SOD1-WT (cyan, PDB ID: 1spd) structures. Aspartic acid residues at position 2 are represented as sticks; Cu^{2+} and Zn^{2+} ions are represented as spheres.

resolution (Figure 4.2); the SOD1-T2D crystal was twinned, but the structure could be solved in the P_1 space group to 1.99 Å resolution (Figure 4.3). The structures of SOD1-T2E and SOD1-T2D dimers differ little from that of SOD1-WT (Figure 4.2B and 4.3B), with both having overall RMSDs calculated to be less than 0.9 Å with respect to the wild type dimer. The arrangement of monomers in the asymmetric unit is similar for both structures, except for the presence of a 7^{th} monomer (colored pink in Figure 4.2A) adjacent to the central dimer, which corresponds to the biological homodimeric assembly.

While the crystal structure of SOD1-T2E reveals no large-scale rearrangements of the homodimer, we cannot rule out the possibility that this substitution produces subtle alterations in SOD1 dynamics that would only be apparent in the solution state. We are particularly interested in whether this substitution alters the sensitivity of SOD1 to destabilization by the glutathione modification. To approximate the effect of glutathionylation on stability of phosphorylated SOD1, we characterized the effect of this modification on stability of the phosphomimetic SOD1-T2E dimer. SEC and SPR of unmodified and glutathionylated SOD1-T2E were performed as described for WT, A4V, and I112T variants in Chapter 2 Methods. DMD simulations of unmodified and glutathionylated SOD1-T2E followed by evaluation of intermonomer contacts were also performed in an identical manner as described in Chapter 2 Methods. Interestingly, in these preliminary SEC experiments, we observe minimal destabilization of SOD1-T2E dimers by glutathionylation despite increased dimer dissociation rate (as measured by SPR) (Figure 4.4). Thus, SOD1-T2E appears to behave similarly to SOD1-I112T upon glutathionylation: rate of dissociation increases but is not reflected in an increased equilibrium dissociation constant (K_d), indicating that association rate of SOD1-T2E monomers may also increase upon glutathionylation. The change in dimer interface contacts induced by glutathionylation of SOD1-

T2E also mirrored that observed for SOD1-I112T: loss of intermonomer contacts present in unmodified SOD1-T2E dimers was balanced by a gain of new contacts in the dimer interface. (Figure 4.4).

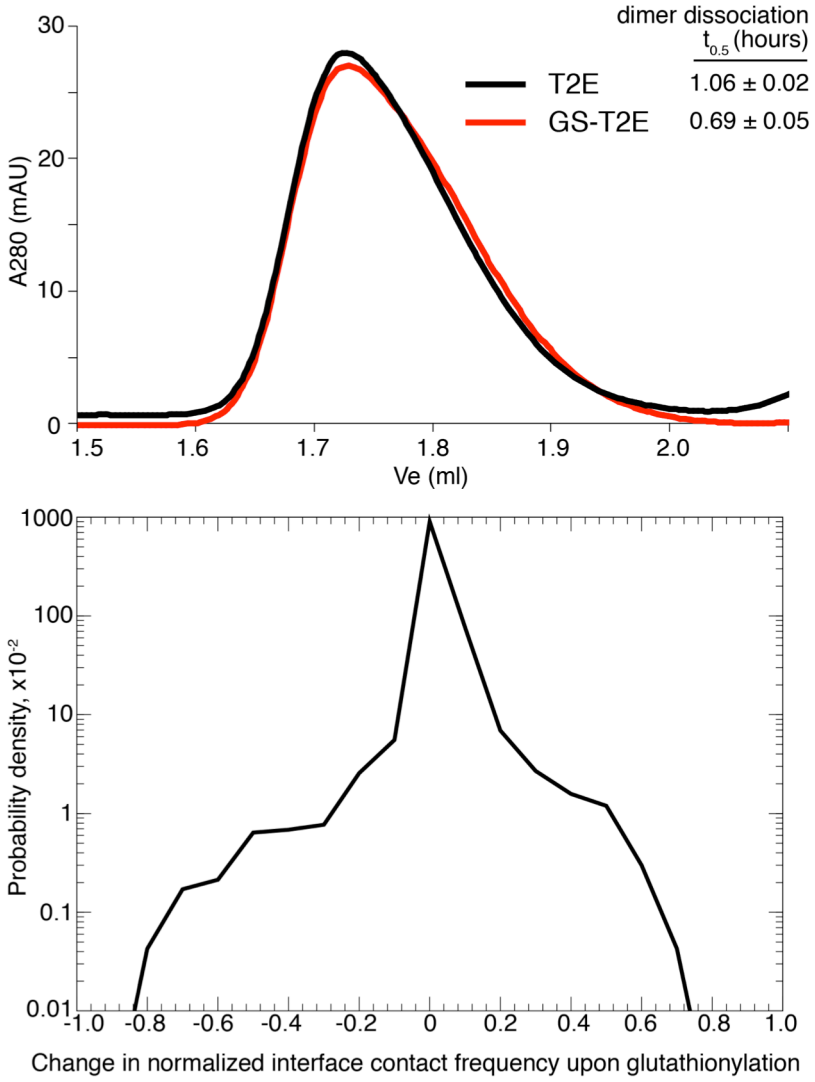

Figure 4.4. Effect of glutathionylation on SOD1-T2E dimer stability and interface composition. Top, SEC separation of unmodified (black curves) and glutathionylated (red curves) SOD1-T2E. Dimeric SOD1 elutes ~1.74 ml after injection onto the column (Superdex 200 PC 3.2/30, GE Healthcare). Half times for dimer dissociation ± S. D. (based on at least three independent SPR experiments) are shown at right. Bottom, distribution of of changes in frequency of Cα interface contacts upon Cys-111 glutathionylation for SOD1-T2E, based on structural models generated using DMD.

Further SEC experiments are currently in progress to confirm the lack of destabilization of SOD1-T2E by glutathionylation and to characterize the effect of glutathionylation on SOD1-T2D, but our preliminary results suggest that phosphorylation of SOD1 may desensitize the protein to the destabilizing effects of the glutathione modification. The potentially protective effect of phosphorylation, allowing SOD1 to remain dimeric under oxidizing conditions, raises the intriguing question of which kinase(s) target SOD1. Identification of the kinase(s) capable of phosphorylating SOD1 would give insight into the cellular conditions under which this modification would likely occur and could potentially enable the production of sufficient p-SOD1 for biophysical characterization through *in vitro* phosphorylation. Recent work implicating Ca^{2+}/calmodulin protein kinase II (CaMKII) in SOD1 phosphorylation that occurs in rat hepatocytes exposed to nodularin (27) motivates further investigation of this protein's ability to phosphorylate human SOD1 *in vitro*.

Assessment of oligomer cytotoxicity

As mentioned above, an outstanding question in the field of SOD1-related ALS is the identity of toxic misfolded SOD1 conformers. We therefore have undertaken efforts to develop a strategy for the generation of structural models of metastable non-native oligomers, which can then be used to identify single amino acid substitutions predicted to alter oligomer stability (Figure 4.5). Briefly, a non-native oligomer of SOD1-WT that can be generated in abundance by incubation at pH 3.5 in the presence of EDTA was subjected to limited proteolysis by multiple proteases of varying specificities. Products of proteolytic cleavage were identified by mass spectrometry, and this information was used to bias molecular dynamics simulations based on

the fact that cleavage sites and flanking residues must be solvent-accessible and flexible (not participating in secondary structural elements). The generated structural model was then used to identify mutations to residues participating in intermonomer contacts that would be expected to alter trimer stability (as calculated by the Eris software, which estimates the effect of amino acid substitutions on the stability of proteins with known structures (28)).

Amino acid substitutions computationally predicted to have greatest effects on trimer stability are currently being evaluated for their aggregation propensities *in vitro* by performing time-resolved SEC of purified SOD1 containing the identified substitutions (under the same conditions utilized to generate the SOD1-WT trimer). These experiments are intended to validate the predictive ability of the structural model, as well as to generate a set of mutations confirmed to alter trimer stability *in vitro*. SOD1 containing substitutions confirmed to promote or inhibit trimer formation will be expressed in motor neuron-like cells (NSC-34 (29)) and their effects on cell viability will be assessed using standard assays. We will test the hypothesis that trimeric SOD1 is cytotoxic by determining whether a correlation exists between the "trimerogenic" character of each substituted variant of SOD1 (i.e., the probability of adopting a trimeric conformation *in vitro*) and its effect on viability of motor neuron-like cells. If the SOD1 trimer is cytotoxic, we would expect that mutations which stabilize the trimeric state would decrease cell viability more than mutations that destabilize the trimer. Immunostaining with the C4F6 conformational antibody and a pan-SOD1 antibody to detect small soluble oligomers and insoluble aggregates, respectively, can be utilized to connect the oligomerization behavior observed *in vitro* with that occurring within the cellular environment.

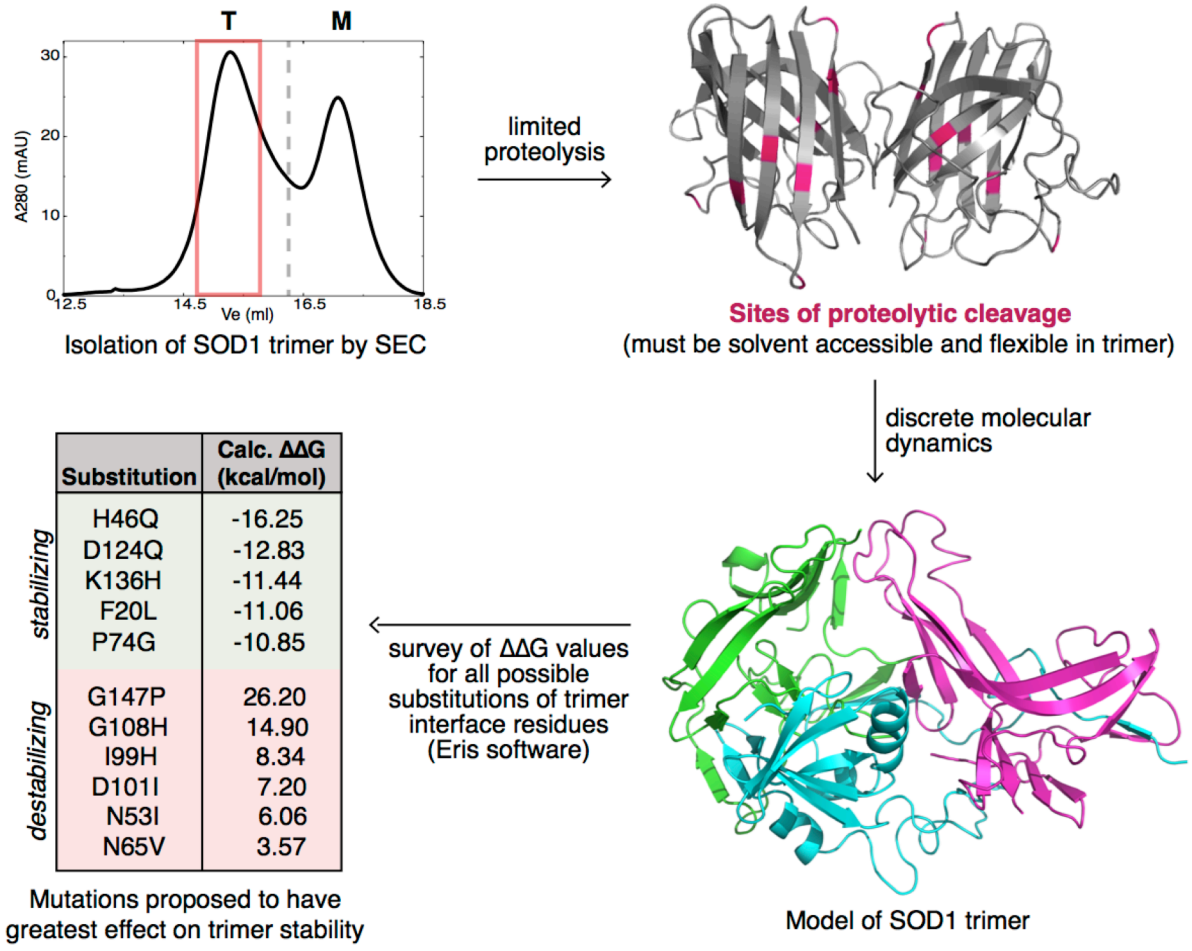

Figure 4.5. Strategy for assessing cytotoxicity of a non-native soluble SOD1 oligomer. Top left, SEC chromatogram of 100 μM SOD1-WT incubated at pH 3.5 in the presence of 10 mM EDTA for 24 hours. The dashed line indicates the elution volume of the native dimer under these conditions (prior to incubation), and peaks corresponding to trimeric and monomeric SOD1 are indicated "T" and "M", respectively. The red box indicates the eluted material that was pooled for subsequent proteolysis experiments. Upper right, sites of initial proteolytic cleavage of SOD1 trimers (by multiple proteases) are shown in pink on the structure of the WT dimer (PDB ID: 1spd). Lower right, structural model of a SOD1 trimer obtained by molecular dynamics simulations biased to penalize contacts made by residues near sites of proteolytic cleavage. Lower left, set of amino acid substitutions within trimer interfaces predicted to have greatest effects on trimer stability, as predicted by Eris software (28).

REFERENCES

1. Wilcox, K.C. et al. (2009) Modifications of superoxide dismutase (SOD1) in human erythrocytes: a possible role in amyotrophic lateral sclerosis. *J Biol Chem* 284:13940–13947.

2. Fujiwara N, Nakano M, Kato S, Yoshihara D, Ookawara T, Eguchi H, Taniguchi N, Suzuki K (2007) Oxidative Modification to Cysteine Sulfonic Acid of Cys111 in Human Copper-Zinc Superoxide Dismutase. J Biol Chem 282:35933–35944.

3. Mulligan VK, Kerman A, Laister RC, Sharda PR, Arslan PE, Chakrabartty A (2012) Early steps in oxidation-induced SOD1 misfolding: implications for non-amyloid protein aggregation in familial ALS. J Mol Biol 421:631–652.

4. Fei E, Jia N, Yan M, Ying Z, Sun Q, Wang H, Zhang T, Ma X, Ding H, Yao X, Shi Y, Wang G (2006) SUMO-1 modification increases human SOD1 stability and aggregation. Biochem Biophys Res Commun 347:406–412.

5. Lin Z-F, Xu H-B, Wang J-Y, Lin Q, Ruan Z, Liu F-B, Jin W, Huang H-H, Chen X (2013) SIRT5 desuccinylates and activates SOD1 to eliminate ROS. Biochem Biophys Res Commun 441:191–195.

6. Antinone SE, Ghadge GD, Lam TT, Wang L, Roos RP, Green WN (2013) Palmitoylation of superoxide dismutase 1 (SOD1) is increased for familial ALS-linked SOD1 mutants. J Biol Chem:jbc.M113.487231.

7. Auclair JR, Johnson JL, Liu Q, Salisbury JP, Rotunno MS, Petsko GA, Ringe D, Brown RH, Bosco DA, Agar JN (2013) Post-Translational Modification by Cysteine Protects Cu/Zn-Superoxide Dismutase from Oxidative Damage. Biochemistry 52:6137–6144

8. Cozzolino M, Amori I, Grazia Pesaresi M, Ferri A, Nencini M, Teresa Carrì M (2008) Cysteine 111 Affects Aggregation and Cytotoxicity of Mutant Cu,Zn-superoxide Dismutase Associated with Familial Amyotrophic Lateral Sclerosis. J Biol Chem 283:866–874.

9. Barber SC, Shaw PJ (2010) Oxidative stress in ALS: key role in motor neuron injury and therapeutic target. Free Radic Biol Med 48:629–641.

10. Khare SD, Caplow M, Dokholyan NV (2004) The rate and equilibrium constants for a multistep reaction sequence for the aggregation of superoxide dismutase in amyotrophic lateral sclerosis. Proc Natl Acad Sci U S A 101:15094–15099.

11. Rakhit R, Crow JP, Lepock JR, Kondejewski LH, Cashman NR, Chakrabartty A (2004) Monomeric Cu,Zn-superoxide dismutase is a common misfolding intermediate in the oxidation models of sporadic and familial amyotrophic lateral sclerosis. J Biol Chem 279:15499–15504.

12. Brotherton TE, Li Y, Cooper D, Gearing M, Julien J-P, Rothstein JD, Boylan K, Glass JD (2012) Localization of a toxic form of superoxide dismutase 1 protein to pathologically affected tissues in familial ALS. Proc Natl Acad Sci 109:5505–5510.

13. Shi Y, Rhodes NR, Abdolvahabi A, Kohn T, Cook NP, Marti AA, Shaw BF (2013) Deamidation of Asparagine to Aspartate Destabilizes Cu, Zn Superoxide Dismutase, Accelerates Fibrillization, and Mirrors ALS-Linked Mutations. J Am Chem Soc 135:15897–15908.

14. Fischer LR, Culver DG, Tennant P, Davis AA, Wang M, Castellano-Sanchez A, Khan J, Polak MA, Glass JD (2004) Amyotrophic lateral sclerosis is a distal axonopathy: evidence in mice and man. Exp Neurol 185:232–240.

15. Lee EB, Lee VM-Y, Trojanowski JQ (2011) Gains or losses: molecular mechanisms of TDP43-mediated neurodegeneration. Nat Rev Neurosci 13:38–50.

16. Redler RL, Dokholyan NV (2012) The complex molecular biology of amyotrophic lateral sclerosis (ALS). Prog Mol Biol Transl Sci 107:215–262.

17. Ladiwala ARA, Bhattacharya M, Perchiacca JM, Cao P, Raleigh DP, Abedini A, Schmidt AM, Varkey J, Langen R, Tessier PM (2012) Rational design of potent domain antibody inhibitors of amyloid fibril assembly. Proc Natl Acad Sci U S A 109:19965–19970.

18. Winner B, Jappelli R, Maji SK, Desplats PA, Boyer L, Aigner S, Hetzer C, Loher T, Vilar M, Campioni S, Tzitzilonis C, Soragni A, Jessberger S, Mira H, Consiglio A, Pham E, Masliah E, Gage FH, Riek R (2011) In vivo demonstration that α-synuclein oligomers are toxic. Proc Natl Acad Sci 108:4194–4199.

19. Oueslati, A., Paleologou, K.E., Schneider, B.L., Aebischer, P., and Lashuel, H.A. (2012). Mimicking phosphorylation at serine 87 inhibits the aggregation of human α-synuclein and protects against its toxicity in a rat model of Parkinson's disease. *J. Neurosci.* 32: 1536–1544.

20. Pondugula, S.R., Brimer-Cline, C., Wu, J., Schuetz, E.G., Tyagi, R.K., and Chen, T. (2009). A phosphomimetic mutation at threonine-57 abolishes transactivation activity and alters nuclear localization pattern of human pregnane x receptor. *Drug Metab. Dispos*. 37: 719–730.

21. Wagner, L.E., 2nd, Li, W.-H., Joseph, S.K., and Yule, D.I. (2004). Functional consequences of phosphomimetic mutations at key cAMP-dependent protein kinase phosphorylation sites in the type 1 inositol 1,4,5-trisphosphate receptor. *J. Biol. Chem.* 279: 46242–46252.

22. Jancarik, J., and Kim, S.H. (1991). Sparse matrix sampling: a screening method for crystallization of proteins. *Journal of Applied Crystallography* 24: 409-411.

23. Otwinowski, Z. and Minor, W. (1997). Processing of X-ray diffraction data collected in oscillation mode. *Methods in Enzymology* 276: 307-326.

24. Navaza, J. (1994) AMoRe: an automated package for molecular replacement. Acta Crystallographica Section A 50, 157-163.

25. Jones, T.A., Zou, J.Y., Cowan, S.W., Kjeldgaard, M. (1991) Improved methods for building protein models in electron density maps and the location of errors in these models. *Acta Crystallogr. A* 47 (Pt 2): 110-119.

26. Brunger, A.T., et al. (1998) Crystallography & NMR system: A new software suite for macromolecular structure determination. *Acta Crystallogr. D Biol Crystallogr*. 54: 905-921.

27. Hjørnevik, L.V., Fismen, L., Young, F.M., Solstad, T., and Fladmark, K.E. (2012). Nodularin exposure induces SOD1 phosphorylation and disrupts SOD1 co-localization with actin filaments. *Toxins (Basel)* 4: 1482–1499.

28. Yin S, Ding F, Dokholyan NV (2007) Eris: an automated estimator of protein stability. *Nat Methods* 4:466–467.

29. Cashman NR, Durham HD, Blusztajn JK, Oda K, Tabira T, Shaw IT, Dahrouge S, Antel JP (1992) Neuroblastoma x spinal cord (NSC) hybrid cell lines resemble developing motor neurons. *Dev Dyn* 194:209–221.